Functional Assessment on the Differential Effect of Mutant p53-Plakoglobin Interaction in Carcinoma Cells

by

Chu Shiun Lo

A thesis submitted in partial fulfillment of the requirements for the degree of

Master of Science

Department of Medicine
University of Alberta

Abstract

p53 transcriptional factor and tumor suppressor protein is mutated in over 50% of all cancers and most metastatic tumors. Majority of p53 mutations are single missense mutation and occur in the DNA-binding domain (DBD). The six most common missense mutations in the p53 DBD are known as "hot spots" and are classified into "conformational" and "contact" mutants. Both mutant types interfere with the interaction of p53 with DNA either by altering p53 conformation/structure (conformational) or affecting amino acid residues directly involved in DNA binding (contact). Conformational and contact p53 mutant oncogenic activities have been shown to be cell-context and mutation type dependent. Using carcinoma cell lines of various origins, previously, we showed that plakoglobin interacted with wild-type and several endogenous p53 mutants (e.g., R280K, R273H, S241F, S215R) and this interaction was mediated by the p53 DBD and plakoglobin C-terminus domain. We further showed that plakoglobin expression in carcinoma cell lines deficient in plakoglobin and expressing various p53 mutants restored the tumor suppressor activities of mutants *in vitro*.

To compare the effects of plakoglobin expression on oncogenic activities of contact vs. conformational mutants and to avoid potential confounding cell-context dependent factors, we established an *in vitro* cellular model using the p53-null and plakoglobin-deficient H1299 non-small cell lung carcinoma cell line. This system allowed us to exogenously express p53-R273H contact or p53-R175H conformational mutant with or without plakoglobin to directly compare tumor suppressive effects of plakoglobin on these mutants in the same genetic background. Functional assays were performed to assess cell growth, colony formation, migration, and invasion. qPCR and immunoblotting were used to examine the expression specific genes and level and subcellular distribution of proteins that are typically regulated by or regulate p53 function and

are altered in mutant p53 expressing cell lines and tumors. Plakoglobin interacted with both mutants, affected their oncogenic properties differently, and its tumor suppressive effects were significantly stronger in p53-R175H expressing cells. We further extended our studies and identified potential amino acid residues in p53-R175H and plakoglobin that mediated their interaction. Using *in silico* 3D molecular dynamic modeling, we identified Q167 and R248 on p53-R175H, and N690 on plakoglobin as potential amino acid residues mediating their interaction. We then validated the *in silico* model by generating plasmids encoding p53-R175H in which Q167 and R248 residues were substituted by alanine individually or together. Similarly, we developed a plasmid encoding plakoglobin in which N690 was substituted by alanine. Different combinations of plasmids were expressed in H1299 cells and the resulting transfectants characterized for changes in p53-R175H and plakoglobin interaction and the functional consequences of these changes was measured by the *in vitro* invasiveness of various transfectants. The results showed decreased p53-R175H- plakoglobin interaction when p53-R175H Q167 and R248 residue were substituted by alanine. In contrast, plakoglobin N690A substitution had no effect on its interaction with p53-R175H. Intriguingly, plakoglobin co-expression with all forms of p53-R175H reduced their invasiveness by more than 80%. These observations suggested the potential ability of plakoglobin to interact with various conformational mutants. The larger implication of these studies is the potential for exploring plakoglobin interactions with p53 conformational mutants as a useful approach to develop cancer therapeutics for tumors expressing this type of mutations.

Preface

This thesis is an original work by Chu Shiun (Tiffany) Lo. No part of this thesis has been previously published. Contents form Chapter 2 and Chapter 3 of this thesis are currently in submission process.

Parnian Alavi contributed to the RT-PCR experiments described in Chapter 2 and Dr. Jinlan Chang contributed to the preparation of plasmids used in Chapter 3. *In silico* modeling of p53-R175H -plakoglobin interaction was performed by Dr. Sara Omar.

We would like to thank Dr. William Weis for the PG-GST and Drs. Giovanni Blandino and Silvia Di Agostino for the $p53^{R175H}$ constructs used in Chapter 2. We also thank Dr. Rashmi Panigrahi for reagents and advice in GST pull down experiments in Chapter 2 of this thesis, as well as her advice for the *in silico* modeling in Chapter 3.

Acknowledgement

I would like to take this opportunity to thank my co-supervisors Dr. Manijeh Pasdar and Dr. Nadia Jahroudi. Their dedication and passion in their work were inspiring, and their feedback and encouragement always pushed me to strive and achieve higher. The amount of guidance and assistance I have received from my supervisors throughout the duration of this degree had been incredible. The countless weekends and the late nights in the laboratory would not have been as enjoyable without their constant supply of food and snacks. On both the personal and professional level, I am truly grateful and appreciative for the supports I have received.

Additionally, I would like to thank the amazing people I have met from Drs. Tan and Hubbard laboratories, Dr. Qiumin Tan, Brenna Hourigan, Rebekah Van Bruggen, and Jerry Chen. I appreciated all the plasticware and laboratory supplies I was able to borrow during the dark period of plasticware shortage. I would also like to acknowledge and thank the assistance that I have received from colleagues: Parnian Alavi, Powel Crosley, Quinn Storozysky, Dr Rashmi Panigrahi, and Dr. Laiji Li from the laboratories of Drs. Jahroudi, Hitt, Glover, and Ballermann. I am very thankful to Colleen Dluzewski, Darcy Robillard, and Sandy Dieb from the Department of Oncology for their continuous support and patience throughout my studies.

Lastly, I would like to give sincere thanks to my friends and family. I am forever grateful for their understanding and support throughout this journey. My grandparents (Baosheng Lo and Baoyu Lolai) and uncle (Weizhe Lo) who have been giving me so much support and encouragement from across the Pacific Ocean, my parents (Ching-Ju Hsieh and Wen-his Lo), my sisters (Wan Lo, Pei Lo, and Chelsea Lo), and my friends (Lily Huang, Leili Hamidi, Andrea Martin, and Yuexi Jiang) in BC who remained in constant contact through texts and phone calls, my friends in Edmonton who made this city feel like home (Wendy Zhang, Lydia Cao, Nico Wang, Fulin Wang, and Zhuohao Li), I especially thank them for their support throughout the difficult time of the pandemic. I look forward to catching up with many of them after the conclusion of this degree. From the bottom of my heart, I sincerely thank everyone who has contributed and impacted me on this journey.

Table of Contents

List of Figures

List of Tables

Glossary

aMD: Accelerated molecular dynamics

AML: acute myeloid leukemia

ARF (p19ARF): Alternate reading frame protein encoded by ARF-INK4a

ATM: Ataxia telangiectasia mutated

ATR: Rad3-related

BAG2: BAG family molecular chaperone regulator 2

B-ALL: B cell acute lymphoblastic leukemia

β-cat: Beta-catenin

Bcl2: B-cell lymphoma 2

CBP: Cyclic adenosine monophosphate Response Element Binding protein (CREB) Binding Protein

cDNA: Complementary DNA

c-jun: Cellular Transcription factor Jun

cMD: Classical molecular dynamics

CML: Chronic myeloid leukemia

COTH: CO-THreader

CTC: Circulating tumor cell

CTD: C-terminal regulatory domain

DBD: DNA-binding domain

DNA: Deoxyribonucleic acid

DNA-PK: DNA-dependent protein kinase

E-cadherin: Epithelial cadherin

EFN: Ephrin

EGR1: Early growth response protein 1

eHsp90α: Extracellular human heat shock protein 90 alpha

EMT: Epithelial-mesenchymal transition

ERK: Extracellular signal-regulated kinases

Ets2: Erythroblast Transformation Specific Proto-Oncogene 2

GOF: Gain of function

HAI-I: Hepatocyte growth factor activator inhibitor type I

HDM2: Human double minute 2

IRF8: Interferon regulatory factor 8

JNK: c-Jun N-terminal kinases

KRAS: Kirsten rat sarcoma virus

L: Linker region

LOF: Loss of function

MAPK: Mitogen-activated protein kinases

MDM2: Mouse double minute 2

MET: Mesenchymal-epithelial transition

MM-GBSA: Molecular mechanics-generalized born surface area

MMPBSA: Molecular mechanics-generalized born surface area

MDR1: Multi-drug resistance 1

N-cadherin: Neural cadherin

NES: Nuclear export signal

NFAT1: Nuclear factor of activated T cells 1

NF-Y: Nuclear transcription factor Y

NLS: Nuclear localization signal

NM23: Non-metastasis 23

NPM: Nucleophosmin

NSCLC: Non-small cell lung carcinoma

OB-cadherin: Osteoblastic cadherin

p300: Histone acetyltransferase p300

P-cadherin: Placental cadherin

PDB: Protein data bank

PDGF-β: Platelet-derived growth factor beta

PG: Plakoglobin

PKB: Protein kinase B

PML: Promyelocytic leukemia

PRD: Proline-rich domain

PTM: Post-translational modification

PUMA: p53 upregulated modulator of apoptosis

RAS: Rat sarcoma virus

RE: Response element

RIPA: Radio Immunoprecipitation Assay

RMSD: Root-mean-square-deviation

SATB1: SATB Homeobox 1

SFN: Stratifin, 14-3-3 σ

SH-3: Src Homology-domain 3

SOX4: Sex Determining Region Y-Box Transcription factor 4

SREBP: Sterol regulatory-element binding proteins

SV40: Simian virus 40

TAD: Transactivation domain

TCF/LEF: T-cell factor/lymphoid enhancer factor

TD: Tetramerization domain

TIP3P: Transferable intermolecular potential with 3 points

VDR: Vitamin D receptor

VE-cadherin: Vascular-endothelial cadherin

Wnt: Wingless and Int1

WT: Wild-type

ZEB: Zinc finger E-box-binding homeobox

CHAPTER 1: INTRODUCTION

1.1 p53, a tumor suppressor or a proto-oncogene

1.1.1. p53: Initial Identification

p53 protein was originally identified as an oncogene due to its co-immunoprecipitation with SV40 large T-antigen in transformed cells (1). Several subsequent studies supported this initial observation. p53-transfected rat chondrocyte sensitized these cells to Ras-mediated transformation (2). Co-transfection of *TP53* and *Ras* into normal rat embryonic fibroblasts resulted in cellular transformation (3, 4). The seemingly critical role of p53 in cell transformation was consistent with the presence of high level of p53 in transformed cell lines and tumors relative to untransformed cells and normal tissues, which express low levels of p53 (5). However, contrasting evidences, such as lack of p53 expression in acute myeloid leukemia (AML), and several studies that failed to demonstrate the cell-transforming property of p53 created contradictory views on role of p53 in cellular function (6, 7, 8). This controversy was resolved in the late 1980s by a number of studies demonstrating that p53 mutations led to its unregulated expression and the onset of cellular transformation, which led to p53-mediated cellular transformation observed in the aforementioned studies (9). Subsequent studies confirmed the role of wild-type p53 (p53-WT) as a tumor suppressor. Transfection of cDNA construct encoding p53-WT did not induce cellular transformation in rat embryo fibroblasts, while constructs encoding mutant p53s did (9, 10). p53-WT expression suppressed foci formation in primary rat embryo fibroblasts transformed by mutant p53 and ras, or other oncogene combinations such as *myc* and *ras* or *E1A* and *ras*.(11). Following these observations, numerous studies further supported the notion that p53-WT suppresses cell transformation while mutant p53 may lead to oncogenesis (12, 13, 14). In summary, *TP53* is a tumor suppressor gene and a proto-oncogene that, when mutated in certain amino acid residue(s), can promote oncogenesis.

1.1.2. p53 and its role in tumor suppression

p53 is a transcription factor and a tumor suppressor that mediates cellular response to stress signals (15). This response is facilitated by the regulators of p53 and lead to modulations in the p53 protein stability and its activities (16). Downstream signaling events of p53 activation include, but are not limited to, activation of cell cycle arrest, recruitment of DNA damage repair machinery, activation of apoptotic programs and autophagy, and regulation of cellular metabolism, energetics and the oxidation state of cells (16, 17).

Due to its ability to maintain genome stability in response to genetic/oncogenic mutations, p53 is dubbed as "the guardian of the genome" (16, 17). The p53 regulated physiological pathways and programs are often dysregulated or non-functional in tumor cells (17). Germline p53 mutations is associated with Li-Fraumeni syndrome, which is presented by the early onset of various tumors including bone and soft tissue sarcomas, brain and breast carcinomas, acute leukemias, etc (17, 18, 19). p53 is mutated in over 50% of all cancers, making it the most frequent somatic mutation in tumors (17). While mutant p53 lacks p53-WT tumor-suppressing function, it may also activate novel pathways that promote all hallmarks of cancers and contribute to tumor development and metastasis (20, 21, 22).

1.1.3 p53 protein structure

Human p53 is a 393 amino acid protein with various structural and functional domains that govern p53 stability and functions (**Figure 1-1A**) (23). p53 contains two transactivation domains (TAD I and TAD II), a proline-rich domain (PRD) and a DNA binding domain (DBD) that is connected to the tetramerization domain (TD) via a linker region (L), followed by a C-terminal regulatory domain (CTD) (**Figure 1-1A**) (23).

TAD is critical for p53 transcriptional activities. Upon recognition of the target gene by DBD, TAD activates transcription by binding to the components of the transcriptional machinery and other coactivators/corepressors (23, 24, 25). TAD is also the binding site for the E3-ubiquitin ligase mouse double minute (MDM2), a major regulator of p53 stability (23, 26). TAD contains multiple phosphorylation sites which when phosphorylated by a group of kinases [including ataxia telangiectasia mutated (ATM), Rad3-related (ATR), and DNA-dependent protein kinase (DNA-PK)], directly affect p53 binding to MDM2 and its coactivators (e.g., p300 and CBP) (**Figure 1-1A)** (23, 27, 28, 29, 30).

Proline-rich domain (PRD) spans amino acid 55-100 of the p53 protein (31). As the name implies, this domain is rich in proline (31). Mutations in the PRD often occurs on proline residue (P82, P89, P98, and the frequently observed P72R polymorphism) (31). These mutations can interfere with p53 transcriptional activity or its interaction with binding partners. Specifically, repeats of PXXP in PRD confers affinity and specificity for Src homology-domain 3 (SH-3)-containing proteins and may alter their interaction with PRD (31, 32). For example, polymorphism

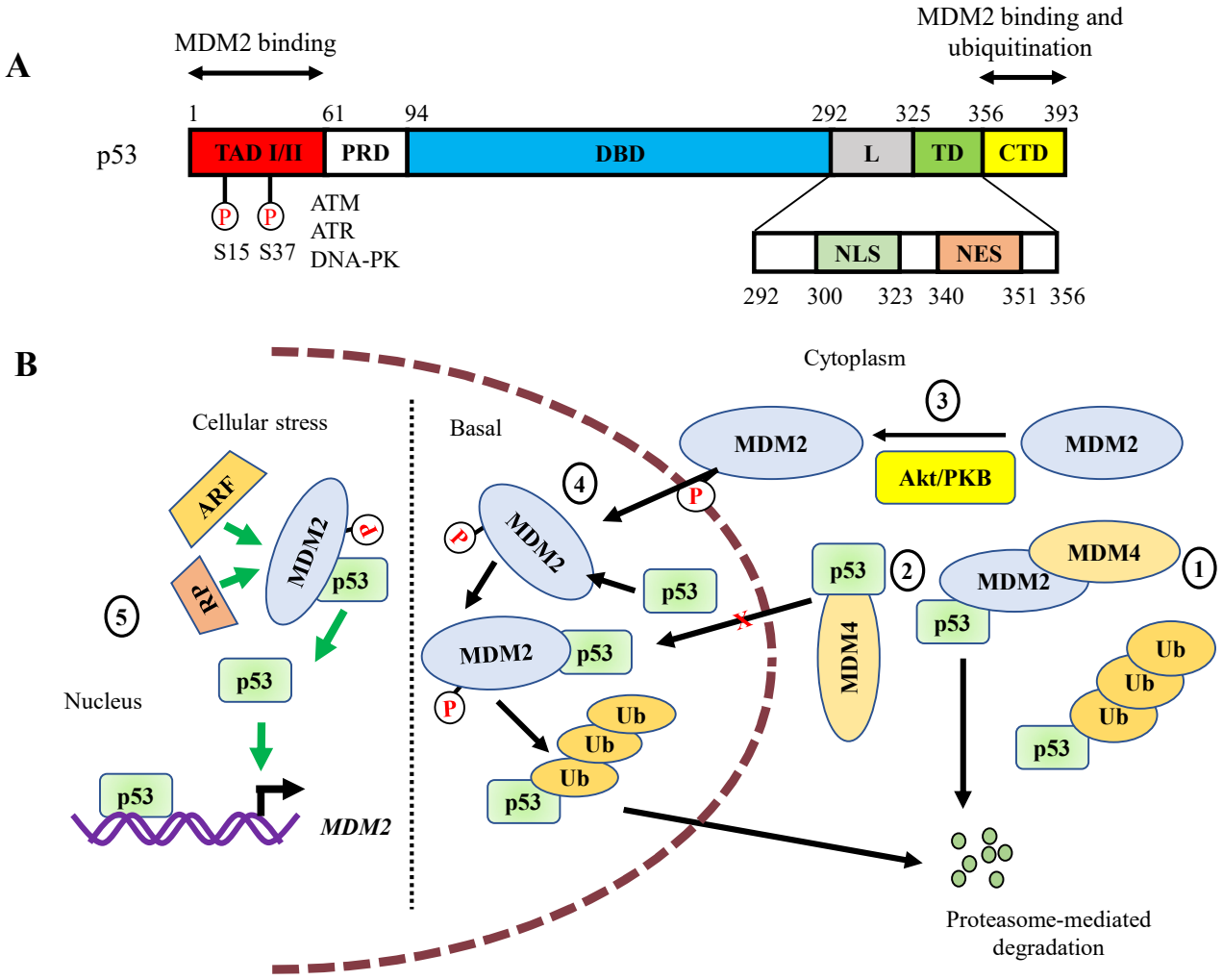

Figure 1-1. Domain structure of p53 and its regulation of stability and function. (A). p53 consists of 393 amino acids divided into five structural and functional domains . A transactivation domain (**TAD**), which consists of TAD I and TAD II, a proline-rich domain (**PRD**), a DNA-binding domain (**DBD**), a linker region (L), a tetramerization domain (**TD**), and a C-terminal regulatory domain (**CTD**). p53 CTD is a binding site for MDM2 E3-ubiquitin ligase that ubiquitinate and marks p53 for proteosomal degradation. In addition, **MDM2** can bind to p53 TAD and directly inhibit p53 transcriptional activity. MDM2 binding and p53 level is tightly controlled by phosphorylation induced by ataxia telangiectasia mutated (**ATM**), Rad3-related (**ATR**), and DNA-dependent protein kinase (**DNA-PK**) kinases that are activated under various kinds of cellular stress. Phosphorylation of Serine15 and Serine37 in the TAD domain and inhibit MDM2 binding and MDM2-mediated p53 degradation. p53 also contains nuclear localization signal (**NLS** in linker region) and nuclear export signal (**NES** in tetramerization domain) that facilitate p53 subcellular localization. **(B)**. The E3 ubiquitin ligase MDM2 functions in both the cytoplasm and nucleus and regulate p53 stability and activity by multiple mechanisms in both the cytoplasm and nucleus. In the cytoplasm: **(1)** MDM2 binds to p53, prevents p53 nuclear translocation and promotes p53 degradation. In addition, MDM4 can interact with MDM2 to enhance MDM2 stability. **(2)** MDM4 can bind to and sequester cytoplasmic p53s. **(3)** MDM2 phosphorylation by **Akt/PKB** induces MDM2 nuclear translocation. In the nucleus: **(4)**. Under basal cellular state, MDM2 binds to and ubiquitinate nuclear p53. Ubiquitinated p53s are transported out of the nucleus and undergo proteasomal degradation. **(5)** Under cellular stress (e.g., UV radiation or ribosomal stress), MDM2 is sequestered from p53 by binding to p19ARF [alternate reading frame (**ARF**)] and ribosomal protein (**RP**), which increases p53 stability. Nuclear p53 can then bind to and activate a number of stress response genes including *MDM2*.

on codon 72 has been shown to change MDM2 binding affinity to p53; e.g., p53-R72 has been shown to interact with MDM2 with higher affinity than its P72 polymorphic counterpart (33).

DBD mediates p53 binding to promoters of target genes in a sequence specific manner via p53 response element (RE) that is usually located upstream of the transcription start site (23). It has been generally accepted that p53 interacts with DNA as a tetramer. Tetramerization begins with dimerization of two p53 monomers that occurs co-translationally and is followed by the tetramerization of the two dimers (34). *In vitro* studies have revealed that p53 dimerization and its translocation into the nucleus is mediated by the nuclear localization signal (NLS; located in the linker region) (35). Nuclear localization function is regulated by the p53 posttranslational modification (PTM) and interacting partners (36). The lysine residues in NLS can be ubiquitinated by MDM2, and this ubiquitination prevents p53 nuclear translocation (36). These lysine residues are also important for p53 binding to the nuclear transport factor importin-α3, which promotes p53 translocation into the nucleus (35).

Tetramerization domain (TD) facilitates p53 oligomerization into transcriptionally active tetramer (37). In response to stress, p53 accumulates in the nucleus where it tetramerizes and regulates the expression of the stress response genes (36). Tetramerization conceals a leucine-rich region (amino acid residues 340-351) that acts as a nuclear export signal (NES). Exposure of the NES upon dissociation of the tetramer lead to p53 export from the nucleus (36).

The C-terminal regulatory domain (CTD) exists in an unfolded state. CTD also contains critical lysine residues that can be post-translationally modified via acetylation, methylation, ubiquitination, sumoylation, neddylation and phosphorylation (23). These PTMs provide complex and diverse ways to modulate p53 activities and allow proper regulation of a wide variety of genes downstream of p53.

1.1.4 Regulation of p53 Stability and Function

MDM2 is a major regulator of p53 stability in both the cytoplasm and the nucleus (**Figure 1-1B)** (38, 39). In the cytoplasm, **1)** MDM2 binding to TAD prevents p53 nuclear localization and promotes its degradation via ubiquitination on CTD (26, 39). Another member of the MDM2 family, MDM4, which does not ubiquitinate p53 can bind to MDM2, enhance its stability and

promote p53 degradation. **2)** MDM4/MDMX can also directly bind to p53 TAD and inhibit its translocation into the nucleus (17). **3)** The protein kinase B (PKB/Akt), which is often found overexpressed in human cancers phosphorylates MDM2 in the cytoplasm and induces MDM2 nuclear localization (40).

In the nucleus, **4)** under basal condition, ubiquitination of the nuclear p53 by MDM2 leads to the exposure of NES and subsequent translocation of p53 into the cytoplasm and its proteasomal degradation. **5)** Under cellular stress, the ribosomal protein (RP) and the tumor suppressor protein $p19^{ARF}$ (alternative reading frame), a cell cycle regulating protein can bind to and sequester MDM2 to inhibit ubiquitination of p53. Stabilized p53 activates the expression of target genes including MDM2 (41).

1.2 Mutant p53 and tumorigenesis

1.2.1 Gain of Function Mutant p53

TP53 is one of the, if not the most, frequently mutated gene in human cancers. The majority of these mutations are missense (a change in one DNA base pair that changes one single amino acid residue in the protein) in the DBD of the protein (**Figure 1-2A**). The six most frequent mutations [Arginine (R) 175, 248, 249, 273, 282 and glycine (G) 245] in the DBD are known as "hot spot" mutations and make up ~30% of all p53 mutations. Compared to the p53-null condition, these mutations are associated with escalated tumorigenesis and poor prognosis (42). Hotspot mutants not only lose p53-WT tumor suppressor function, but also gain new oncogenic function and therefore are known as gain of function (GOF) mutants (42).

GOF mutants are generally classified into two types: conformational mutants (R175, G245, R249, R282) and the contact mutants (R248, R273) (42). Both classes interfere with the ability of the protein to bind to DNA (**Figure 1-2B**), albeit by two different mechanisms. In conformational mutants p53 protein is misfolded; whereas in contact mutants, residues that directly interact with DNA are altered while the protein retains its normal/WT conformation. (**Figure 1-2B**) (42). The intrinsic differences between the two types of p53 mutants may cause a difference in their ability to affect p53 target gene expressions (43). For example, while both contact and conformational mutants are equally effective in increasing invasive capacity and contribute to oncogenesis by

A

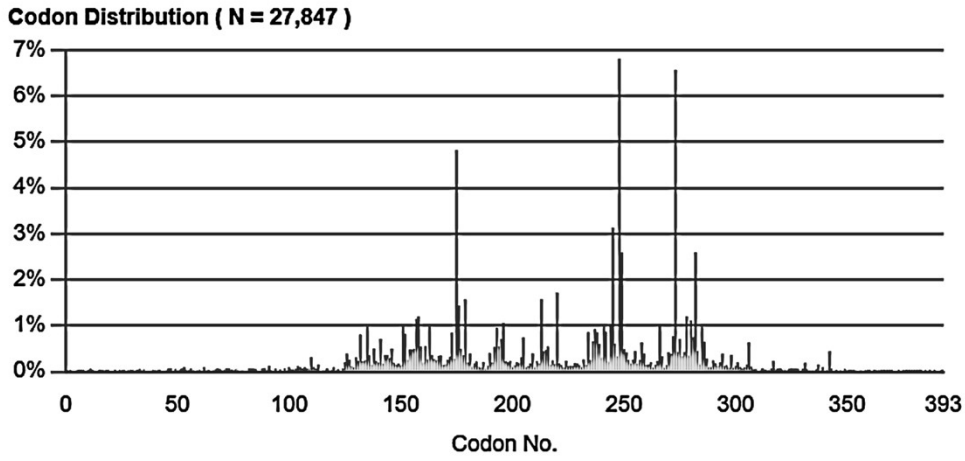

The *TP53* Database (R20, July 2019): https://tp53.isb-cgc.org

B

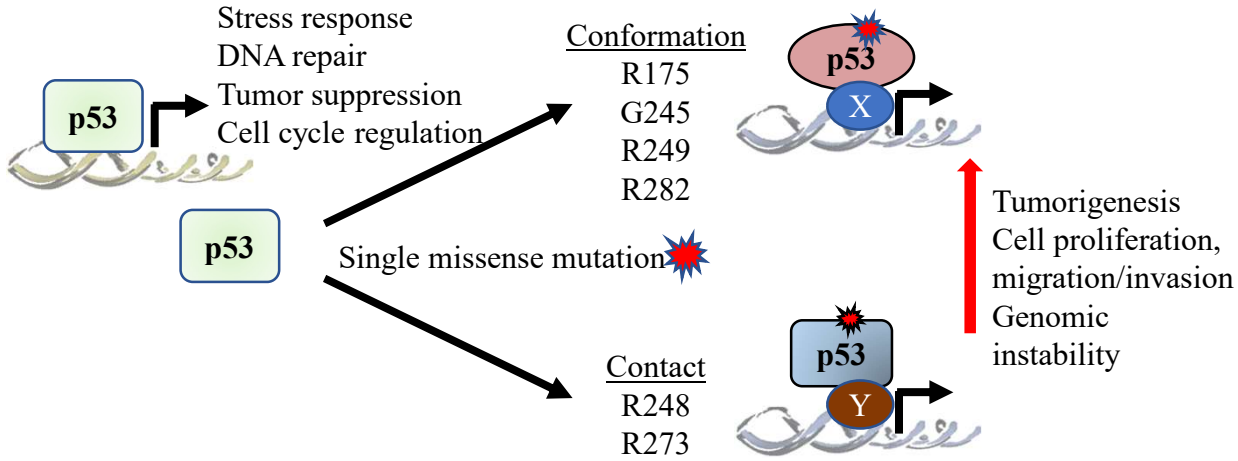

Figure 1-2. (A) Distribution and classification of hotspot p53 mutations. Majority of the mutations occur in the DNA-binding domain (aa. 94-292). The most frequent mutations are known as hotspot mutations and are classified into conformational/structural or contact mutants based on changes in conformation or the involvement of amino acids that directly interact with DNA. **(B) p53 target gene expression.** In non-transformed cells, p53-WT is activated in response to cellular stress, which in turn activates the expression of tumor suppressor genes that induce cell cycle arrest, DNA damage response machinery and apoptosis to maintain genomic stability and cellular homeostasis. In transformed cells expressing conformational (**R175, R245, R249, R282**) or contact (**R248, R273**) mutants, mutant p53 not only loses the ability to bind to p53-WT target genes but it gains novel interacting nuclear partners (depicted by **X** and **Y**) that enable it to induce activation of oncogenic targets and promote tumorigenesis/metastasis.

inducing CXC chemokines (CXCL5, CXCL8, CXCL12) (44). However, only p53 contact mutants, have been shown to increase cell motility, EMT, and activity of promigratory pathways by activating the extracellular human heat shock protein 90 alpha (eHsp90α) (45). Overall, both p53-WT and mutants' effects can be context-dependent and cell-type specific (16). In addition, other factors such as external stress and tumor microenvironment must also be considered when interpreting the GOF properties of mutant p53 (16). Mutant p53 oncogenic function can be activated by several mechanisms as discussed below.

1.2.2 Mutant p53 exerts dominant negative effect on p53-WT

In heterozygous cells expressing both p53-WT and mutant, mutant p53 can form heterotetramers with p53-WT and exert a dominant negative effect on p53-WT since the heterotetramer cannot bind to the p53-WT target genes.(46) For example, using mouse models of human R175H and R273H (mouse R172H and R270H, respectively), it has been demonstrated that homozygous p53-null ($p53^{-/-}$), heterozygous $p53^{R172H/+}$ and homozygous $p53^{R172H/R172H}$ mice suppressed p53-dependent apoptosis induced by irradiation (47). Also, $p53^{R172H/+}$ and $p53^{R270H/+}$ mice formed more tumors compared to $p53^{-/-}$ mice (47). These studies suggest that mutant p53 contributes to loss of tumor suppressor function of p53 by binding to and nullifying the activity of p53-WT.

1.2.3 Mutant p53 can alter activities of p53 regulators

Mutant p53s are often stabilized in cancer cells and are present at much higher levels (48, 49, 50). However, Similar to p53-WT, mutant p53 accumulates in the nucleus in response to stress signals and this accumulation is crucial for the oncogenic activities of GOF mutants (51). As discussed earlier, under basal cellular condition/absence of cellular stress, p53-WT is maintained at low level through its constitutive interaction with MDM2 and degradation. Under cellular stress, MDM2 is inactivated and p53 is stabilized (38). In contrast, mutant p53s are often stabilized in cancer cells and are present at much higher levels (48, 49, 50).

Studies have demonstrated that mutant p53 can bypass MDM2-mediated degradation via several mechanisms. Hotspot p53 mutants lose their abilities to bind to DNA and are unable to activate MDM2 expression. However, this does not explain the high level of p53 mutants present

in cancer cells since MDM2 expression is not mutually exclusive to p53 mutation status (49). Other transcriptional factors [such as human nuclear factor of activated T cells 1 (NFAT1) or interferon regulatory factor 8 (IRF8)] have been demonstrated to activate *MDM2* expression in a p53-independent manner (52, 53). These observations imply that p53 mutants use additional mechanisms to evade MDM2-mediated degradation (52, 53, 54). For example, it has been shown that mutant p53s (including R175H and R273H) interact with BAG2 [a member of the Bcl-2 associated BAG family of athanogenes (inhibitor of apoptosis)] prior to its translocation into the nucleus. This association inhibits mutant p53 interaction with MDM2 and its degradation (55). Additionally, transient co-transfections with the conformational mutant p53-R175H and MDM2 in H1299 cells have shown that MDM2-mediated degradation of mutant p53 occurs at a significantly lower efficiency compared to MDM2-mediated degradation of p53-WT.(56) Yet another mechanism for stability/activity of mutant p53 is its constitutive phosphorylation by ERK1/2 and activation of MAP kinase pathway (57). This phosphorylation event may act similarly to ATM-mediated phosphorylation of p53-WT, which decreases its interaction with MDM2 and its degradation (57). Overall, these observations suggest that p53-WT and mutant stability and activity are regulated by distinct mechanisms.

It is important to consider cellular contexts when studying mutant p53s. Tumors are typically heterogeneous and genetic background of each tumor, or even cell line, is complicated by differences in selective pressure and stochasticity of mutation (16). These factors further complicate the possibility of generalizing the effect and the downstream signaling of mutant p53 solely based on factors such as the kind of mutation or the type of cancer cells. As stated by Kastenhuber and Lowe in their 2017 review, "It seems naive to expect that oncogene activation in different tissues (for example, KRAS activation in colon, pancreas, and lung) would precipitate an identical p53 transcriptional response. Moreover, one would not presume a priori that the p53 output generated by DNA damage would exactly mirror the gene expression signature elicited by oncogene activation, even in a single cell type." (16). Despite the complexities discussed above, it is generally accepted that one major mechanism of mutant p53 oncogenic activation is by interacting with and altering the activities of transcriptional factors.

1.2.4 Mutant p53 and regulation of gene expression

Due to its inability to arrest cell cycle progression following DNA damage and/or to activate DNA repair or apoptosis, mutant p53 can induce genetic instability and unregulated cell proliferation (42, 58). p53 GOF mutants promote tumorigenesis by several non-mutually exclusive mechanisms. Mutant p53 can activate the epithelial-mesenchymal transition (EMT) by inducing the expression of EMT-associated factors (e.g., Slug, Twist1, ZEB) (59, 60, 61). Mutant p53 can also modulate cellular metabolism by upregulating glycolytic enzymes which contribute to the Warburg effect often observed in cancer patients (62). Upregulating multi-drug resistance 1 (*MDR1*) gene which leads to chemoresistance in patients is another activity of mutant p53 (63, 64). These functions are accomplished by binding of mutant p53 to oncogenic and/or tumor suppressor protein partners in a cell context dependent manner. One class of these binding partners are transcription factors including but not limited to p63, p73, Ets2, NF-Y, VDR, SREBPs, etc., which typically do not interact with p53-WT (42, 58). Mutant p53 interaction with these nuclear factors alters the transcription of their target genes. For example, in the murine pancreatic cancer cell line KPC, the oncogenic transcriptional factor NF-Y is inhibited by interaction with the p53 homologue and tumor suppressor p73 (65). Mutant p53 can bind to and sequester p73 from the NF-Y transcriptional complex, which then activates the expression of platelet-derived growth factor β (PDGF-β) (65). High expression of PDGF-β has been shown to correlate with worse disease-free survival in pancreatic cancer patients. Mutant p53 can also recruit NF-Y to activate the expression of other tumor promoting factors. In colorectal adenocarcinoma cell lines with mutant p53 expression, mutant p53 recruits NF-Y to ephrin (*EFN)B2* promoter region and induce EMT and chemoresistance via activation of JNK/c-JUN pathway (66). Genomic expression analysis has revealed the upregulation of mevalonate pathways by mutant p53 in breast adenocarcinoma cell lines by binding to sterol regulatory-element binding protein (SREBP) transcription factors. This correlated with the elevated sterol biosynthesis and tissue architecture disruption (67). Mutant p53 interaction with Ets2 transcription factor in mouse models of osteosarcoma and pancreatic ductal adenocarcinoma activated expression of oncogenic genes involved in lipid biosynthesis, nucleotide synthesis, increased cell proliferation, invasiveness and metastasis (68). Also, mutant p53 binding to the transcription regulator early growth response protein 1 (EGR1) has been shown to drive invasion in breast cancer cell lines in a MAPK/ERK

pathway dependent manner (69). Finally, we have recently identified the cell adhesion and signaling protein plakoglobin as a novel interacting partner of p53-WT and various mutants in cells and tissues of different origins (70, 71). Interestingly, our results have suggested that plakoglobin-mutant p53 interaction led to a partial restoration of mutant p53 tumor suppressor function *in vitro* by reducing cellular growth, colony formation, migration and invasion in these cells (70, 71, 72).

1.3 Plakoglobin and its role in tumorigenesis

1.3.1 Plakoglobin: role in cell adhesion

Plakoglobin is an 83 kDa protein that was initially identified as a component of the desmosomal plaque (73). Later studies showed that plakoglobin is also present in the adherens junction and being the only common component of both adhesive junctions, a major regulator of the cell adhesive properties (**Figure 1-3A)** (74). Both adherens junction and desmosomes are cadherin-based adhesive junctions. Cadherins are calcium-dependent cell adhesion proteins that initiate cell-cell contact between adjacent epithelial cells and are essential for the maintenance of integrity and function of epithelial tissues (75, 76, 77). Structurally, cadherins consist of three domains: an extracellular domain, which mediates homotypic or heterotypic contact with cadherin on the adjacent cell, a transmembrane domain that spans the plasma membrane and a cytoplasmic domain that interacts with the cytoplasmic proteins, which in turn, interact with cytoskeleton to stabilize the junction (77).

Adherens junctions are ubiquitously present in all tissues. At this junction, the extracellular domain of classical cadherins [E-cadherin (epithelial), N-cadherin (neural), P-cadherin (placental), VE-cadherin (vascular-endothelial), and OB-cadherin (osteoblastic)] interacts with the extracellular domain of the cadherin on the adjacent cell to mediate adhesion (**Figure 1-3A)** (75, 77)**.** Intracellularly, cadherins cytoplasmic domain bind to proteins known as catenins [α, β, γ (plakoglobin) and δ (p120)] (78, 79). δ (p120) Catenin binds to the juxtamembrane domain of cadherins and stabilizes the cadherin dimers.(78) β-Catenin or plakoglobin interact with the cytoplasmic tail of cadherin in a mutually exclusive manner and associate with α-catenin, which in turn interacts with actin filaments and links the cadherin-catenin complex to the cytoskeleton (**Figure 1-3A)** (77, 80).

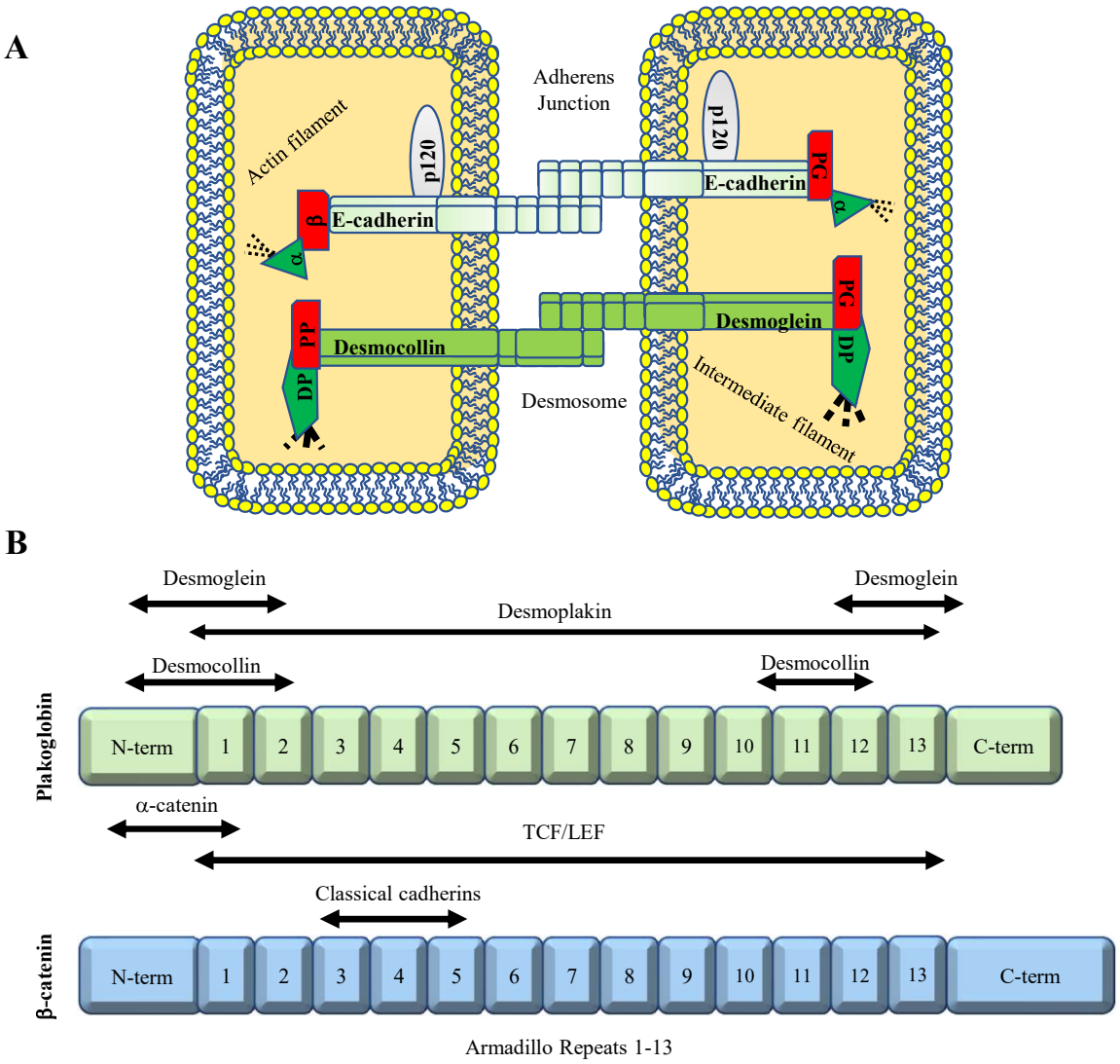

Figure 1-3. Cadherin mediated cell adhesion complexes; adherens junction and desmosomes.
A. Schematic diagram of adhesive junctions. Adherens Junction: the extracellular domains of classical cadherins such as E-cadherins interact with each other in the adjacent cells whereas their cytoplasmic domain interacts with p120 catenin (juxtamembrane) and β-catenin or γ-catenin/plakoglobin (cytoplasmic tail, mutually exclusive). β-catenin and plakoglobin, in turn, interact with α-catenin ,an actin binding protein that associates the cadherin-catenin complex to the actin microfilaments and stabilizes the adherens junction at the membrane. Desmosome: the extracellular domain of desmosomal cadherins (desmocollin and desmoglein) associates with the corresponding domain in the adjacent cell, while their cytoplasmic tails interact with plakophilin or plakoglobin and desmoplakin, which in turn connects to the intermediate filaments.
B. Schematic diagram of plakoglobin and β-catenin domain structure. Plakoglobin is a paralogue of β-catenin and a member of the Armadillo protein family characterized by the presence of 13 armadillo repeats flanked by a N-terminus and C-terminus. Armadillo repeats are protein-protein interaction domains that mediate plakoglobin and β-catenin interactions with a number of common and/or unique intracellular partners that regulate adhesive vs. signaling function of these proteins. The N-terminus of both proteins interacts with α-catenin to mediate cell-cell adhesion and their C-terminus is the transactivation domain and essential for their transcriptional activity. α, α-catenin ; β, β-catenin ; PG, plakoglobin/γ-catenin; DP, desmoplakin; PP, plakophilin.

Desmosomes are adhesive structures that are primarily present in tissues that endure significant mechanical stress and require stronger adhesion such as epithelial tissues, cardiac muscle and meninges.(81) Similar to adherens junction, the extracellular domain of desmosomal cadherins (desmogleins and desmocollins) interact with the corresponding domain of desmosomal cadherins on the adjacent cells. (**Figure 1-3A)** (81). The cytoplasmic domains of desmosomal cadherins bind to cytoplasmic proteins plakoglobin, plakophilins, and desmoplakins forming the desmosomal plaque, which in turn, associates with intermediate filaments (**Figure 1-3A)** (81, 82). Intermediate filaments are tissue specific and different types are expressed in different tissues such as keratins (epithelia), desmin (muscle), vimentin (mesenchymal), etc. (82).

Plakoglobin expression is essential for formation of desmosomes and important for the initiation of adherens junction formation where it interacts with classic cadherin in a mutually exclusive manner with β-catenin (74, 83, 84). Plakoglobin and β-catenin are paralogues and belong to the Armadillo family of proteins with similar dual adhesive and signaling functions (85). The two proteins have similar structure and interact with many common intracellular protein partners to mediate cell adhesion or participate in signaling pathways that regulate cell proliferation, growth and tumorigenesis (**Figure 1-3B**) (85).

β-Catenin has well studied oncogenic signaling function via its role as the terminal cytoplasmic component of the Wnt pathway (86). Wnt is a developmentally regulated pathway that was initially identified in *Drosophila* (87). Activation of Wnt pathway during development is essential for body axis patterning, cell fate determination, proliferation and migration.(85) In the absence of Wnt ligand, the cadherin-independent cytoplasmic pool of β-catenin is degraded. When activated by Wnt ligand, β-catenin degradation is inhibited, excess β-catenin accumulate in the cytoplasm and can translocate into the nucleus (86). In the nucleus, β-catenin binds to TCF/LEF transcription factor and activate transcription of Wnt target genes (86). Products of the Wnt signaling pathway are essential in embryonic development, but activation of the pathway in adult cells induces tumorigenic events such as cell proliferation and cell migration and cancer stem cell survival and function (86). While plakoglobin also interacts with the components of the Wnt

pathway, it generally acts as a tumor suppressor (85). The rest of this thesis will focus on plakoglobin and its role(s) in tumorigenesis and potential mechanisms underlying its tumor suppressor function.

1.3.2 Clinical significance of plakoglobin in tumors

Numerous studies have associated reduced plakoglobin expression with adverse patient outcomes (85, 88, 89, 90, 91, 92, 93, 94). Plakoglobin deficiency is associated with poor prognosis in various tumor such as neuroblastoma, non-small cell lung carcinoma, squamous cell, breast and bladder carcinomas etc. (88, 91, 92). Reduced plakoglobin, but not α-catenin or β-catenin, was associated with higher lymph node metastasis and poor survival in oral squamous cell carcinoma (89). In human bladder tumors, reduced level of plakoglobin was associated with shorter overall survival while its cytoplasmic localization was associated with lymph node metastasis (90). It has also been shown that reduced plakoglobin level is associated with increased metastatic potentials in soft tissue sarcomas (93).

In contrast to solid tumors, several studies have suggested a tumor promoting role for plakoglobin in leukemia and lymphomas. Abnormal expression of both plakoglobin and β-catenin has been reported in leukemia (95, 96). Overexpression of plakoglobin in acute myeloid leukemia (AML) patients is frequently observed and is associated with poor prognosis (97). Plakoglobin knockdown from the human acute monocytic leukemia cell line THP-1 induced growth inhibition and increased apoptosis, concurrent with reduced level of nuclear β-catenin (98). These observations suggested that plakoglobin does not directly participate in the pathogenesis in AML, instead, plakoglobin overexpression may promote β-catenin nuclear translocation and activate Wnt signaling pathway, a pathway that is involved in hematopoiesis. This is consistent with Niu *et al.* observations, which showed plakoglobin downregulation resulted in reduced nuclear β-catenin level in chronic myeloid leukemia (CML) (99). Other studies have reported a β-catenin-independent role of plakoglobin in leukemic cancers. Using mouse models expressing BCR-ABL, which is associated with B-ALL or CML, it has been shown that plakoglobin is essential for the initiation and maintenance of B-ALL, while β-catenin may potentially suppress B-ALL and promote CML in hematopoietic stem cells (100). Interestingly, Niu *et al.* also observed higher plakoglobin expression in BCR-ABL-positive CML cell line compared to the BCR-ABL negative

CML cell line, which suggested that BCR-ABL may play an important role in facilitating plakoglobin function in non-solid tumors (99). Lastly, exogenous overexpression of plakoglobin in myeloid leukemia cell lines resulted in the stabilization and nuclear localization of β-catenin, as well as increased TCF-dependent transcription activities (97). Similarly, plakoglobin siRNA treatment in CML led to decreased nuclear β-catenin, increased cytoplasmic β-catenin, and reduced β-catenin target gene expression (97). This study suggests that overexpression of plakoglobin may indirectly contribute to oncogenesis via displacement of junctional β-catenin, and promotion of its stabilization and nuclear localization.

Aside from reports in non-solid tumors, high plakoglobin expressions in circulating tumor cells (CTCs) were also observed and were associated with increased metastasis and worse prognosis in patients (101, 102). This is consistent with the observation that CTCs have better odds of survival and increased metastatic potential as CTC clusters than as single CTCs and it is supported by the presence of multiple homotypic and heterotypic cell-cell adhesion molecules and tight junction proteins (103, 104). Presence of plakoglobin may promote survival by promoting cell-cell adhesion within the cluster. However, it is important to note that some of these studies did not investigate the expression and localization of other cell adhesion proteins including cadherins, as well as α- and β-catenin, which are essential for holding cells in CTC clusters. This suggest that plakoglobin, along with other cell-cell adhesion molecules, may increase cell-cell adhesion in CTC clusters, consequently, confers a survival advantage for CTCs, and increase their metastatic potential.

1.3.3 Potential Mechanisms of Plakoglobin Tumor Suppressor Activity

While many clinical and experimental studies support a tumor suppressor function for plakoglobin but the mechanism(s) by which it acts as a tumor suppressor was until recently unclear. To gain insight into how plakoglobin act as a tumor suppressor, our laboratory has developed several experimental models of squamous cell, breast, lung and ovarian carcinoma cell lines to investigate potential mechanism(s) of plakoglobin tumor suppressor function (70, 71, 72, 105, 106, 107, 108, 109, 110, 111). These studies have provided strong evidence and have led us to posit a model that supports at least four potential mechanisms by which plakoglobin suppresses tumorigenicity and metastasis (**Figure 1-4). 1)** Plakoglobin is a major regulator of cell adhesive

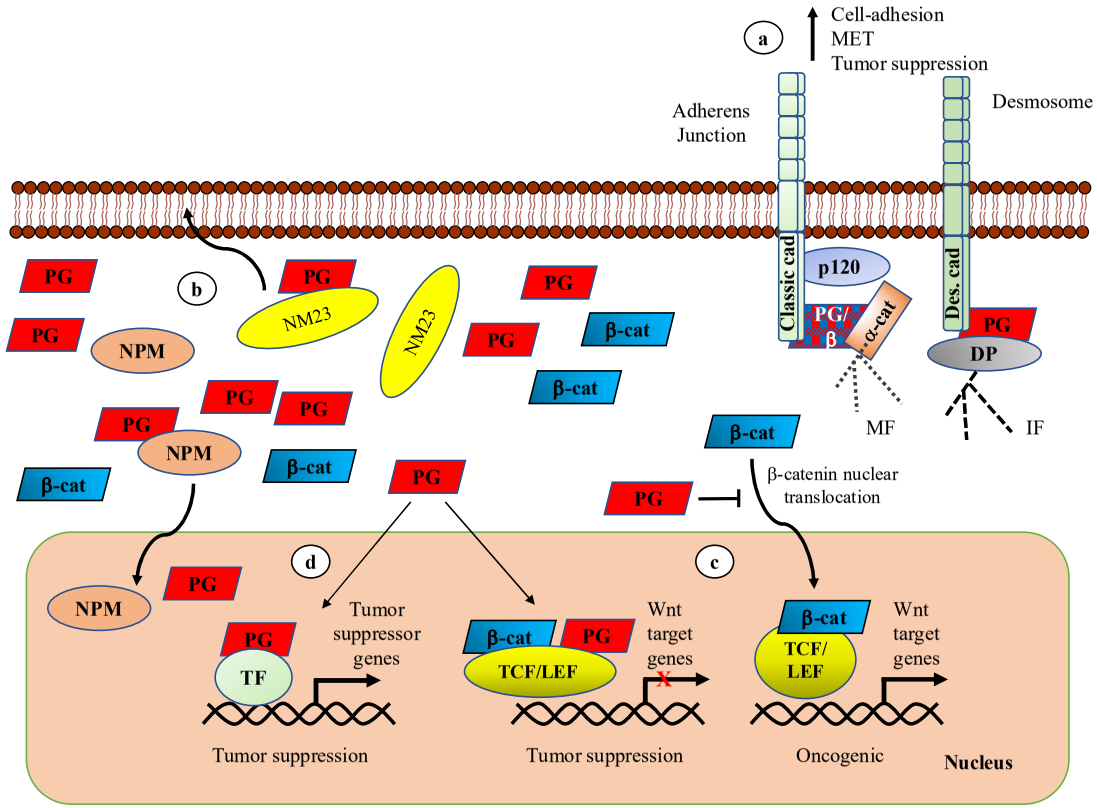

Figure 1-4. Potential mechanisms of plakoglobin tumor suppressor activity. Four potential mechanisms may regulate plakoglobin tumor suppressor activity. **a.** Plakoglobin (**PG**) mediates extensive cell-cell adhesion by participating in adherens junction and desmosome formation, which is essential for the maintenance of epithelial integrity and function. **b.** Plakoglobin interacts with and regulates the subcellular localization of intracellular protein partners (e.g.,**Nm-23 or NPM**) that participate in growth regulatory pathways, promote tumor suppression, and inhibit tumorigenesis and metastasis. **c.** Plakoglobin modulate the oncogenic potential of β-catenin (**β-cat**) and activation of the Wnt signaling pathway. Excess cytoplasmic β-catenin can translocate to the nucleus, where it binds to **TCF/LEF** transcription factor and activate downstream Wnt/β-catenin target genes associated with cell proliferation and cell motility. Plakoglobin can decrease β-catenin nuclear localization and inhibit Wnt/β-catenin target genes expression. **d.** Plakoglobin can interact with transcription factors (**TF**) and regulate their target gene expression involved in tumorigenesis and metastasis. Des.cad, desmosomal cadherin; Classic cad, classical cadherin; α, α-catenin ; β, β-catenin ; PG, plakoglobin; DP, desmoplakin; TCF/LEF, T cell factor/lymphoid enhancer factor; NM23, non-metastatic 23; NPM, nucleophosmin; TF, transcription factor; MF, microfilament; IF, intermediate filament; MET, mesenchymal-epithelial transition.

properties and participate in the formation of adhesive junctions (adherens junction and desmosomes) to promote extensive cell-cell adhesion, which holds cells together, induces contact inhibition of growth and is essential for the maintenance of integrity and function of epithelial monolayer. During tumorigenesis, loss of cell-cell adhesion and contact inhibition of growth leads to a more mesenchymal phenotype associated with unregulated cell proliferation, increased motility, and migratory phenotype (**Figure 1-4a)**. **2)** Plakoglobin can interact with and alter the subcellular distribution of intracellular protein partners involved in signaling pathways that regulate tumorigenesis (**Figure 1-4b)**.**3)** Plakoglobin can modulate the subcellular distribution of β-catenin, its oncogenic function, and activation of Wnt target genes. (**Figure 1-4c)**. Finally, plakoglobin can interact with transcription factors and regulate the expression of their target genes involved in growth regulatory pathways **(Figure 1-4d)**. The next section will be focused on the work form our group has provided evidence in support of the above model.

1.3.4 Plakoglobin promotes cell-cell adhesion and mesenchymal to epithelial transition (MET, Figure 1-4a)

The earliest evidence for the potential tumor suppressor function of plakoglobin was the association of its loss of heterozygosity with a predisposition to familial breast and ovarian cancers (112). Following this report, Simcha *et al.* showed that plakoglobin overexpression in SV40-transformed 3T3 cells suppressed the tumorigenicity of these cells in syngeneic mice and furthermore, this effect was augmented when N-cadherin was co-transfected (113). The authors also reported that the expression of plakoglobin in cadherin, α-, β-catenin and plakoglobin-deficient renal carcinoma cells reduced tumor formation in a dose-dependent manner in nude mice. More importantly, in these transfectants, plakoglobin was diffusely distributed in the cytoplasm and nucleus (113). Consistent with these observations, we have shown that generally ~ 20-30% of plakoglobin is present in the cytoplasm (105). Furthermore, the expression of either plakoglobin or E-cadherin in the plakoglobin and E-cadherin deficient and N-cadherin-expressing human tongue squamous carcinoma cells SCC9 induced a mesenchymal to epithelial transition (MET) phenotype, along with decreased cell proliferation, increased cell-cell adhesion and desmosome formation (105). This phenotypic transition was concurrent with decreased level of soluble/cytoplasmic β-catenin.(105) Interestingly and in agreement with Simcha *et al*, plakoglobin expression in SCC9 cells led to stabilization and increased level of N-cadherin (113). This

suggested that in the absence of E-cadherin, plakoglobin may use N-cadherin to form junctions and induce an epidermoid phenotype. Similar results were obtained with breast, lung, and ovarian carcinoma cell lines **(Figure 1-4a)** (107, 111).

1.3.5 Plakoglobin interacts with other growth regulating proteins, change their cellular distribution and growth regulating activities (Figure 1-4b)

In addition to regulation of β-catenin subcellular localization and oncogenic activity, plakoglobin has been shown to interact with and affect the level, subcellular localization, and function of other growth regulating cellular partners (**Figure 1-4b**). Comparison of the proteomic profiles of plakoglobin deficient carcinoma cells and their plakoglobin expressing transfectants by our group identified a number of differentially expressed proteins and we further characterized two of them (71, 108). The following section is a brief summary of these studies.

The nucleocytoplasmic protein nucleophosmin (NPM) is a multifunctional protein with dual oncogenic and tumor suppressing function that shuttles between cytoplasm and nucleus (114). The function of NPM is determined by its subcellular localization; the cytoplasmic NPM acts as a tumor promoter, whereas the nuclear NPM promotes tumor suppression.[(115), (116)] NPM acts as a tumor suppressor by its role in stabilizing p53 (117). Nuclear NPM promotes ARF nuclear localization and ARF interaction with MDM2 and this interaction sequesters MDM2 from p53 and promotes p53 stabilization (118). In contrast, cytoplasmic NPM is generally considered oncogenic by conferring a survival and proliferative advantage. Our group has shown that plakoglobin interacts with and promotes nuclear localization of NPM (109). Plakoglobin expression in the plakoglobin-deficient MDA-MB-231 invasive breast carcinoma cell line resulted in increased nuclear NPM, which was concurrent with decreased cell growth, cell migration and invasion. In support of the association between plakoglobin and NPM observed in *in vitro* experiments, examination of the biopsies from normal breast tissue demonstrated primarily membranous plakoglobin and primarily nuclear NPM, whereas breast tumors with reduced /no plakoglobin expression showed decreased/no nuclear NPM distribution (109).

The non-metastatic 23 (NM23 H1/H2) is the first identified anti-metastasis protein (119, 120). Our proteomic analysis identified Nm23-H2 as differentially upregulated in plakoglobin expressing transfectants relative to the plakoglobin-deficient parental SCC9 cells (108). Further

studies demonstrated that plakoglobin interacted with and stabilized the cytoskeleton-associated pool of Nm23-H2 at the membrane and this interaction required the α-catenin binding domain of plakoglobin (108). Overall, these studies further suggested that increased level and stabilization of NM23-H2 may be a potential mechanism by which plakoglobin functions as a tumor/metastasis suppressor **(Figure 1-4b)** (108).

1.3.6 Plakoglobin modulates β-catenin signaling and oncogenic potential (Figure 1-4c)

The membrane-associated pool of β-catenin and plakoglobin interacts with cadherins and forms adhesive junctions, whereas their cytoplasmic pool can interact with an array of intracellular partners and participate in cellular signaling (86). Due to their structural similarities, plakoglobin and β-catenin share many common interacting partners and as such, they can play independent and interdependent roles in signaling pathways (85).

As a homolog of β-catenin, the role of plakoglobin in the Wnt signaling pathway has been investigated. Multiple studies have demonstrated that plakoglobin can alter the signaling activities of β-catenin. Overexpression of plakoglobin in the plakoglobin-deficient SCC9 cells increased cell proliferation and foci formation and decreased apoptosis (106). These observations were correlated with the increased expression of the anti-apoptotic protein BCL-2 in these cells (106). To determine the underlying mechanism for induction of BCL-2 expression, a subsequent study was done using the same cell line. SCC9 cells were transfected with either plakoglobin cDNA fused with nuclear export signal (NES) to express plakoglobin exclusively in the cytoplasm (PG-NES) or plakoglobin cDNA fused with nuclear localization signal (NLS) to express plakoglobin exclusively in the nucleus (PG-NLS) (107). The results of this study revealed that expression of exclusively cytoplasmic plakoglobin (PG-NES) resulted in β-catenin nuclear distribution, increased β-catenin/TCF transcriptional activities, and BCL2 expression. In contrast, PG-NLS expression decreased nuclear β-catenin, TCF/β-catenin transcriptional activity and BCL-2 expression (107). Overexpression of β-catenin alone in SCC9 further confirmed that nuclear β-catenin induced BCL-2 expression whereas SCC9 cells expressing mutant plakoglobin proteins unable to interact with N-cadherin and α-catenin, had noticeably lower Bcl-2 levels (107). Overall, these studies suggested that plakoglobin can modulate the oncogenic potential of β-catenin by

regulating promoting its degradation/subcellular distribution and by decreasing TCF/β-catenin signaling in the nucleus (**Figure 1-4c**).

1.3.7 Plakoglobin regulates gene expression by interaction with p53

Studies from various groups have demonstrated that plakoglobin can directly or indirectly alter the activity of transcription factors. Plakoglobin was shown to sequester exogenously expressed TCF in the cytoplasm and inhibit Wnt target gene activation (121). Plakoglobin also interacts with TCF in the nucleus and inhibits TCF/β-catenin target gene activation (**Figure 1-4c**). The SOX4 transcription factor enhances β-catenin signaling. It has been shown that plakoglobin interacts with SOX4 in the cytoplasm, inhibit its nuclear translocation and activation of β-catenin signaling (122). Recently, our group identified plakoglobin as a novel p53 interacting protein.(70, 71, 72) Comparison of transcriptome profiles of plakoglobin deficient and their plakoglobin expressing transfectants identified a number of differentially regulated p53 target genes in plakoglobin expressing cells, including tumor/metastasis suppressors *NME1* (NM23-H1*)* and *SFN (*stratifin*,* 14-3-3 σ) and tumor promoter *SATB1* (71). Subsequent studies showed plakoglobin interacted with p53 and together they induced/upregulated *NME1* and *SFN* and downregulated *SATB1* (71, 108, 110). Work from other groups further confirmed these observations. Using the p53-null and plakoglobin-deficient H1299 non-small cell lung carcinoma (NSCLC) cells, plakoglobin was shown to activate the expression of promyelocytic leukemia (PML) and hepatocyte growth factor activator inhibitor type I (HAI-I) in a p53-dependent manner (123). Plakoglobin expression in H1299 cells with either WT-p53 or mutant p53 regulated WT-p53 target gene promoter (70, 71, 72, 123). Taken together, the association of plakoglobin with transcription factors including p53 provides another potential mechanism for its tumor suppressor function (**Figure 1-4d**). Intriguingly, work from our group showed that plakoglobin interaction with different mutant p53 restores their *in vitro* tumor suppressor activity (70, 71, 72). Co-immunoprecipitation and immunoblotting experiments using various cell lines demonstrated that plakoglobin interaction with p53 (WT or mutant) is not cell-line/tissue specific **(Figure 1-4d)** (71).

1.3.8 Identification of plakoglobin-p53 interacting domains

To identify p53 and plakoglobin interacting domains involved in their association, constructs encoding different fragments of p53 (N-terminal, DBD, C-terminal) and deletions of

plakoglobin (ΔN, ΔArm, ΔC) were expressed in various combinations in H1299 cells (70). These studies revealed that the C-terminus of plakoglobin and the DNA-binding domain of p53 are critical in p53-plakoglobin interaction, and that this interaction is important in the synergistic decrease in cellular invasion and migration in H1299 cells co-expressing plakoglobin and p53-WT (70). Overall, the results of the aforementioned studies have provided the basis for this thesis, which specifically examines the effect of plakoglobin on restoration of tumor suppressor activity of conformational/structural vs. contact p53 GOF mutant.

1.4 Rationale and hypothesis

p53 is mutated in over 50% of all cancers and the majority of metastatic tumors (124). Apart from the hereditary cases. p53 mutations generally occur when adenomas progress to carcinomas (125). In addition to tumorigenesis/metastasis, p53 mutations also promote drug resistance and interfere with therapies targeting many signaling pathways (126, 127, 128).

Studies have demonstrated that the functional consequences of p53 mutation is both mutant and cell context dependent. Further insights into mechanisms and signaling pathways by which mutant p53 drives tumorigenesis/metastasis is essential for the development of effective cancer therapies. In this thesis, my hypothesis is "plakoglobin affects conformational and contact mutants similarly to restore their tumor suppressor activity and this occurs by restoration of p53-WT regulated target gene expression via similar signaling mechanisms.". To validate this possibility, I have investigated how plakoglobin expression affects the tumorigenic properties of conformation vs. contact mutants under identical genetic background in order to avoid confounding factors brought on by cellular context. The promise of plakoglobin's ability to bind various p53 mutants and potentially restore their tumor suppressor function *in vitro* provides important insights for development of plakoglobin targeted therapeutics for various cancers.

CHAPTER 2: DIFFERENTIAL EFFECT OF PLAKOGLOBIN ON RESTORING THE TUMOR SUPPRESSOR ACTIVITIES OF CONTACT VS. CONFORMATIONAL P53 MUTANTS

2.1 INTRODUCTION

TP53 encodes a transcription factor and tumor suppressor protein (p53) that plays essential roles in the maintenance of genome integrity, cell cycle progression, DNA damage repair, apoptosis, etc. (42, 129, 130). Inactivation of p53 function contributes to tumor development and metastasis. p53 is mutated in 50% of cancers whereas, in the other 50%, mutations in other components of the p53 pathway account for its functional inactivation (131, 132). p53 mutants often lose the tumor suppressor function of the wild-type p53 protein (p53-WT), and/or gain new oncogenic function (gain-of-function; GOF) that promotes tumorigenesis (15, 125, 133, 134, 135, 136, 137). The majority of p53 mutations are missense and in the DNA binding domain (DBD) (124, 138). The six most frequently occurring DBD mutations are known as the "hot spot" and account for ~30% of p53 mutations (124, 127, 133). These mutants can be classified into two categories: conformational/structural and contact (16, 17, 42, 124, 139). While both categories are compromised in their ability to bind to p53-WT target DNA sites, conformational mutants (R175H, G245S, R249S, and R282H) do so by disrupting the conformation and folding of the p53 protein whereas contact mutants (R248W, R248Q, and R273H) do so by affecting the amino acid residues that are directly involved in p53-WT DNA binding while maintaining a p53-WT-like structure (16, 17, 42, 124, 139, 140).

As the central player in managing the cellular response to environmental stress signals, p53 levels and functions are tightly controlled. The most important regulator of p53 function is the E3-ubiquitin ligase MDM2 (mouse double minute 2), which targets p53 protein for degradation, or interacts with and sequesters p53 from the transcriptional machinery (38, 39, 141, 142, 143). GOF mutants often bypass MDM2 and p53 regulatory mechanisms, gain stability and activate oncogenic gene expression and pathways (125, 134, 144, 145, 146, 147). In addition to ubiquitination, p53 stability and function is regulated by other post-translational modifications such as phosphorylation, acetylation, sumoylation, methylation, and interactions with other proteins. We recently identified plakoglobin as a p53 interacting protein partner (148, 149).

Plakoglobin (PG, γ-catenin) is a dual cell-cell adhesion and signaling protein and a paralog of β-catenin (150). These proteins interact with cadherins at the membrane to mediate cell-cell adhesion and associate with an array of intracellular proteins to participate in signaling pathways (85, 94). In contrast to the well-known oncogenic function of β-catenin via its interaction with

TCF/LEF and activation of the Wnt signaling pathway (151, 152, 153), plakoglobin generally acts as a tumor/metastasis suppressor (85, 105, 113, 123, 154, 155, 156). We have shown that one mechanism by which plakoglobin acts as a tumor suppressor is via its interaction with p53 (70, 71, 72, 85, 94).

We previously demonstrated plakoglobin interaction with endogenously expressed WT or various p53 mutants (e.g., R280K, R273H, S241F, S215R) in cell lines of different tissue origins and genetic backgrounds (70, 71, 72, 110, 111). These studies showed for the first time, p53-plakoglobin interactions and the consequences of this association on p53 function. Herein, we specifically compared the effects of plakoglobin expression on exogenously expressed contact $p53^{R273H}$ and conformational $p53^{R175H}$ mutants in the same genetic background. We have used the p53-null and plakoglobin-deficient H1299 non-small cell lung carcinoma cell line (70), which has been used routinely to assess the function of exogenously expressed WT and mutant p53 proteins under the same genetic background. To the best of our knowledge, H1299 is the only available plakoglobin-deficient and p53 null cell line that is uniquely suited for this study. We show for the first time that plakoglobin differentially affected the oncogenic properties of contact $p53^{R273H}$ and conformational $p53^{R175H}$ mutants. We found that plakoglobin co-expression led to a stronger inhibition of the oncogenic properties of $p53^{R175H}$ transfectants relative to that of the $p53^{R273H}$ transfectants. Our findings suggest that plakoglobin interaction with p53 conformational mutants may have the potential to be exploited for the development of effective therapeutic strategies for tumors expressing this type of p53 mutant.

2.2 MATERIALS AND METHODS

2.2.1 Cell lines and culture conditions

All tissue culture reagents were purchased from Gibco unless otherwise stated. H1299, the non-small cell lung carcinoma cell line has been previously described (70). H1299 cells and its transfectants were maintained in minimum essential medium (MEM) supplemented with 10% fetal bovine serum (HyClone Laboratories, USA), 1% penicillin-streptomycin and 5 μg/mL kanamycin (complete MEM, CMEM). SKOV-3 ovarian carcinoma cell line was purchased from American Type Culture Collection (ATCC) and cultured in dulbecco's modified eagle medium:

F12 medium (DMEM/F12, 1:1) supplemented with 10% fetal bovine serum, 1% penicillin-streptomycin and 5 μg/mL kanamycin.

2.2.2 Plasmid construction and transfection

HA-tagged p53, pcDNA3-plakoglobin-FLAG and $p53^{R175H}$ (p53 in which arginine 175 is replaced with histidine) expression constructs and their respective H1299 transfectants have been described previously (70, 72, 107, 157). The pCMV-Neo-Bam-$p53^{R273H}$ (p53 in which arginine 273 is replaced with histidine) plasmid was purchased from Addgene (USA).

$p53^{R273H}$ transfectants were generated using the jetOPTIMUS® (Polyplus, France) DNA transfection reagent following the manufacturer's protocol. Cells were transfected with either 5 μg of pCMV-$p53^{R273H}$ (hereafter H1299-p53-273) alone or with 10 μg of pcDNA3-plakoglobin plasmids (H1299-PG-p53-273). Stable cell lines were selected by supplementing CMEM with 800 μg/mL G418 (p53-273 transfectants) or 800 μg/mL G418 and 600 μg/mL hygromycin (PG-p53-273 transfectants) 48 hours post-transfection. Stable transfectants were maintained in 400 μg/mL G418 (H1299-p53-273) or 400 μg/mL G418 and 400 μg/mL hygromycin (H1299-PG-p53-R273H). p53 and plakoglobin expression were verified using immunofluorescence (not shown) and immunoblot assays. All experiments were carried out with stable transfectants unless indicated otherwise.

2.2.3 Cell extraction and immunoblotting

Equal amounts of total cellular proteins from 100 mm cultures were processed for extraction with RIPA lysis buffer (150 mM NaCl, 50 mM Tris-HCl pH 7.4, 1% NP-40, 0.25% sodium deoxycholate, 1 mM EDTA, 1 mM PMSF, 1 mM NaF, 1 mM Na3VO4, and Roche protease inhibitor cocktail, Sigma, Canada) and resolved with SDS-PAGE, transferred to nitrocellulose membrane and processed for immunoblotting using primary and secondary antibodies **(Table 2-1)**. Blots were developed using LICOR IR fluorescent dyes, scanned, and protein bands quantitated using the NIH ImageJ software. Protein levels were normalized to internal controls (tubulin/actin or lamin) in the same cell line.

2.2.4 Immunoprecipitation

Confluent 100 mm culture dishes were extracted with 1 mL RIPA buffer as described above. Cells were removed from the plates and centrifuged at 48,000 xg for 10 minutes. The resulting supernatant was divided into equal aliquots and processed for immunoprecipitation. Duplicate aliquots were incubated with 50 μL protein G (Pierce, Canada) and anti-p53 or anti-plakoglobin antibodies, at concentrations indicated in **Table 2-1,** and incubated overnight on a rocker-rotator at 4°C. To ensure complete depletion, samples were centrifuged briefly and the resulting supernatants were processed for another round of immunoprecipitation for 3 hours. Beads from the two immunoprecipitations were combined, washed three times with RIPA buffer and immune complexes eluted in hot 4X-SDS sample buffer. Equivalent amounts of total cellular proteins immunoprecipitated from each cell line were resolved on SDS polyacrylamide gels and processed for immunoblot as described above.

2.2.5 Preparation and purification of GST-plakoglobin

A construct encoding pGEX-TEV-PG was kindly provided by Dr. William Weis (158). *Escherichia coli* DH5α cells were transformed by pGEX-TEV-PG constructs to express PG-GST. Cells were grown in Luria-Bertani broth at 37°C to an A_{600} of 0.6–0.8 and then induced with 0.5 mM IPTG (isopropyl-β-D-1-thiogalactopyranoside, Thermo Fisher, Canada). Cultures were grown for an additional 6 hours at 30°C, harvested by centrifugation at 4,000 x g at 4°C for 12 min and the supernatants were discarded. Pellets were resuspended in 6 mL of cold bacterial lysis buffer (500 mM NaCl, 0.5% NP-40, 50 mM Tris-HCl pH 7.6, 5 mM EDTA, 5 mM EGTA, 1 mg/mL lysozyme, 10 mM DTT, 2.5 U/mL DNase, 1 mM PMSF and an EDTA-free protease inhibitor cocktail tablet) and lysed via sonication. Lysates were centrifuged at 10,000 x g for 25 min at 4°C and the supernatants were divided into 1 mL aliquots, snap frozen and stored at -80°C.

2.2.6 GST pull-down assay

A one mL aliquot of PG-GST bacterial lysate was incubated with 150 μL of glutathione sepharose beads (GE Life Sciences) on a rocker-rotator at 4°C for 6 hours. Beads were centrifuged at 21,000 x g for 1 min and supernatants were aspirated. Beads were washed 3x using cold KCl-PBS (0.137 M NaCl, 0.0027 M KCl, 0.01 M Na_2HPO4, 0.0018 M KH_2PO_4) and stored in KCl-PBS at 4°C.

Cells from 100 mm cultures of H1299 and H1299-p53-(WT, R175H, R273H) transfectants were extracted in 750 µL RIPA lysis buffer for 20 min on a rocker-rotator at 4°C. The lysates were centrifuged at 48,000 x g for 10 min at 4°C and supernatants were removed. For pull down assays, 600 µL of cell lysates were mixed with 50 µL PG-GST or GST (control) beads and incubated on a rocker rotator for 4-6 hours at 4°C. The beads were washed 3x with RIPA lysis buffer, eluted with 4x SDS sample buffer and processed for immunoblot using p53 and plakoglobin antibodies.

2.2.7 Subcellular fractionation

Cell pellets from 100 mm cultures were extracted with NE-PER™ Nuclear and Cytoplasmic Extraction Reagents (Thermo Scientific) according to the manufacturer's protocol. Unless otherwise stated, cytoplasmic and nuclear extracts of equal cell numbers were resolved by SDS-PAGE and processed for immunoblot (71, 72). The purities of cytoplasmic and nuclear extracts were verified by immunoblotting with tubulin and nuclear lamin antibodies.

2.2.8 *In vitro* soft agar colony formation assay

Cultures were seeded at 7,500 cells in 35 mm culture plates containing 0.6% base agar and 0.35% top agar (Noble Agar, Thermo Scientific) in CMEM. Plates were incubated at 37°C, 5% CO_2 for two weeks and supplemented with 0.3 mL CMEM every three days. The colonies were fixed and stained with a solution containing 0.05% w/v crystal violet, 1% formaldehyde and 1% methanol in PBS for 20 minutes, destained in water overnight at room temperature and colonies counted under a dissecting microscope. Colony formation results are presented as means ± SD in histograms.

2.2.9 *In vitro* migration and invasion assays

Migration and invasion assays were performed in triplicates using transwell insert (Fisher Scientific) For cell migration assays, 2×10^5 cells were resuspended in 500 µL serum-free media and plated in the upper chamber of transwell inserts (3µm pore, 6.5mm diameter; Corning, Life Sciences). Normal media containing 10% FBS was added to the lower chamber. Cultures were incubated at 37°C in 5% CO_2 for 24 hours to allow cell migration. Inserts were transferred into new dishes and rinsed with PBS to remove un-attached cells. Inserts were stained using NovaUltra™ Hema-Diff Stain Kit (IHC World Life Science Products & Services, USA) following

manufacturer's protocol. Following staining, inserts were viewed under an inverted microscope using a 20x objective lens and photographed.

Matrigel invasion assays were performed according to the manufacturer's protocol (Corning, Life Sciences). Cells were starved in serum free media 24 hour prior to plating. For each cell line, 5×10^4 cells in 0.2ml serum-free media were plated in the top compartment of Matrigel-coated invasion chambers (8 μm pore PET membrane). Fibroblast conditioned media (0.8ml) was added to the bottom chambers and plates were incubated overnight at 37°C in 5% CO_2. After 24 hour, membranes were recovered and processed as described for the migration assay. Inserts were viewed under a 20x objective lens of an inverted microscope and photographed.

The number of migrated/invaded cells was counted in five random fields for each membrane using NIH ImageJ Cell Counter software. Migration and invasion results are presented as means ± SD in histograms. constructed by normalizing the values of the H1299 mutant p53 cells to p53-WT cells, and the values of the PG-p53 transfectants to their corresponding p53 only expressing cells.

2.2.10 RNA isolation, RT-PCR and real-time PCR

Cells grown in 100 mm culture dishes were processed for total RNA extraction using the RNeasy Plus Mini Kit (Qiagen) and 1 μg of RNA was used to synthesize cDNA with a QuantiTect Reverse Transcription Kit (Qiagen). For real-time PCR, SYBR Green Master Mix (Thermo Fisher) and specific primers for *PUMA*, *S100A4*, *MDM2*, *BAX* and *ACTB* **(Table 2-2)** were used. Quantitative reverse transcriptase PCR (qRT-PCR) was done using a 7500 ABI Thermocycler. Data were normalized to the internal control (ACTB) and fold changes were calculated based on the $2^{-\Delta\Delta CT}$ method. Results are presented as means ± SD in histograms constructed by normalizing the values of the H1299 mutant p53 cells to p53-WT cells, and the values of the PG-p53 transfectants to their corresponding p53 only expressing cells.

2.2.11 Statistical data analysis

All quantitative data were presented as mean ± standard deviation (SD). Statistical significance between groups were assessed using Student's t-test for all assays except qPCR, which was analyzed by One-way ANOVA. p-values < 0.05 were considered significant in all cases. All biochemical experiments were repeated at least 3-6 times and the figures are

representative of one typical experiment for each assay. All functional assays were repeated at least three times and the histograms represent the average of all assays.

Table 2-1: Antibodies and their dilutions in various assays

Antibody	Species	Assays		Manufacturer/Catalogue #
Primary		IP	WB	
Akt2	Mouse	-	1:1000	Santa Cruz # sc-5270
β-Actin	Mouse	-	1:1000	Santa Cruz # sc-47778
β-catenin	Mouse	-	1:1000	MilliporeSigma # c-7207
β-tubulin	Mouse	-	1:1000	Developmental Studies Hybridoma Bank (E7)
Glutathione S-transferase (GST)	Goat	-	1:1000	Cytiva # 27-4577-01
Lamin B	Rabbit	-	1:1000	Abcam # ab16048
Nucleophosmin (NPM)	Mouse	-	1:2000	Abcam # ab10530
p53	Mouse	1:100	1:1000	Santa Cruz # sc-126
Plakoglobin	Mouse	1:100	1:1000	BD Bioscience # 610253
Secondary				
AlexaFluor 790 Mouse anti-Rabbit	Mouse	-	1:30,000	Jackson Immuno Research # 211-652-171
AlexaFluor 790 Goat anti-Mouse	Goat	-	1:30,000	Jackson Immuno Research # 115-655-174
AlexaFluor 680 Goat anti-Mouse	Goat	-	1:30,000	Jackson Immuno Research # 115-625-174
Li-Cor IRDye®-800CW-Donkey anti-goat	Donkey	-	1:20,000	LiCor # LIC926-32214

Table 2-2. List of primers and their sequences used for qRT-PCR assays

Gene	Primers	Sequences (5-′3′)
PUMA	Forward	ACGACCTCAACGCACAGTACGA
	Reverse	CCTAATTGGGCTCCATCTCGGG
BAX	Forward	TCAGGATGCGTCCACCAAGAAG
	Reverse	TGTGTCCACGGCGGCAATCATC
S100A4	Forward	CAGAACTAAAGGAGCTGCTGACC
	Reverse	CTTGGAAGTCCACCTCGTTGTC
ACTB	Forward	CACCATTGGCAATGAGCGGTTC
	Reverse	AGGTCTTTGCGGATGTCCACGT

2.3 RESULTS

2.3.1 Plakoglobin interacts with p53-WT, p53-R175H and p53-R273H mutants in H1299 cells

We previously reported plakoglobin interactions with endogenous p53-WT and several p53 mutants in various carcinoma cells (70, 71, 72, 110). To determine if plakoglobin interacts with exogenously expressed p53-WT, $p53^{R175H}$ (p53-175) and $p53^{R273H}$ (p53-273) similarly, H1299 cells were transfected with p53 (WT, 175 or 273) with or without plakoglobin. The expression of transfected proteins was validated by immunoblotting of total cell extracts (TCEs) using anti-p53 or -plakoglobin (PG) antibodies (**Figure 2-1A**). As mentioned earlier, H1299 cells lack plakoglobin expression. However, we observed a non-specific band in plakoglobin immunoblots (depicted with the asterisk * in **Figure 2-1**) with the specific plakoglobin antibody used in this study. Hence, we validated the absence of plakoglobin protein in H1299 parental cells via immunofluorescence. As seen in **Figure 2-2**, no plakoglobin expression was observed in H1299 cells, which confirmed the absence of plakoglobin expression in these cells.

Transiently co-expressing p53-(WT, 175 or 273) and plakoglobin cells were processed for sequential and reciprocal co-immunoprecipitation and immunoblotting with p53 and plakoglobin antibodies. The results demonstrated that all p53 transfectants (WT, 175 and 273) co-precipitated plakoglobin. Similarly, plakoglobin co-precipitated p53 in all transfectants, whereas control immunoprecipitates using mouse IgG were negative for both p53 and plakoglobin (**Figure 2-1B**). We also examined plakoglobin interaction with exogenously expressed p53- (WT, 175, 273) in SKOV-3 ovarian carcinoma cells that express endogenous plakoglobin and are p53 null **(Figure 2-3A)**. The results of these experiments showed plakoglobin interacted with wild type p53 and both p53 mutants, suggesting that plakoglobin-p53-(WT, 175, 273) interaction is independent of tissue and cellular backgrounds **(Figure 2-3B)**.

Plakoglobin interactions with the three forms of p53 were also confirmed by GST pull-down assays. TCEs from untransfected (UT) H1299 cells and H1299 cells transiently expressing p53-(WT, 175 or 273) were mixed with PG-GST beads and processed for pull-down and immunoblotting with p53 antibodies. PG-GST beads pulled down p53 in all three transfectants whereas GST alone beads pulled down GST but not p53 (**Figure 2-1C**). Finally, subcellular fractionation followed by immunoblotting with p53 and plakoglobin antibodies showed the presence of both proteins in the same subcellular compartments in all transfectants co-expressing

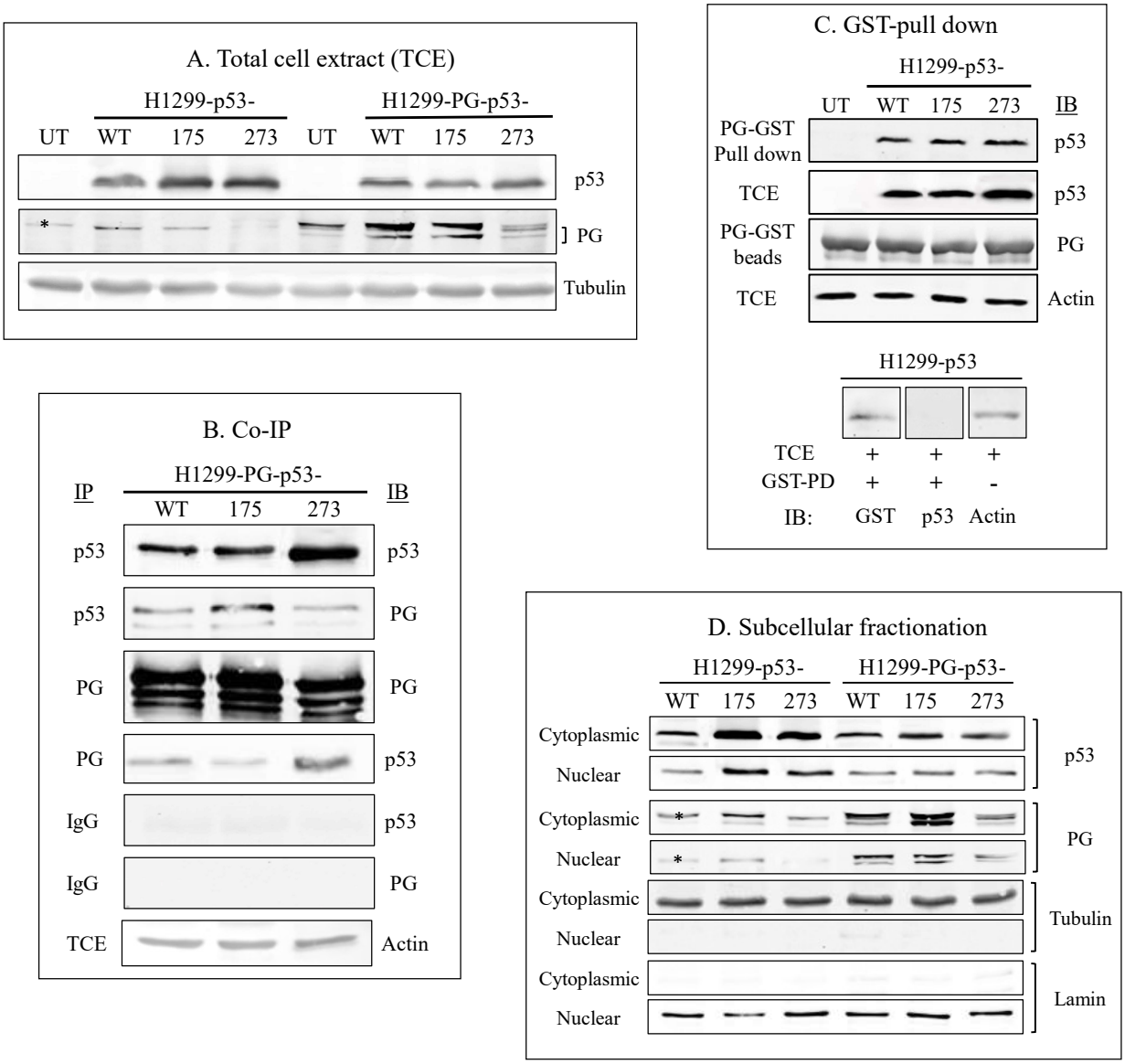

Figure 2-1. Protein expression and interaction of plakoglobin with p53-WT, p53-R175H conformational and p53-R273H contact mutants. A. Total cellular extracts (TCEs) from untransfected H1299 cells (UT) and H1299 transfectants expressing p53-(**WT, 175 or 273**) alone or together with plakoglobin **(PG)** [**H1299-PG-p53-(WT, 175, 273)**] were processed for immunoblot using p53 and plakoglobin antibodies. Beta-tubulin was used as a loading control. **B.** TCEs from H1299-PG-p53-(WT, 175, 273) were processed for sequential reciprocal co-immunoprecipitation (**Co-IP**) and immunoblotting (**IB**) using p53, plakoglobin and control (IgG) antibodies. Beta-actin was used as loading control. **C. Top:** TCEs from H1299-p53- (WT, 175 or 273) transfectants were incubated with GST-tagged plakoglobin (**PG-GST**) and processed for GST-pull down assays and immunoblotting with p53 and plakoglobin antibodies. Beta-actin was used as a loading control. **Bottom:** TCE from H1299-p53-WT cells was incubated with GST only beads and processed for pull down and immunoblot with GST and p53 antibodies. **D.** H1299 transfectants were processed for subcellular fractionation using NE-PER reagent and **Cytoplasmic** and **Nuclear** extracts of equal cell numbers were processed for immunoblot with p53 and plakoglobin antibodies. The purity of cytoplasmic and nuclear fractions was confirmed by immunoblotting with tubulin and lamin antibodies, respectively. * Non-specific.

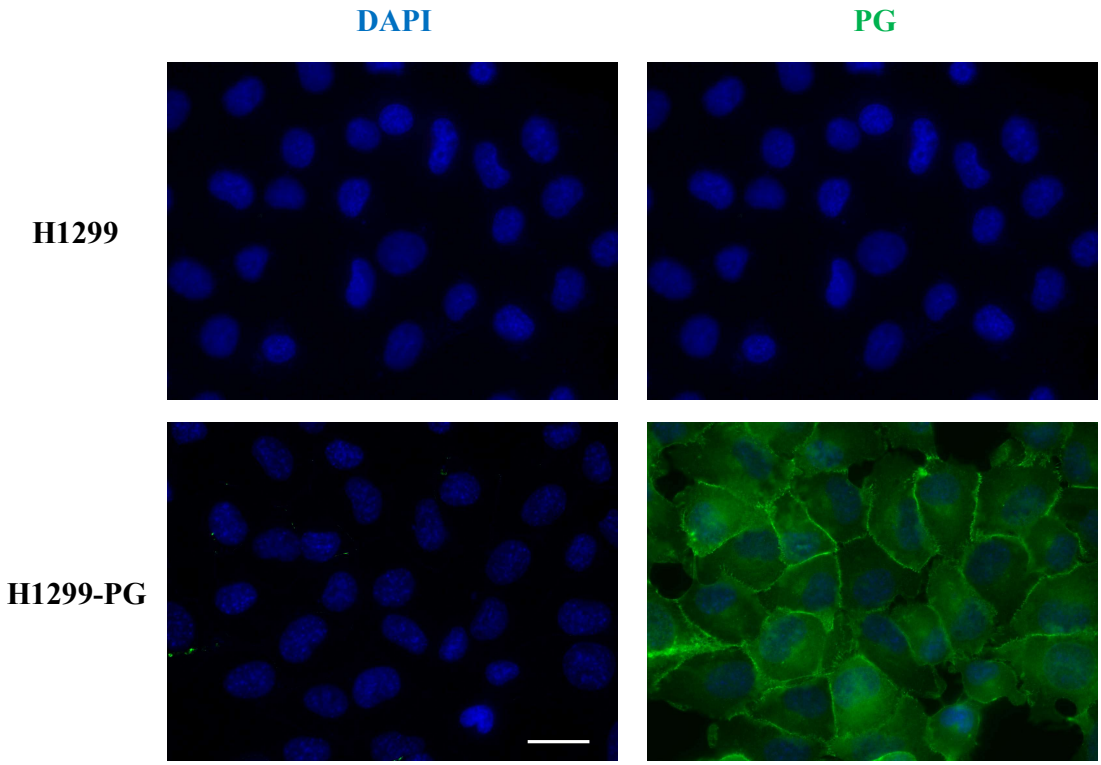

Figure 2-1. Plakoglobin (PG) expression and localization in H1299 parental cells and H1299-PG transfectants. Confluent cultures of H1299 and H1299-PG cells grown on coverslips were processed for immunofluorescence using plakoglobin (**PG**) antibodies. Nuclei were counterstained with DAPI and coverslips imaged using a 40x objective of a Zeiss confocal microscope. Bar, 40 μm.

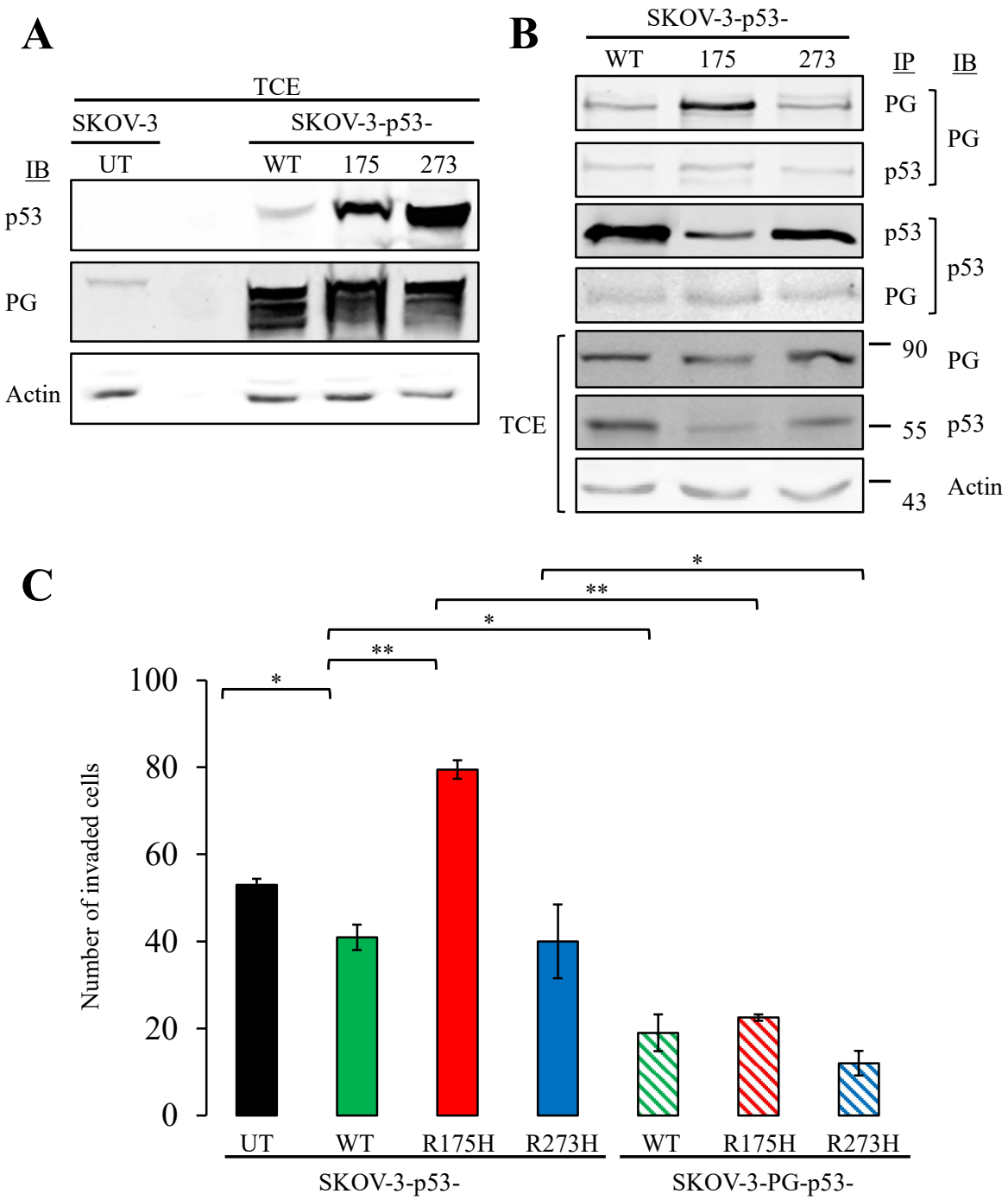

Figure 2-3. Plakoglobin (PG) interacted with p53- (WT, 175, 273) in SKOV-3 cells and reduced cellular invasion. (A) Total cellular extracts (TCEs) from SKOV-3 cells co-expressing p53- (WT, 175, 273) with plakoglobin were processed for sequential reciprocal co-immunoprecipitation (**IP**) and immunoblotting (**IB**) using p53 and plakoglobin antibodies. Beta-actin was used as loading control. Triplicate cultures of transfectants were processed for 24-hour transwell Matrigel invasion **(B)** assays. Inserts were fixed, stained, and imaged under an inverted microscope at 20x magnification. The number of migrated or invaded cells was quantitated from five random fields using NIH ImageJ Cell Counter software. Results are presented as means ± SD in histograms. *p* values, * < 0.05, ** < 0.01.

p53 and plakoglobin (**Figure 2-1D)**. Overall, these results showed that plakoglobin interacted with all three forms of exogenously expressed p53 and both proteins localized to the cytoplasm and nucleus.

2.3.2 Plakoglobin co-expression with different p53s differentially affects their colony formation, migration and invasion

To assess how plakoglobin expression affects the oncogenic properties of mutant p53 (175 and 273), we performed soft agar colony formation, migration, and invasion assays on H1299-p53-(WT, 175 and 273) transfectants independently or co-expressed with plakoglobin.

When expressed individually in H1299 cells, p53-WT reduced colony formation by over 50%, whereas plakoglobin had no significant effect on clonogenicity **(Figure 2-4A)**. Compared with H1299-p53-WT cells, H1299-p53-175 and -273 cells exhibited increased colony formation by ~55% and 62%, respectively (**Figure 2-5A**). Co-expression of plakoglobin with p53-175 or -273 reduced anchorage-independent growth by > 60% (**Figure 2-5A**), indicating that plakoglobin is able to suppress the anchorage-independent growth induced by p53-175 and -273 in H1299 cells.

While PG expression significantly decreased cellular migration and invasion in H1299 cells, reduction in these properties were more drastic in p53-WT expressing H1299 cells **(Figure 2-4B)**. Similarly, compared with p53-WT cells, both p53-175 and -273 transfectants showed increased cell migration (75% and 43%; **Figure 2-5B**) and invasion (45% and 17%; **Figure 2-5C**), respectively. Interestingly, co-expression of plakoglobin only decreased cell migration and invasion in p53-175 transfectants (35% and 65%, respectively) but had no significant effect on these properties in p53-273 cells (8% and 6%, respectively) (**Figure 2-5B and C**). Notably, when co-expressed, plakoglobin also significantly decreased migration and invasion in H1299-p53-WT cells by 66% and 58%, respectively (**Figure 2-5B and C**), consistent with our previous studies (70, 72). These observations suggested that plakoglobin expression exerted differential *in vitro* anti-tumorigenic effects in different p53 mutant backgrounds in H1299-p53-175 and -273 cells. Specifically, plakoglobin reduced the colony formation properties of both H1299-p53-175 and -273 transfectants, but only reduced the invasive and migratory properties of H1299-p53-175 transfectants. To validate the anti-tumorigenic effect of plakoglobin on exogenously expressed p53 mutants in a different cellular background, p53-175 and -273 mutants were transiently expressed in SKOV-3 ovarian carcinoma cells and invasion assays performed on the transfectants. We found

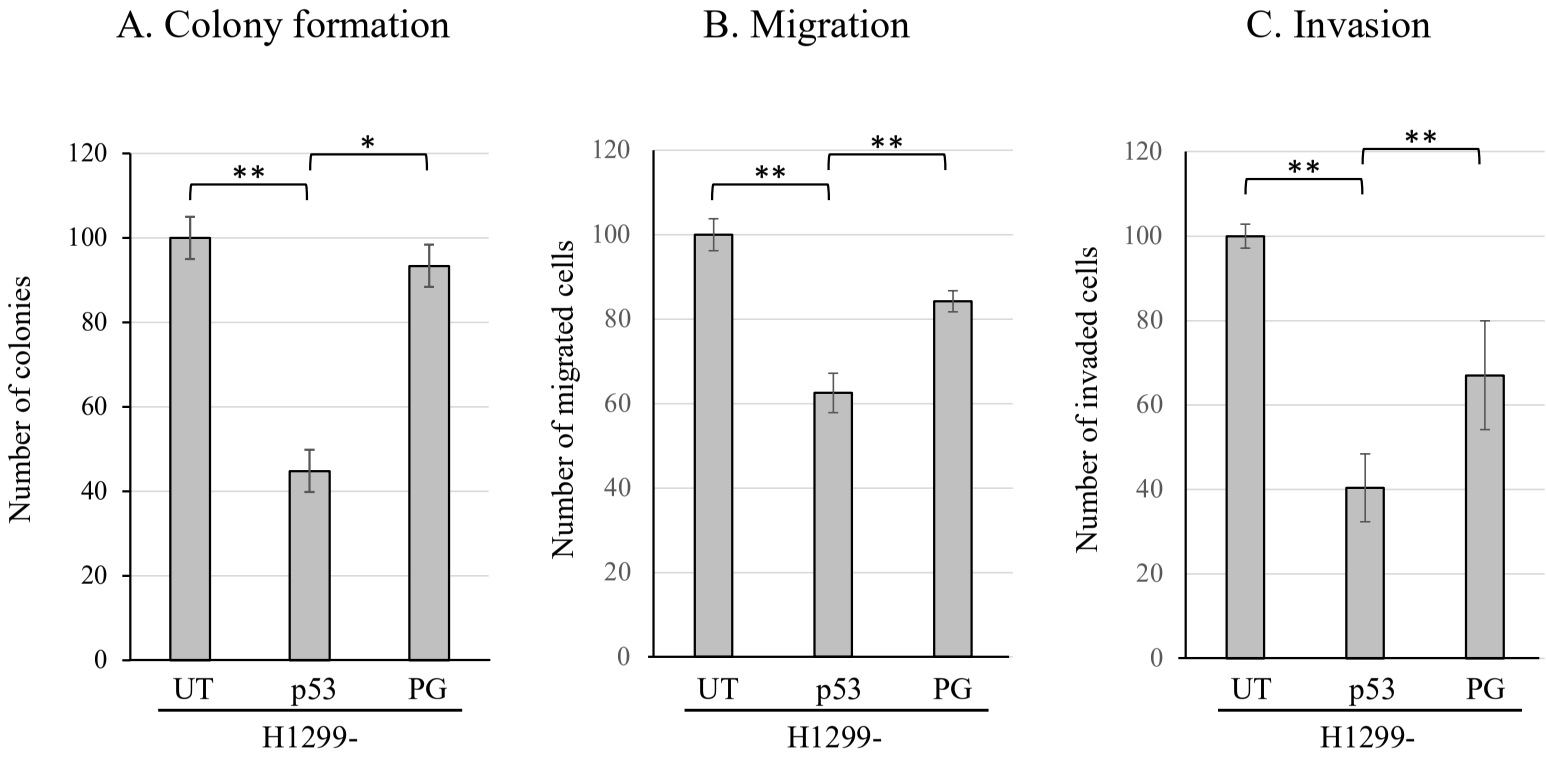

Figure 2-4. Colony formation, migration, and invasion of H1299, H1299-p53-WT and H1299-plakoglobin (PG) cells . A) H1299 cells transfectants were seeded in triplicates at $7.5x10^3$ cells in 35 mm dishes containing 0.35% top agar and 0.6% base agar and grew for two weeks. At the end of the two weeks, colonies were fixed, stained, counted and the results presented as means ± SD. **(B)** and **(C)** Triplicate cultures of transfectants were processed for 24-hour transwell migration **(B)** and Matrigel invasion **(C)** assays. Inserts were fixed, stained, and imaged under an inverted microscope at 20x magnification. The number of migrated or invaded cells was quantitated from five random fields using NIH ImageJ Cell Counter software. Results are normalized to H1299 untransfected cells (UT) and presented as means ± SD in histograms. *p* values, * < 0.05, ** < 0.001.

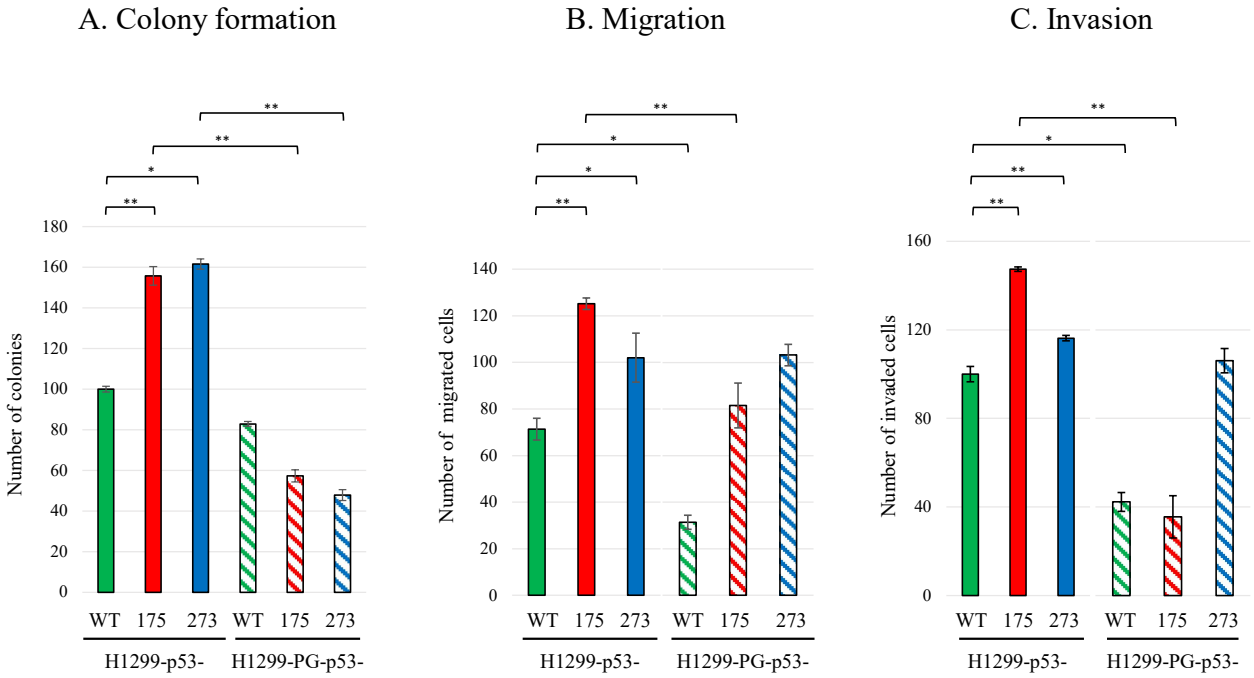

Figure 2-5. Colony formation, migration and invasion of H1299 cells expressing p53-(WT, R175H, R273H) without or with plakoglobin (PG). A. H1299 cells transfectants were seeded in triplicates at $7.5x10^3$ cells in 35 mm dishes containing 0.35% top agar and 0.6% base agar and grew for two weeks. At the end of the two weeks, colonies were fixed, stained, counted and the results presented as means ± SD. **B and C.** Triplicate cultures of transfectants were processed for 24-hour transwell migration **(B)** and invasion **(C)** assays. Inserts were fixed, stained, and imaged under an inverted microscope at 20x magnification. The number of migrated or invaded cells was quantitated from five random fields using NIH ImageJ Cell Counter software. Results are presented as means ± SD in histograms. *p* values, * < 0.05, ** < 0.001.

that only p53-175 expression significantly elevated cellular invasion relative to p53-WT in SKOV-3 cells. Nonetheless, when co-expressed, plakoglobin decreased cellular invasion in both SKOV-3-p53-175 and -273 cells and also SKOV-3-p53-WT cells **(Figure 2-3C)**. These findings indicated that although p53-R175H and -R273H oncogenic functions are cellular-context dependent as has been reported previously (106, 159, 160, 161, 162, 163, 164), plakoglobin co-expression was still able to suppress their invasive properties.

2.3.3 Plakoglobin co-expression alters PUMA, BAX and S100A4 mRNA levels

Mutant p53 has been shown to promote tumorigenesis by altering the expression of p53-WT target genes (15, 124, 130, 132, 133, 134, 135, 138). Since our earlier studies showed a role for plakoglobin in regulating the expression of a number of p53-WT target genes (71, 72, 106, 110, 123, 155, 165, 166), we investigated the effect of plakoglobin on the expression of two well-studied p53-WT target genes: *PUMA* (p53 upregulated modulator of apoptosis) and *BAX* (Bcl2-associated X protein) that are growth-regulating, proapoptotic (149, 167, 168, 169, 170, 171, 172, 173, 174, 175), in mutant p53 expressing cells. We also examined the effect of plakoglobin on the expression of tumor invasion and metastasis promoting S100A4 protein that is known to promote mutant p53 accumulation and oncogenic target gene expression in cancer cells (176, 177).

We first assessed the effects of individual expression of p53-WT or plakoglobin in H1299 cells. We found that while p53-WT had no effect on the expression of *PUMA*, *BAX* and *S100A4*, plakoglobin significantly increased *PUMA* and *BAX* but not *S100A4* expression in H1299 cells **(Figure 2-6, A, B and C)**.

Expression of mutant p53-(175, 273) in H1299 cells did not affect the expression of *PUMA* or *BAX* transcripts. However, when co-expressed, plakoglobin resulted in a significant increase in *PUMA* but not *BAX* expression in H1299-p53-175 and -273 cells (**Figure 2-7A and B)**. We also observed a significant increase in *PUMA* and *BAX* expression upon plakoglobin co-expression in control H1299-p53-WT cells **(Figure 2-7A and B)**.

With respect to *S100A4,* we found that p53-175 significantly increased while p53-273 significantly decreased *S100A4* transcripts level in H1299 cells relative to p53-WT. Interestingly, co-expression of plakoglobin resulted in a significant decrease in *S100A4* levels in both H1299-

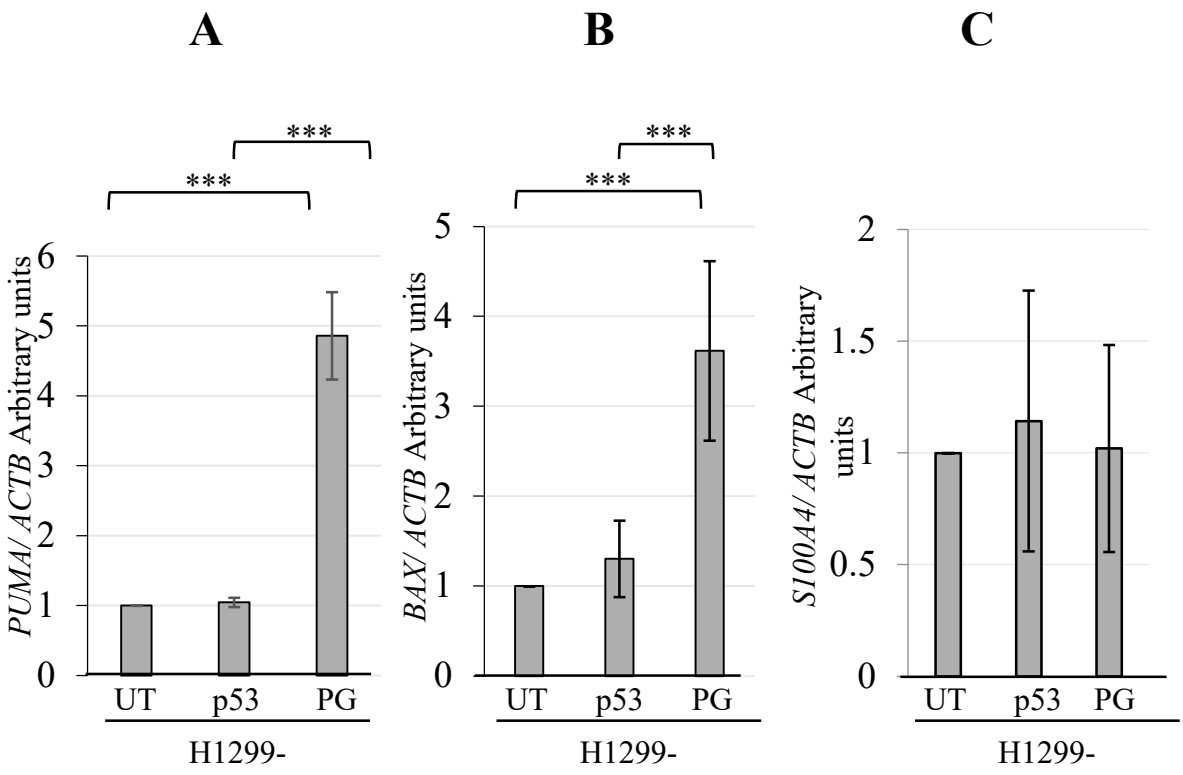

Figure 2-6. Changes in the mRNA expression of p53 or β-catenin target genes in H1299 cells expressing p53 or plakoglobin (PG). Total cellular RNA was extracted from confluent cultures of H1299, H1299-p53 and H1299-PG, reverse transcribed and processed for real-time PCR for ***PUMA*** **(A)**, ***BAX*** **(B)** and ***S100A4*** **(C)**, using specific primers (**Table 2-2**). Expression levels were normalized to the amount of *ACTB* in the same cell line. Histograms were constructed based on the mean ± SD. The values of transfectants were normalized to that of the untransfected H1299 cells. **P < 0.01, ***P < .001, ****P < .0001.

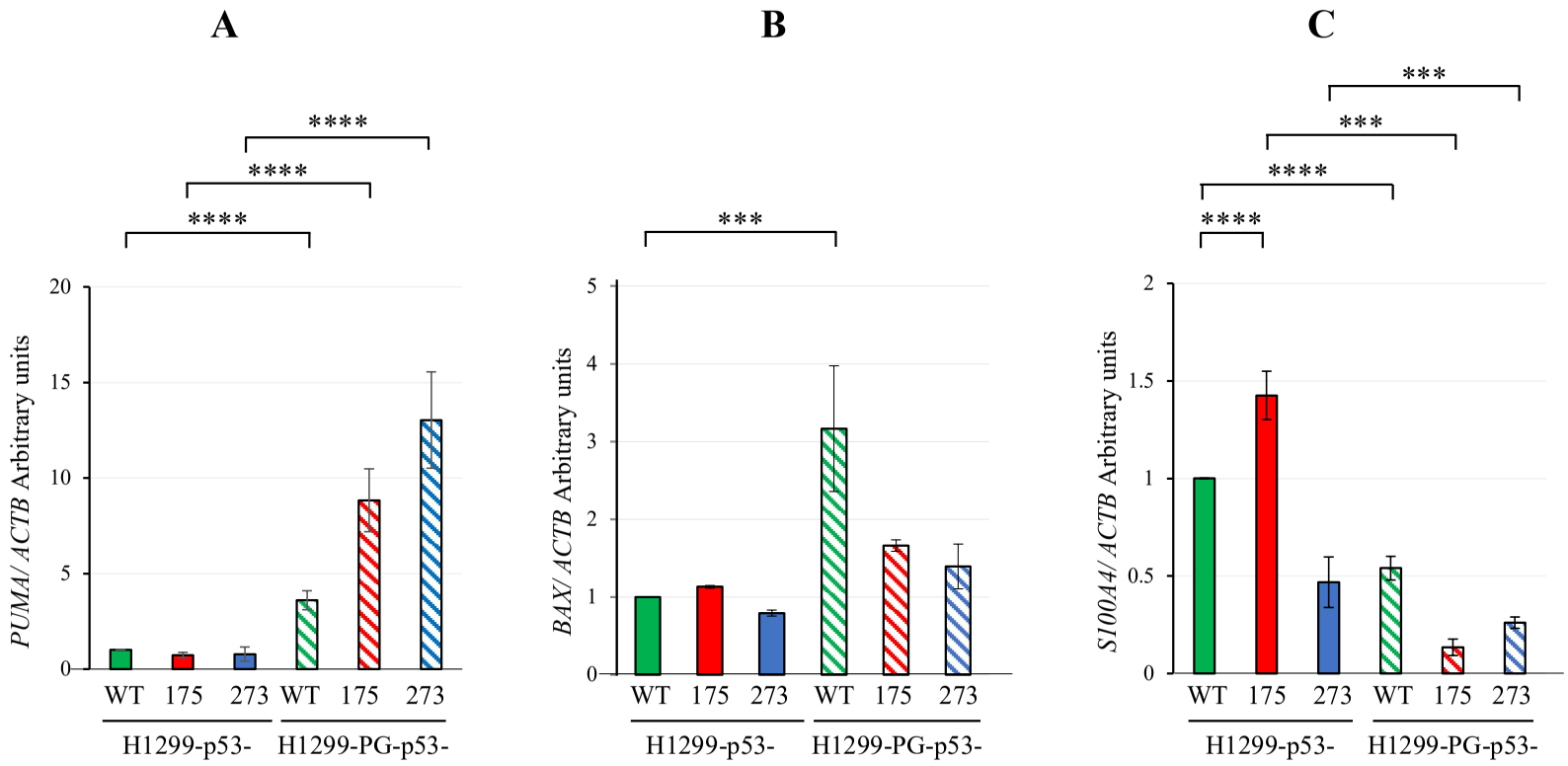

Figure 2-7. Changes in the expression of p53 and β-catenin target genes by plakoglobin co-expression. Total cellular RNA was extracted from confluent cultures, reverse transcribed and processed for real-time PCR for ***PUMA*** **(A)**, ***BAX*** **(B)** and ***S100A4*** **(C)**, using specific primers (**Table 2-2**). Expression levels were normalized to the amount of *ACTB* in the same cell line. Histograms were constructed based on the mean ± SD. The values of mutant p53-(175, 273) transfectants were compared to p53-WT cells, and PG-p53 expressing transfectants to their p53 only expressing counterparts. **P < 0.01, ***P < .001, ****P < .0001.

p53-175 and -273 transfectants (**Figure 2-7C**). We also noticed a significant decrease in *S100A4* transcripts when plakoglobin was co-expressed in control H1299-p53-WT cells **(Figure 2-7C)**.

Together, these findings demonstrated that with regards to *PUMA* and *BAX* expression, plakoglobin had a mutant p53 independent effect as demonstrated by the significantly increased *PUMA* and *BAX* transcript levels when only plakoglobin was expressed in H1299 cells. Conversely, plakoglobin has a p53-dependent effect on *S100A4* expression as evidenced by the decreased trend of *S100A4* expression when plakoglobin was co-expressed with p53- (WT, 175, and 273) in H1299 cells. Notably, our findings showed that plakoglobin had similar effects on *PUMA, BAX,* and *S100A4* mRNA expression when co-expressed with either the conformational or the contact p53 mutants.

2.3.4 Plakoglobin decreases nuclear β-catenin and increases nuclear nucleophosmin (NPM) levels in mutant p53 expressing H1299 cells

We next investigated the effects of plakoglobin on the subcellular distribution of β-catenin and nucleophosmin (NPM) that have been linked to plakoglobin anti-tumor roles in cancer cells (107, 109, 156, 178). Indeed, our lab and others have previously demonstrated that a potential mechanism of plakoglobin tumor suppressive function is the regulation of the subcellular distribution and oncogenic activities of β-catenin (91, 109, 156, 158, 179). We have also shown that plakoglobin expression in the mutant p53 (R280K)- expressing and highly invasive breast carcinoma cells MDA-MB-231 increased nuclear NPM level and this redistribution was concurrent with decreased *in vitro* tumorigenic properties of these cells **[(109) and Figure 4 and 5 therein]**.

First, we examined the effect of the p53 mutants on the subcellular distribution of β-catenin and NPM. We found that while p53-175 had no significant effect on the level of nuclear β-catenin in H1299 cells, p53-273 significantly decreased (~50%) nuclear β-catenin expression in H1299 cells relative to H1299-p53-WT cells. When co-expressed, plakoglobin resulted in a significant reduction (60%) in nuclear β-catenin levels in H1299-p53-175 cells. We also observed a significant decrease (50%) in nuclear β-catenin expression in H1299-p53-WT cells upon co-expression of plakoglobin. Contrastingly, though not statistically significant, we observed an

increase in nuclear β-catenin level upon co-expression of plakoglobin in H1299-p53-273 transfectants **(Figure 2-8A and B)**.

On the other hand, we found that the levels of nuclear NPM were similar in all H1299-p53-(WT, 175, 273) transfectants, when co-expressed, plakoglobin increased the nuclear pool of NPM by 89% and 55% in H1299-p53-175 and -273 cells, respectively **(Figure 2-8C and D)**. We also observed a significant increase (54%) in the nuclear pool of NPM in H1299-p53-WT cells when plakoglobin was co-expressed in these cells **(Figure 2-8C and D)**. It is important to note that we found plakoglobin in complex with NPM in all H1299-PG-p53- (WT, 175, 273) transfectants (**Figure 2-9)**. These findings provide a potential mechanism via which PG may exert its tumor suppressor activity in these cells.

2.3.5 Plakoglobin differentially affects AKT activation in H1299-p53-175 and -273 transfectants

The PI3K/AKT signaling pathway is hyperactivated in various cancers and promotes cell survival and proliferation (180, 181, 182, 183, 184, 185). Assessment of the pAKT level in breast carcinoma cell lines expressing p53-175 and -273 showed no change in pAKT level in p53-175 cells but significantly increase in pAKT levels in p53-273 expressing cells (159). Consistent with these observations, we found that the expression of p53-273 contact mutant but not p53-175 conformational mutant in H1299 cells resulted in a significant increase in pAKT levels in H1299-p53-273 transfectants only. Co-expression of plakoglobin led to a significant decrease in pAKT levels only in the H1299-PG-p53-273 cells (**Figure 2-10**). These results suggest a potential mechanism for the differences in the tumor suppressor effects of plakoglobin on the oncogenic properties of p53-175 and -273 in H1299 transfectants.

2.4 DISCUSSION

We have previously shown that plakoglobin interacts with endogenously expressed p53-WT and p53 mutants (70, 71, 72) and that exogenous expression of plakoglobin in plakoglobin deficient and mutant p53 (e.g., R280K, R273H, S241F, S215R) expressing carcinoma cell lines of different origins restored p53 tumor suppressor activity *in vitro* (70, 71, 72, 110, 111). Herein, we

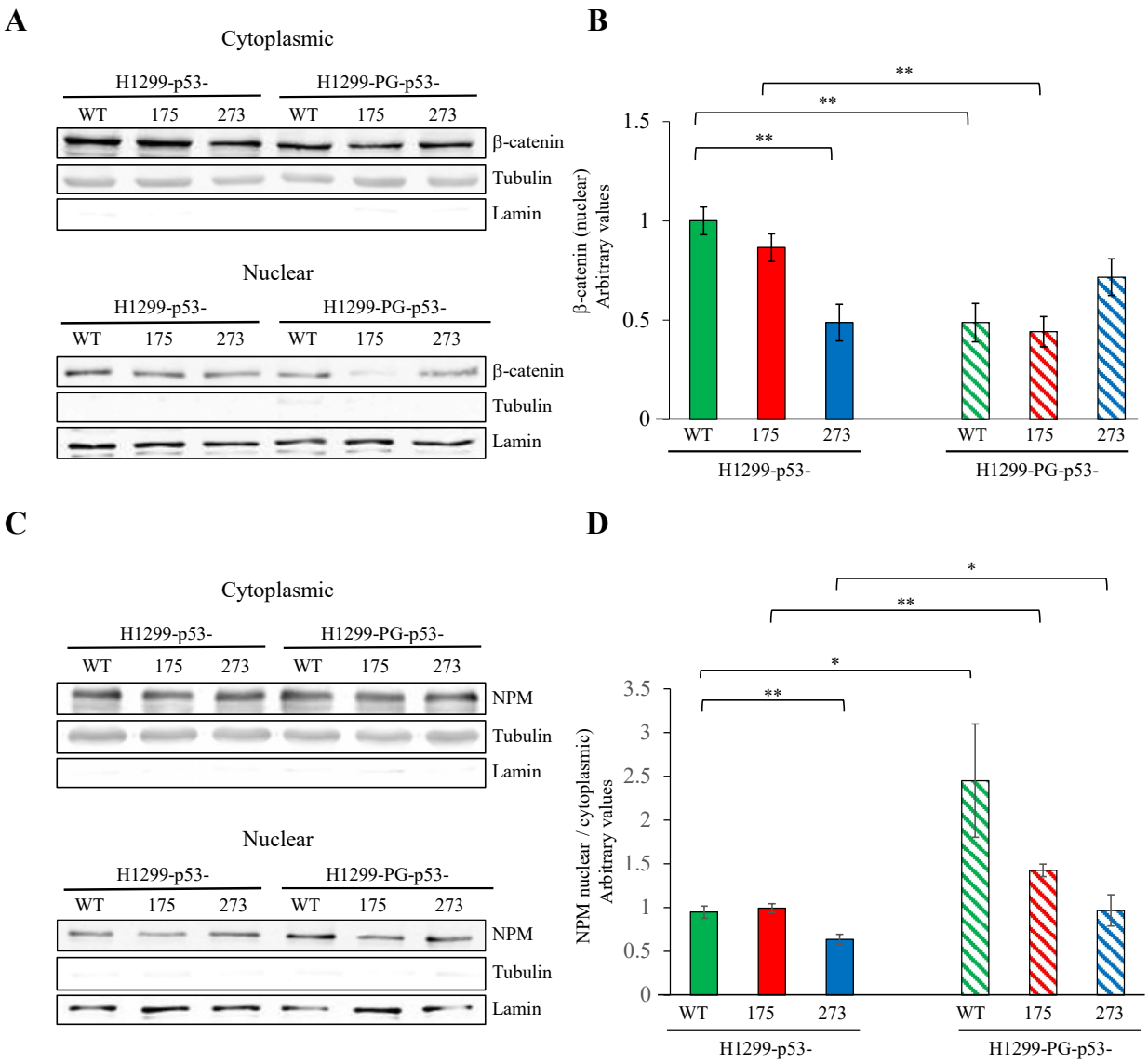

Figure 2-8. Plakoglobin differentially affects the subcellular distribution of β-catenin and nucleophosmin (NPM) in H1299 cells expressing p53- (WT, R175H, R273H). Equal amounts of cytoplasmic and nuclear extracts from various transfectants were processed for immunoblotting using **β-catenin (A, B) and NPM (C, D).** The purity of the cytoplasmic and nuclear fraction was confirmed by immunoblotting with tubulin and lamin antibodies, respectively. **(A)** Nuclear and cytoplasmic distribution of β-catenin in various transfectants. **(B)** β-catenin nuclear blots in A were quantitated by NIH Image software and histograms constructed, which represent means ± SD of at least 3 independent experiments. **(C)** Immunoblots representative of the cytoplasmic and nuclear distribution of NPM. **(D)** Histograms depicting the means ± SD nuclear/cytoplasmic ratio of NPM in various transfectants were generated by quantifying cytoplasmic and nuclear blots in C. Histograms were constructed based on the mean ± SD. *P < .05, **P < 0.01.

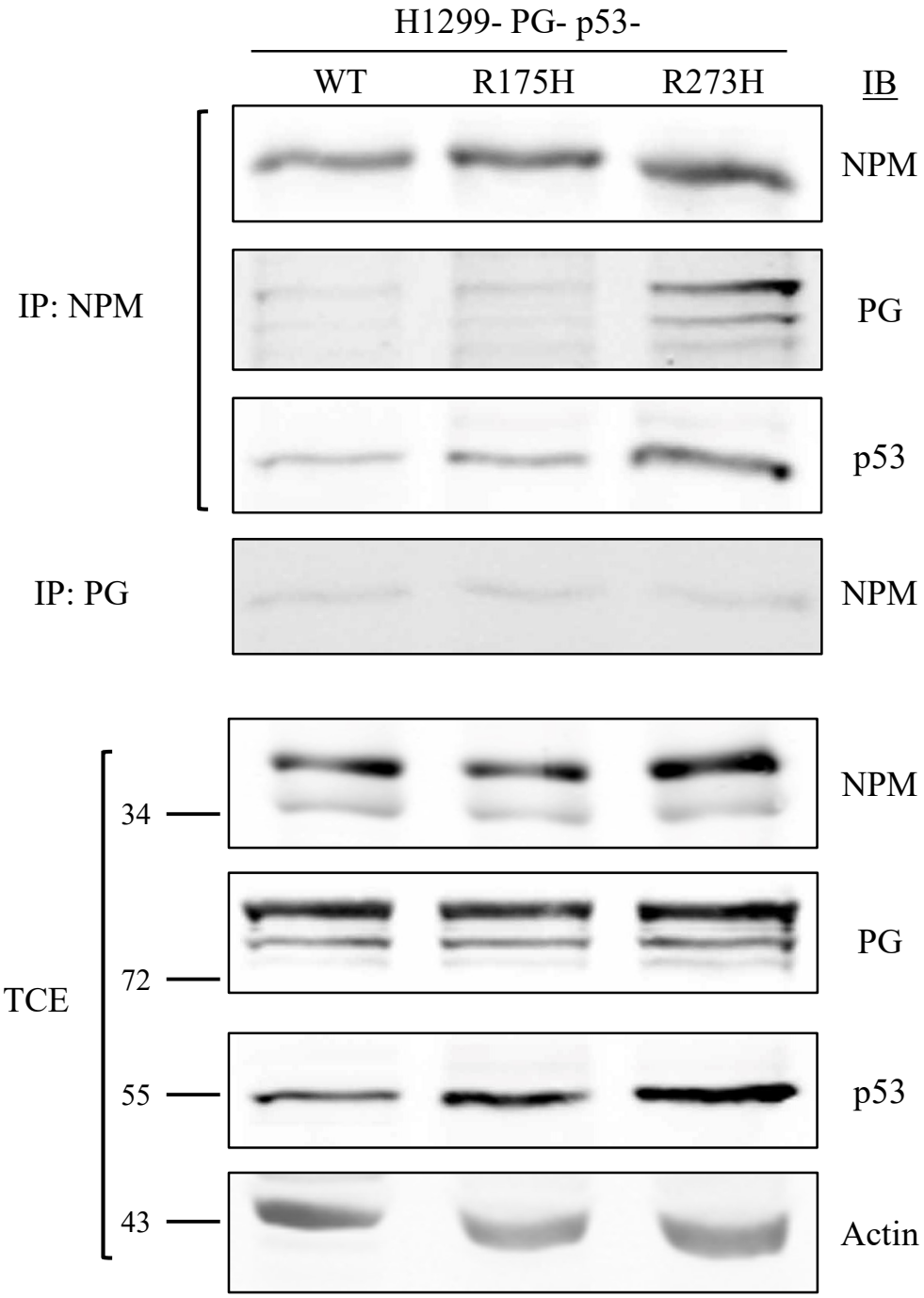

Figure 2-9. Nucleophosmin (NPM) interacted with plakoglobin (PG) in H1299-p53- (WT, 175, 273) transfectants. Total cellular extracts (TCEs) from H1299-PG-p53- (WT, 175, 273) cells were processed for sequential co-immunoprecipitation (**IP**) and immunoblotting (**IB**) with nucleophosmin, plakoglobin and p53 antibodies. Beta-actin was used as loading control.

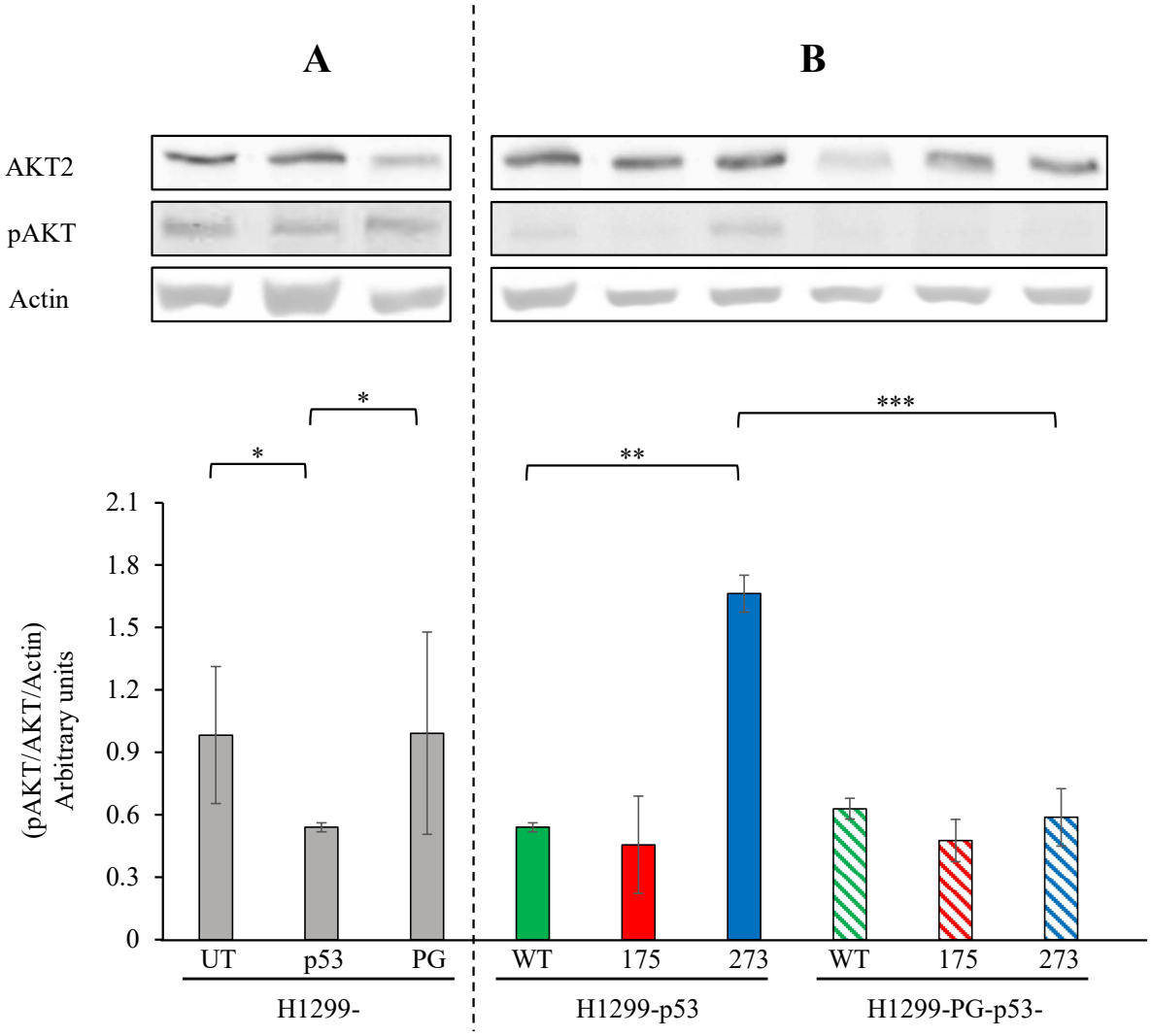

Figure 2-10. Protein expression and phosphorylation of AKT in H1299 cells and H1299 transfectants expressing plakoglobin (PG) or p53-(WT, R175H, R273H) or both. Total cell extracts were processed for immunoblotting for **AKT2** and **pAKT** antibodies and the same blots were probed with actin to confirm comparable loadings. Histograms represent means ± SD of the ratio of pAKT/AKT/actin. **Left panel**: Representative immunoblot and histogram depicting the ratio of pAKT/AKT/actin of H1299 cells and H1299 transfectants expression PG or p53-WT only. **Right panel**: Representative immunoblot and histogram of the ratio of pAKT/AKT/actin of the mutant p53 expressing cells and of the PG-p53 expressing cells. *P < .05, **P < 0.01, ***P < .001.

show that exogenously expressed plakoglobin interacted with both exogenously expressed $p53^{R175H}$ conformational and $p53^{R273H}$ contact mutants in the plakoglobin-deficient and p53-null H1299 cells and differentially affected their *in vitro* oncogenic functions. Specifically, plakoglobin co-expression significantly reduced the tumorigenic properties of H1299-p53-175 cells, whereas it minimally affected the tumorigenic properties of H1299-p53-273 cells. It is important to mention that we observed a more tumorigenic effect of p53-175 compared to p53-273 in H1299 cells that is H1299-p53-175 cells exhibited significantly increased anchorage-independent growth, migratory and invasive properties relative to their p53-273 expressing counterpart.

Several studies have demonstrated that the oncogenic functions of p53 mutants are mediated in part by their altered transcriptional effects on p53-WT target genes. We found that both p53-175 and p53-273 had no effect on the transcription of the p53-WT target genes *PUMA* and *BAX,* as have been reported in other studies (159, 186, 187). Interestingly, plakoglobin co-expression significantly increased *PUMA* but not *BAX* transcript levels in both the p53-175 and p53-273 transfectants suggesting a direct regulation of *PUMA* but not *BAX* transcripts by plakoglobin in H1299-p53-175 and -273 cells. *PUMA* is a well-known proapoptotic/anti-tumorigenic p53-WT target gene (169, 170, 174). Its increase in both H1299-p53-175 and p53-273 cells by plakoglobin may explain how plakoglobin was able to inhibit the anchorage-independent growth features displayed by both these transfectants.

Investigation of a different gene, *S100A4* known to promote mutant p53 accumulation and oncogenic target gene expression in cancer cells revealed that *S100A4* is significantly increased by p53-175 but greatly reduced by p53-273 in H1299 cells. S100A4 is a well-known promoter of cancer cell migration, invasion and metastasis (188, 189). As such, its upregulated expression in response to p53-175 but not p53-273 in H1299 cells may be responsible for the increased migratory and invasive properties exhibited by the H1299-p53-175 relative to -273 cells. Importantly, co-expression of plakoglobin appreciably reduced *S100A4* transcript levels in the p53-175 cells, which may provide an explanation for plakoglobin's suppressive effect on the migration and invasion of H1299-p53-175 cells.

Another interesting finding in this study is that plakoglobin co-expression differentially affected the levels of nuclear β-catenin, which is pro-tumorigenic in the H1299-p53-175 and p53-273 transfectants. Specifically, while a significant decline in nuclear β-catenin levels was observed

in the H1299-PG-p53-175 cells there was a slight increase in nuclear β-catenin levels in the H1299-PG-p53-273 cells, though it was not significant. Plakoglobin suppression of nuclear β-catenin localization in the H1299-PG-p53-175 cells could further explain the anti-tumorigenic effect that it has on these cells. While its lack of inhibition of the nuclear β-catenin localization in the H1299-PG-p53-273 cells could explain why plakoglobin had no significant effect on the tumorigenic (migratory and invasive) properties displayed by the H1299-PG-p53-273 cells. We also found that plakoglobin co-expression in H1299-p53-175- and -273 cells increased the nuclear pool of NPM, which has been associated with decreased *in vitro* tumorigenic properties– specifically decreased growth of mutant p53-expressing cells (109). This may further explain the suppressive effects of plakoglobin on the anchorage-independent growth of H1299-p53-175- and -273 cells.

Finally, we found that the p53-273 contact mutant but not the p53-175 conformational mutant resulted in a drastic increase in pAKT levels in H1299 cells, which was attenuated by the co-expression of plakoglobin. Hyperactivated/phosphorylated form of AKT has been reported to affect the oncogenic properties of p53 contact and conformational mutants differently (159). Particularly, certain contact mutants have been shown to enhance anoikis resistance and thus anchorage-independent growth in an AKT-dependent manner (159). Correspondingly, we postulate that the significant suppression of anchorage-independent growth by plakoglobin observed in the p53-273 cells relative to its other tumorigenic (migration and invasion) properties, which plakoglobin co-expression had no effect on may be due to plakoglobin's ability to suppress the high pAKT levels induced by p53-273 in H1299 cells.

Overall, our results suggested that plakoglobin has the ability to reactivate tumor suppression in mutant p53-expressing cells especially conformational mutant p53-expressing cells and can thus potentially be used for the development of effective therapeutic strategies in highly aggressive mutant p53-expressing cancer cells. Using *in silico* modeling, we have determined the 3-D structure of PG-p53-WT and PG-p53^{R175H}, identified the amino acid residues involved in their interaction and validated the *in silico* model (190). Information derived from these studies will be utilized to develop compounds that mimic plakoglobin-p53 interaction and have the potential to be used as therapeutics in various cancers. These compounds will further have the advantage of representing a naturally occurring biological interaction that positively promote p53

tumor/metastasis suppressor function, potentially, with less side effects in patients with mutant p53-expressing tumors.

CHAPTER 3: EXPERIMENTAL VALIDATION OF AN *IN SILICO* MODEL OF P53-R175H-PLAKOGLOBIN INTERACTION

3.1 INTRODUCTION

The tumor suppressor and transcription factor p53 plays a central role in the regulation of the cell cycle, apoptosis, DNA repair, senescence, metabolism, and immune system (20, 21). In normal cells, p53 responds to cellular stress such as DNA damage, hypoxia and oncogenic insults, among other stimuli/insults, by regulating the expression of genes and pathways that maintain homeostasis and normal cellular functions (17, 136, 191) The inactivation or abnormal activation of p53 is one of the most frequent and effective strategies that cancer cells use to maintain survival and growth as well as the ability to invade normal tissues and metastasize (136). p53 is inactivated by several mechanisms including mutations, posttranslational modifications, and interactions with its primary endogenous inhibitor HDM2 (39, 134). p53 mutations are observed in >50% of all cancers and the majority of metastatic tumors (192). Consequently, restoring p53 activity is currently one of the most promising therapeutic strategies in fighting cancer (126).

Majority of p53 mutations occur in the DNA-binding domain (DBD) of the protein with more than 80% being single missense mutations, 30% of which are represented by six hot spot mutations (42). The hot spot mutations are generally classified into DNA contact, which affect residues involved in the direct DNA-protein interaction [Arginine (R), 273, 248] without conformational changes; and structural/conformation mutations, which change the protein conformation [R (175, 245, 249, 282)] (42). Functionally, there are three types of p53 mutants: loss/partial loss of wild-type (p53-WT) function, dominant-negative (negatively regulates p53-WT), and gain of function (GOF; loss of tumor suppressor function and gain of oncogenic function) (15, 135). Strategies used for p53-targeted therapy are dependent on p53 status (126, 193, 194). For p53-WT loss of function (LOF) mutants, therapies are generally based on drugs that target its interaction with its major negative regulator, the E3 ubiquitin ligase MDM2. For GOF mutants, therapies are centered on drugs/small molecules that promote mutants p53 degradation, restore the wild-type transcriptional activity/function of mutants, and inhibit downstream oncogenic pathways activated by mutants (126, 193, 194).

Plakoglobin (PG) is a dual adhesion and signaling protein that we have identified as a novel interacting partner of p53 (70, 71, 72, 111). Previously, we have shown that plakoglobin interacted with p53-WT and several p53 mutants, including p53-R175H, in carcinoma cell lines of different tissue origins (70, 71, 72, 111). p53-R175H is the most frequently occurring p53 mutant in various

cancers, with potent GOF oncogenic properties (195). Co-expression of plakoglobin in cells expressing p53-R175H restored its tumor suppressor function *in vitro* by significantly reducing cell proliferation and migratory and invasive properties (72). To gain further insights into p53-R175H-plakoglobin interaction and its potential therapeutic application, herein, we used *in silico* 3D molecular dynamic modeling to identify amino acids residues in p53-R175H and plakoglobin that are involved in their interaction. The model identified Q167 and R248 in p53-R175H and N690 in plakoglobin as residues critical in mediating their interaction. Using site-directed mutagenesis, we generated constructs encoding p53-R175H in which Q167 and R248 were substituted with alanine individually or together. Similarly, a construct was developed to encode plakoglobin in which N690 was substituted by alanine.

To validate the model prediction, we exogenously expressed various p53-R175H constructs without or with plakoglobin in the p53 null and plakoglobin deficient H1299 non-small cell lung carcinoma cells. Similarly, wild type or N690A plakoglobin was co-expressed with p53-R175H expressing cells. Transfectants were then characterized for changes in p53-plakoglobin interaction and its functional consequence by measuring invasiveness of cells expressing various combinations of p53-R175H and plakoglobin. Our results suggested that Q167 and R248 amino acid residues are important for p53-R175H interaction with plakoglobin and their respective substitution with alanine individually or together significantly reduced p53-R175H-plakoglobin interaction. In contrast, there were no differences in p53-R175H-plakoglobin interaction when PG-WT or PG-690A was co-expressed with p53-R175H. Intriguingly, plakoglobin co-expression with any of the p53-R175H constructs similarly decreased their invasiveness. Overall, the results showed that Q167 and R248 residues in p53-R175H are important for its interaction with plakoglobin. The results also provide further insights for development of potential cancer therapeutics that could function by mimicking plakoglobin effects in cancers expressing this type of mutant p53.

3.2 MATERIALS AND METHODS

3.2.1 *In silico* modeling of p53-R175H and plakoglobin interaction

3.2.1.1 Cothreading of p53-R175H and plakoglobin

COTH webserver (196) was initially used to predict the complex structure of p53-R175H core domain and the C-terminal residues of plakoglobin **(Figure 3-1A)**. All ten predictions from COTH were of the p53 core-domain in a tetramer assembly with PDB IDs: 3KMD, 3D0A, 3EXJ, 4IBU, 1TSR, 3EXL, 4GUO,1TUP, 4G82 AND 1KZY. Since COTH webserver only outputs the alpha-carbon coordinates of the query residues, the top prediction, based on PDB ID: 3KMD (196) was used as a starting point to build the model. More specifically, COTH predictions yielded the alpha-carbon coordinates of p53-R175H core domain and residues 724-736 of plakoglobin. Tleap of Ambertools18 (197) was then used to place the missing atoms for each residue to build an all-atom model from the predicted alpha-carbon positions.

3.2.1.2 Construction of the p53-R175H-plakoglobin complex structure

There is a single experimentally-resolved structure of plakoglobin of residues 126-673 (PDB ID: 3IFQ (158)). It was necessary to construct the missing C-terminal residues of plakoglobin involved in the interaction with p53. Therefore, Quark webserver (198, 199) was used for the *ab initio* structure prediction of residues 674-723 and 737-745 of plakoglobin, which were not mapped by COTH. A model of plakoglobin residues 126-745 was then constructed by joining residues 126-673 from PDB ID: 3IFQ (158). Quark predicted residues 674-723 followed by COTH predicted residues 724-736 in their relative positions with respect to p53-R175H. Quark predicted residues 737-745 were then joined to residue 736.

p53-R175H-plakoglobin complex was then solvated in a neutralized 12 Å TIP3P water box with 0.15 M NaCl and parameterized using Amberff114SB force-field. To increase conformational sampling of the complex we used accelerated molecular dynamics (aMD) using Amber software (200). For this, the solvated complex was first minimized then gradually heated from 0 to 310 K using heavy restraints on the backbone atoms. Restraints were gradually decreased until they were completely removed before the complex was simulated for 150 ns using classical molecular dynamics (cMD) to obtain parameters required for aMD. The latter simulation was run for 200 ns.

3.2.1.3 Trajectory processing

Root-mean-square-deviation (RMSD**)** based clustering of 10,000 frames obtained from aMD were clustered based on a 2 Å cut-off for residues 670-745 of plakoglobin using CPPTRAJ of Ambertools18 (197). This yielded 101 different clusters that represent distinct complex conformations sampled during the simulation. The average Molecular Mechanics-Generalized Born Surface Area (MM-GBSA) binding energy of each cluster was calculated using MMPBSA.py (198). Additionally, the pairwise binding energy decomposition was also calculated.

3.2.2 Cell lines and culture conditions

All tissue culture reagents were purchased from Gibco unless stated otherwise. H1299, the non-small cell lung carcinoma cell line deficient in p53 and plakoglobin expression was provided by Dr. Roger Leng, University of Alberta and has been described previously (70, 72, 199). H1299 cells and its transfectants expressing plakoglobin and various p53-R175H constructs were maintained in minimum essential medium (MEM) supplemented with 10% fetal bovine serum (HyClone Laboratories, USA), 1% penicillin-streptomycin and 5 μg/mL kanamycin (complete MEM, CMEM).

3.2.3 Plasmid construction and transfection

Mutant p53 constructs were generated from HA-tagged p53 cDNA and has been described previously (70, 72). Site directed mutagenesis was used to generate plasmids encoding wild type plakoglobin (70, 72, 107) in which N690 was replaced by alanine; and p53-R175H and p53-R175H in which glutamine (Q) 167 or arginine (R) 248 or both were mutated to alanine to express mutants p53-R175H-Q167A, p53-R175H-R248A, and p53-R175H-Q167A-R248A (Synthego Corporation, USA). The authenticity of all constructs was validated by sequencing both at Synthego and the University of Alberta Molecular Biology Service Unit (MBSU).

Transfectants were generated using the jetOPTIMUS® (Polyplus, France) DNA transfection reagent following the manufacturer's protocol. Cells were transfected with 2 μg of plasmids encoding p53-R175H or p53-R175H-Q167A or p53-R175H-R248A or p53-R175H-Q167A-R248A alone or together with 3 μg of plakoglobin (WT or N690A). For transient transfections, cultures were processed within 30h for various assays. Stable transfectants were

selected by supplementing CMEM with 800 μg/mL G418 (p53 transfectants) or 800 μg/mL G418 and 600 μg/mL hygromycin (PG-p53 transfectants) 48 hours post-transfection. Multiple single cell clones for each transfectants were obtained using limiting dilution and the expression of p53 or co-expression of p53 and plakoglobin was verified using immunofluorescence and immunoblot assays. All experiments were repeated at least 3 times and conducted with stable transfectants, unless indicated otherwise.

3.2.4 Preparation of total cell extracts and Immunoblotting

Confluent 100 mm culture dishes were rinsed with cold PBS and extracted with 1mL RIPA lysis buffer [150 mM NaCl, 50 mM Tris-HCl pH 7.4, 1% NP-40, 0.25% sodium deoxycholate, 1 mM EDTA, 1 mM PMSF, 1 mM NaF, 1 mM Na_3VO_4, and Roche protease inhibitor cocktail (Sigma, Canada)] for 20 minutes on a rocker at 4 °C. Cells were scraped and centrifuged at 48,000 x g for 10 minutes and supernatants were processed for immunoblotting. Equal amounts of total cellular lysates (100 μL) were solubilized in 20 μL hot 6X-SDS sample buffer (10 mM Tris-HCl pH 6.8, 2% (w/v) SDS, 50 mM dithiothreitol (DTT), 2 mM EDTA, 0.5 mM PMSF), boiled for 10 minutes. Proteins were resolved by SDS-PAGE, transferred onto nitrocellulose membranes, and processed for immunoblotting with primary and secondary antibodies at concentrations indicated in **Table 3-1.** Membranes were scanned using an Odyssey CLx infrared imaging system. Comparable loadings among various cell lines were confirmed by immunoblotting of the same membrane with anti-actin antibodies.

3.2.5 Immunofluorescence

Cells were grown to 80% confluency on glass coverslips and processed for immunofluorescence staining as described previously (70, 111). Briefly, coverslips were rinsed with cold PBS, fixed with 3.7% formaldehyde solution and permeabilized with cytoskeletal extraction buffer (CSK; 50 mM NaCl, 300 mM sucrose, 10 mM PIPES pH 6.8, 3 mM $MgCl_2$, 0.5% Triton X-100, 1.2 mM PMSF, and 0.1 mg/mL DNase and RNase) for 7 minutes. Coverslips were blocked with 4% goat serum and 50 mM NH_4Cl in PBS, rinsed with PBS-BSA and incubated with primary antibodies for 1 hour, followed by 30 minutes in species specific secondary antibodies **(Table 3-1)**. Nuclei were stained with 1:2000 DAPI. Coverslips mounted in elvanol containing 0.2% paraphenylene diamine (PDD, w/v) and viewed using a 40x objective of a Zeiss confocal microscope.

3.2.6 Co-immunoprecipitation

All steps were carried out at 4C. Confluent 100 mm culture dishes were extracted with 1 mL RIPA buffer as described above. Cells were removed from the plates and centrifuged at 48,000 x g for 10 minutes. The resulting supernatant was divided into equal aliquots. Duplicate aliquots were incubated with 50 µL protein A/G (Pierce, Canada), anti-p53 or anti-plakoglobin antibodies (**Table 3-1)** and incubated overnight on a rocker-rotator. Beads containing immune complexes were washed three times with RIPA buffer and immune complexes eluted in hot 4X-SDS sample buffer. Equivalent amounts of total cellular proteins immunoprecipitated from each cell line were loaded onto SDS-polyacrylamide gels and processed for immunoblot using p53 and plakoglobin antibodies.

3.2.7 Preparation of GST-plakoglobin

A construct encoding pGEX-TEV-PG was kindly provided by Dr. William Weis (158). To express PG-GST protein, *Escherichia coli* DH5α cells were transformed by pGEX-TEV-PG constructs. Transformed cells were grown in Luria-Bertani broth at 37°C to an A_{600} of 0.6–0.8 and induced with 0.5 mM IPTG (isopropyl-β-D-1-thiogalactopyranoside, Thermo Fisher, Canada). Cultures were grown for an additional 6 hours at 30°C, harvested by centrifugation at 4,000 x g at 4°C for 12 min and the supernatants discarded. Pellets were resuspended in 6 mL of cold bacterial lysis buffer (500 mM NaCl, 0.5% NP-40, 50 mM Tris-HCl pH 7.6, 5 mM EDTA, 5 mM EGTA, 1 mg/mL lysozyme, 10 mM DTT, 2.5 U/mL DNase, 1 mM PMSF and an EDTA-free protease inhibitor cocktail tablet) and lysed via sonication. Lysates were centrifuged at 10,000 x g for 25 min at 4°C and the supernatants were divided into 1 mL aliquots, snap frozen and stored at -80°C.

3.2.8 PG-GST purification and GST pull-down assay

A one mL aliquot of PG-GST bacterial lysate was incubated with 150 µL of glutathione sepharose beads (GE Life Sciences) on a rocker-rotator at 4°C for 6 hours. Beads were centrifuged at 21,000 x g for 1 min and supernatants were aspirated. Beads were washed 3x using cold KCl-PBS (0.137 M NaCl, 0.0027 M KCl, 0.01 M Na_2HPO_4, 0.0018 M KH_2PO_4) and stored in KCl-PBS at 4°C.

Cells from 100 mm cultures of H1299 and H1299-p53-(R175H, R175H-Q167A, R175H-R248A, R175H-Q167A-R248A) transfectants were extracted in 1 mL RIPA lysis buffer for 20 min on a rocker-rotator at 4°C. The lysates were centrifuged at 48,000 x g for 10 min at 4°C and supernatants were removed. For pull down assays, 900 µL of cell lysates were mixed with 40 µL PG-GST or GST (control) beads and incubated on a rocker rotator for 4-6 hours at 4°C. The beads were washed 3x with PBS-KCl buffer (0.137 M NaCl, 0.0027M KCl, 0.01 M Na_2HPO_4, 0.0018 M KH_2PO_4), eluted with 4x SDS sample buffer, and processed for immunoblot using p53 and plakoglobin antibodies.

3.2.9 *In vitro* invasion assays

Matrigel invasion assays were performed according to the manufacturer's protocol (Corning, Life Sciences). For each cell line, 5×10^4 cells in 0.2 mL serum-free media were plated in the top compartment of Matrigel-coated invasion chambers (8 µm pore PET membrane). Fibroblast conditioned media (0.8mL) was added to the bottom chambers and plates were incubated overnight at 37°C in 5% CO_2. After 24 hours, inserts were stained using NovaUltra™ Hema-Diff Stain Kit (IHC World Life Science Products & Services, USA) following manufacturer's protocol. Following staining, inserts were viewed under an inverted microscope using a 20x objective lens and photographed.

The number of invaded cells was counted in seven random fields for each membrane using NIH ImageJ Cell Counter software. Migration and invasion results are presented as means ± SD in histograms.

3.2.10 Statistical data analysis

All quantitative data were presented as mean ± standard deviation (SD). Statistical significance between groups were assessed using Student's t-test for all assays.

All biochemical experiments were repeated at least 3-6 times and the Figures are representative of one typical experiment for each assay. All functional assays were repeated at least three times and the histograms represent the average of all assays.

Table 3-1: Antibodies and their dilutions in various assays

Antibody	Species	Assays			Manufacturer/Catalogue #
Primary		IP	WB	IF	
β-Actin	Mouse	-	1:1000	-	Santa Cruz # sc-47778
p53 (DO-1)	Mouse	1:100	1:1000	-	Santa Cruz # sc-126
p53 (FL-393)	Rabbit	-	-	1:100	Santa Cruz # sc-6243
Plakoglobin	Mouse	1:100	1:1000	1:100	BD Bioscience # 610253
Secondary					
AlexaFluor 790 Mouse anti-Rabbit (LC)	Mouse	-	1:30,000	-	Jackson Immuno Research # 211-652-171
AlexaFluor 790 Goat anti-Mouse (LC)	Goat	-	1:30,000	-	Jackson Immuno Research # 115-655-174
AlexaFluor 488 Goat anti-Mouse (H+L)	Goat	-	-	1:1000	Thermo Fisher # A-11029
AlexaFluor 546 Goat anti-Mouse (H+L)	Goat	-	-	1:1000	Thermo Fisher # A-11035

Table 3-2: Lowest molecular mechanics-generalized born surface area (MM-GBSA) binding energy (in kcal/mol) of the residue pairs in the modeled p53-R175H-plakoglobin complex.

p53 residue	Plakoglobin residue	MM-GBSA calculated binding energy (kcal/mol)
P62	H717	-6
L93	H717	-7
Q167	Y724	-5
Q167	D719	-15
E171	**N690**	-17
R174	P692	-14
G245	**N690**	-5
N247	**N690**	-5
N247	P688	-5
R248	D741	-10
R248	A740	-4
R248	E654	-23

3.3 RESULTS AND DISCUSSION

Previously, we have shown that plakoglobin interacted with wild type and mutant p53 via the DNA binding domain of p53 and C-terminal domain of plakoglobin (70). Remarkably, plakoglobin interaction with several mutant p53 expressed in carcinoma cell lines of different tissue origins restored their tumor suppressor activity *in vitro* (71, 72, 108, 109, 110, 111).

p53-R175H is the most frequently occurring p53 mutant in cancer in which the wild type p53 arginine 175 is mutated to histidine. p53-R175H is a structural/conformation mutant that changes the DBD conformation and disrupts p53 interaction with target DNA (42). p53-R175H is classified as a gain of function (GOF) mutant that not only loses the tumor suppressor activity, but also gains potent oncogenic functions (15, 42, 125, 135). Our previous studies have shown that when co-expressed, plakoglobin significantly reduced growth, migratory and invasive properties of p53-R175H expressing cells. This reduction of tumorigenic properties was associated with suppression of oncogenic genes expression such as *c-MYC* and *S100A4* (72). We hypothesized that plakoglobin interaction with conformational mutants potentially changes the conformation of the mutant protein and restores its binding to the promoters of wild type target genes. The larger implication of these observations is the potential of developing therapeutic agents that mimic mutant p53-plakoglobin interaction and restore tumor suppressor activity of p53 conformational mutants. In this study, we used *in silico* modeling and identified potential amino acid residues that mediate p53-R175H-plakoglobin interaction and validated the *in silico* model experimentally**.**

3.3.1 *In silico* modeling identified Q167, R248 on p53-R175H and N690 on plakoglobin as residues critical for the interaction between p53-R175H and plakoglobin

There are no experimentally resolved structures of the C-terminal residues 674-745 of plakoglobin, which are involved in the interaction with p53-R175H. COTH webserver was used to predict the relative position of p53-R175H core domain to plakoglobin. This only yielded the alpha-carbon positions of p53-R175H and residues 724-736 of plakoglobin (**Figure 3-1A**). Quark ab initio webserver was used to predict the structure of residues 674-723 and 737-745 that constitute the missing residues of plakoglobin C-terminal domain. To construct the protein complex, we assembled the experimentally resolved structure of armadillo domains, residues 126-

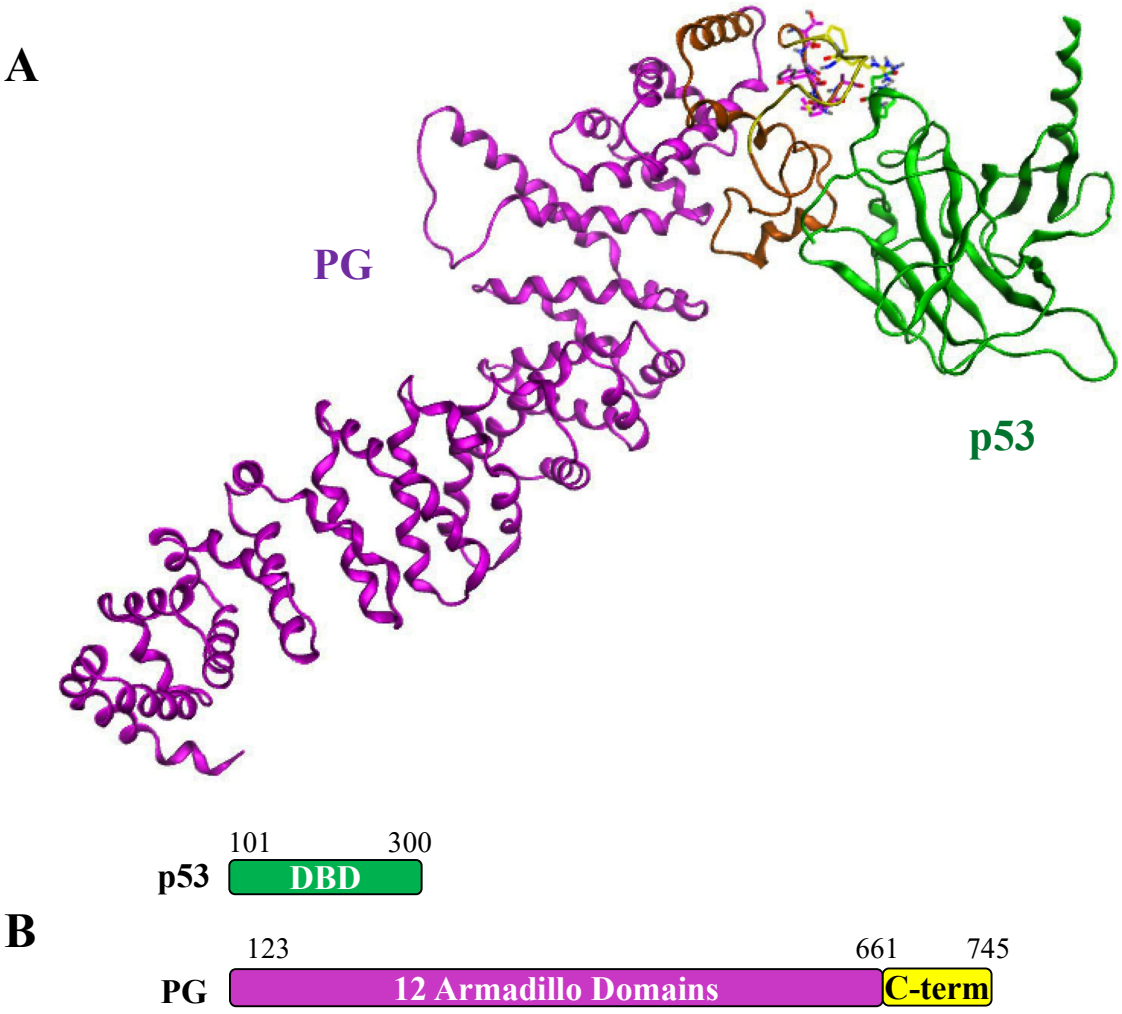

Figure 3-1. DNA binding domain of p53 interacts with the C-terminus of plakoglobin (PG). (A) Ribbon representation of the Armadillo domain of plakoglobin (PG) in complex with p53 DNA-binding domain (DBD). **(B)** Schematic of the p53 and plakoglobin domains used in the *in silico* modelling. p53 DNA-binding domain (residue 101-300) and plakoglobin armadillo and C-terminus (residue 661-745).

673, of plakoglobin (PBD; ID: 3IFQ), as well as the Quark *ab initio* (Quark. Bio.tools) predicted structures of residues 674-723 and 674-745 to the COTH predicted residues (158).

Due to the crudeness of the initial structure and the intrinsically disordered nature of the C-terminal domain of plakoglobin, it was important to equilibrate the protein structures and efficiently sample the conformational landscape of the complex. We, therefore, ran cMD for 150 ns for equilibration and to obtain parameters for aMD, which was performed for 200 ns. Sampled conformations were clustered based on the C-terminal residues closest to p53 with a RMSD cut-off of 2 Å to distinguish distinct complex conformations. A total of 101 clusters were obtained. The MM-GBSA binding energy of each cluster was calculated. The distribution of the size of each cluster and its average binding energy is shown in **Figure 3-1B.** Cluster 6 had the lowest average MMGBSA binding energy between p53-R175H and plakoglobin of -49 kcal/mol (**Figure 3-1).** We also decomposed the calculated average binding energy to identify the residue pairs that contributed the most to the interaction (**Table 3-2).** Our results indicate that R248 and Q167 of p53-R175H as well as N690A of plakoglobin contributed the most to the total binding energy of the complex. To validate this prediction, site-directed mutagenesis was performed to substitute these residues by alanine (A). We then examined the expression and localization of p53, its interaction with plakoglobin and its effect on the invasive properties of p53-R175H.

The representative structure of cluster 6 is shown in **Figure 3-2A**. Several hydrogen bond networks can be observed at the interaction interface of the two proteins (**Figure 3-2B** and **C**). Specifically, hydrogen bonds are formed between the side-chains of Q167 (p53) and D719 (plakoglobin) while the backbone of D719 forms an intra-chain hydrogen bond with the side-chain of H717 (**Figure 3-2B**). Additionally, a hydrogen-pi interaction is formed between the side-chain of H717 (PG) and backbone of L93 of p53 (**Figure 3-2B**). Furthermore, a dense hydrogen-bond network between residues P692 (PG)-R174 (p53)-E171 (p53)-N690 (PG)-G245 (p53)-N247(p53) is formed, which would stabilize the interaction between the two proteins. Additionally, a salt bridge is formed between R248 of p53 and E654 of plakoglobin and another between R174 and E171 of p53 (**Figure 3-2C**). To validate this prediction, we performed site-directed mutagenesis of these residues and assessed the binding of the two proteins.

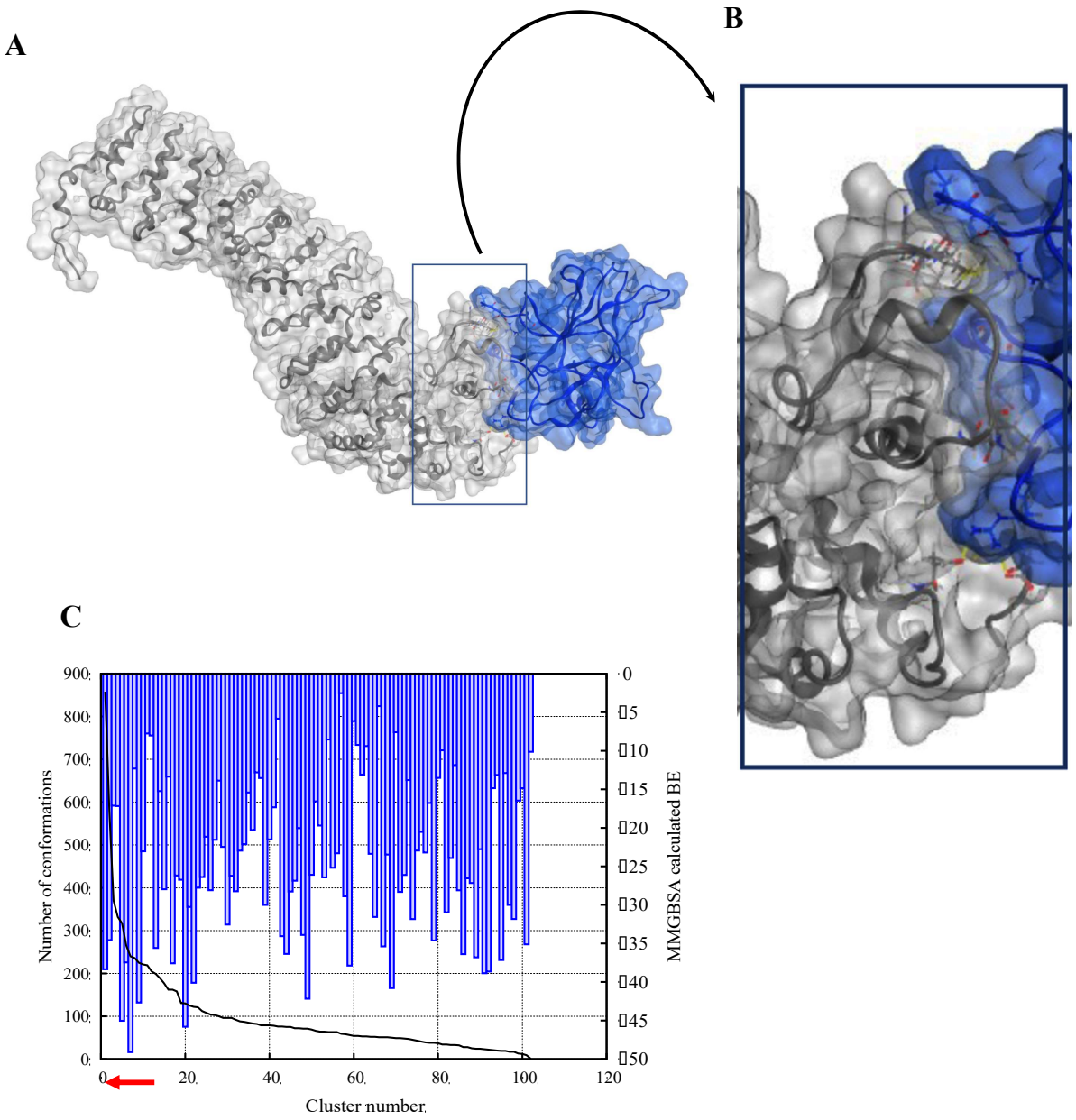

Figure 3-2. (A and B) Ribbon representation of the plakoglobin **(grey)** in complex with the p53-R175H DBD **(blue)** in the representative structure of the least binding energy cluster. Dark gray bands represent Armadillo domains. **(C)** A plot demonstrating the number of conformations of the complex in each cluster and the corresponding average binding energies of each cluster. **Cluster 6 (red arrow)** has the lowest binding energy of -49 kcal/mol.

3.3.2 Expression and subcellular localization of p53-(R175H, R175H/Q167A, R175H/R248A and R175H/Q167A/R248A) with and without plakoglobin in H1299 cells

To validate the *in silico* model, site-directed mutagenesis was used to develop plasmids encoding p53-R175H -Q167A, p53-R175H-R248A, p53-R175H-Q167A-R248A and PG-N690A mutant proteins. These plasmids were used to generate transient and stable H1299-p53-R175-(Q167A or R248A or Q167A-R248A) transfectants expressing various forms of p53-R175H alone or together with either PG-WT or PG-N690A.

Western blot (**Figure 3-3A**) using p53 and plakoglobin antibodies and total cellular extracts (TCEs) from transfectants expressing p53 alone or together with plakoglobin confirmed similar expression of both proteins in various transfectants.

Immunofluorescence staining using p53 antibodies showed primarily nuclear localization of p53 in cells expressing only p53-(R175H, R175H-Q167A, R175H-R248A and R175H-Q167A-R248A) only (**Figure 3-3B, - Plakoglobin**). Double immunofluorescence staining with p53 and plakoglobin antibodies in transfectants co-expressing both proteins (**Figure 3-3B, + Plakoglobin)** showed that while p53 was mainly localized to nuclei, it was also detected in the cytoplasm. This p53 cytoplasmic staining was more prominent in H1299-PG-p53-R175H and PG-p53-R175H-R248A cells relative to H1299-PG-p53-R175H-Q167A and PG-p53-R175H-Q167A-R248A transfectants (**Figure 3-3B, + Plakoglobin**).

Plakoglobin staining in all mutants showed distinct membrane localization and cytoplasmic/nuclear distribution typical of this protein. The membrane localization of this protein is consistent with its role in cell-cell adhesion via its participation in the formation of adherens junction and the desmosome, whereas its cytoplasmic/nuclear distribution is associated with signaling functions (85). Also, we detected some co-distribution of plakoglobin and p53 in H1299-PG-p53-R175H, PG-p53-R175H-R248A and PG-p53-R175H-Q167A-R248A cells (**Figure 3-3B, + Plakoglobin, arrows**). The co-distribution of p53 and plakoglobin in various cellular compartments is consistent with our previous observations that demonstrated p53-plakoglobin interaction in both the cytoplasm and nuclei of different carcinoma cells expressing various p53 mutants (15-17). Together, these results showed that substituting Q167 and R248 by alanine in p53-R175H does not interfere with the p53-R175H protein expression and nuclear localization.

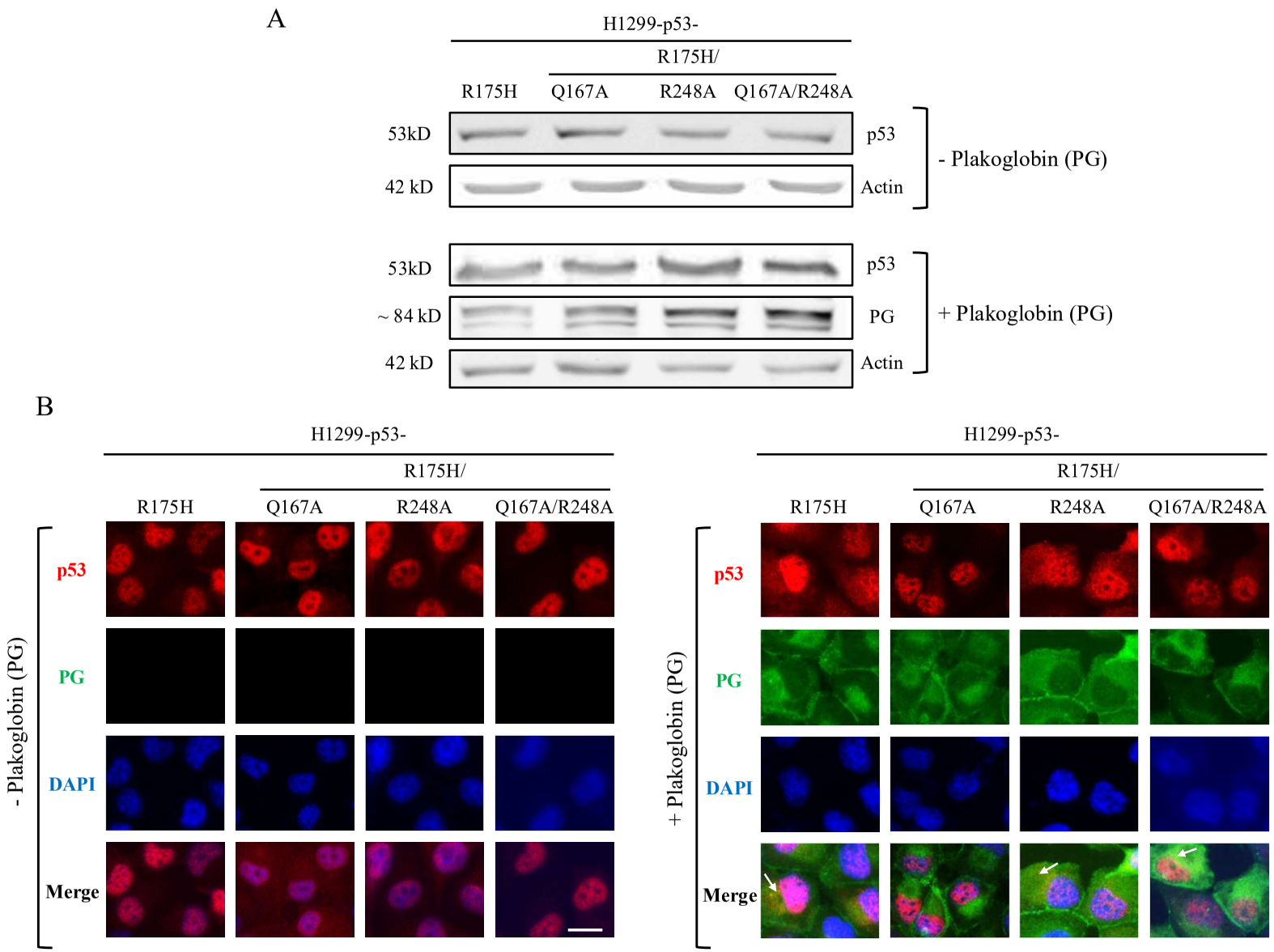
A
H1299-p53-
R175H/
R175H
Q167A
R248A
Q167A/R248A
53kD
p53
42 kD
Actin
- Plakoglobin (PG)
53kD
p53
~ 84 kD
PG
42 kD
Actin
+ Plakoglobin (PG)
B
H1299-p53-
R175H/
R175H
Q167A
R248A
Q167A/R248A
- Plakoglobin (PG)
p53
PG
DAPI
Merge
H1299-p53-
R175H/
R175H
Q167A
R248A
Q167A/R248A
+ Plakoglobin (PG)
p53
PG
DAPI
Merge

Figure 3-3. p53 and plakoglobin (PG) protein expression and localization in H1299-p53-R175H, p53-R175H/Q167A, p53-R175H/R248A, and p53-R175H/Q167A/R248A transfectants.
A. Total cellular extracts from H1299 transfectants expressing p53(R175H, R175H/Q167A, R175H/R248A, or R175H/Q167A/R248A) without **[Top two panels, [- Plakoglobin (PG)]** or with plakoglobin **[Bottom three panels, [+Plakoglobin (PG)]** were processed for immunoblot using p53 and plakoglobin antibodies. Beta-actin was used as a loading control.

B. Stable H1299 transfectants expressing various forms of p53- R175H without **[Left, [- Plakoglobin (PG)]** or with plakoglobin **[Right, [+Plakoglobin (PG)]** were grown to confluence on coverslips, fixed, permeabilized, and processed for immunofluorescence staining using p53 (Red) and plakoglobin (Green) antibodies followed by species-specific secondary antibodies. Nuclei were stained with DAPI (Blue). Bar, 7 μm.

3.3.3 Substitution of Q167 and R248 by alanine in p53-R175H protein reduced its interaction with plakoglobin

We performed co-immunoprecipitation (**Figure 3-4)** and GST pull down (**Figure 3-5)** experiments to examine whether substituting Q167 and R248 with alanine individually or together in p53-R175H affected its interaction with plakoglobin. H1299 cells were transiently co-transfected with plakoglobin and various p53-R175H constructs. Twenty-four -36 hours post transfection, equal amount of cellular total extract from various transfectants were processed for sequential immunoprecipitation and immunoblotting with p53 and plakoglobin antibodies. Immunoblotting of total cellular extracts (TCEs) from various transfectants showed similar level of p53 and plakoglobin expression among all plakoglobin-p53-R175H transfectants [H1299-PG-p53- (R175H, R175H-Q167A, R175H-R248A and R175H-Q167A-R248A)] (**Figure 3-4, TCE, IB: p53, PG, actin**).

Immunoprecipitation assays detected comparable levels of p53 among various transfectants when p53 immunoprecipitates were blotted with p53 antibodies. In contrast, immunoblotting of plakoglobin immunoprecipitates with p53 antibodies detected significantly lower amount of p53 co-precipitated with plakoglobin in p53-R175H- (Q167A, p53-R175H-R248A and p53-R175H-Q167A-R248A) expressing cells relative to PG-p53-R175H transfectants. Compared to p53-R175H, the plakoglobin co-precipitated p53 was reduced by 70%, 60% and 80% in p53-R175H-Q167A, p53-R175H-R248A and p53-R175H-Q167A-R248A transfectants, respectively (**Figure 3-4, IP)**.

Results of co-immunoprecipitations studies were further confirmed by GST-pull down assays (**Figure 3-5**). Here, we used PG-GST beads to pull down p53 from equal amount of cellular lysate from transfectants expressing p53-R175H and p53-R175H- (Q167A, R248A, Q167A-R248A. As shown in **Figure 3-5**, relative to p53-R175H, the amount of p53 pulled down by PG-GST beads was reduced by 30%, 50% and 60% in p53-R175H-Q167A, p53-R175H-R248A and p53-R175H-Q167A-R248A transfectants, respectively. Overall, the results of these two independent assays showed that Q167 and R248 substitution by alanine reduced the binding of plakoglobin to p53-R175H.

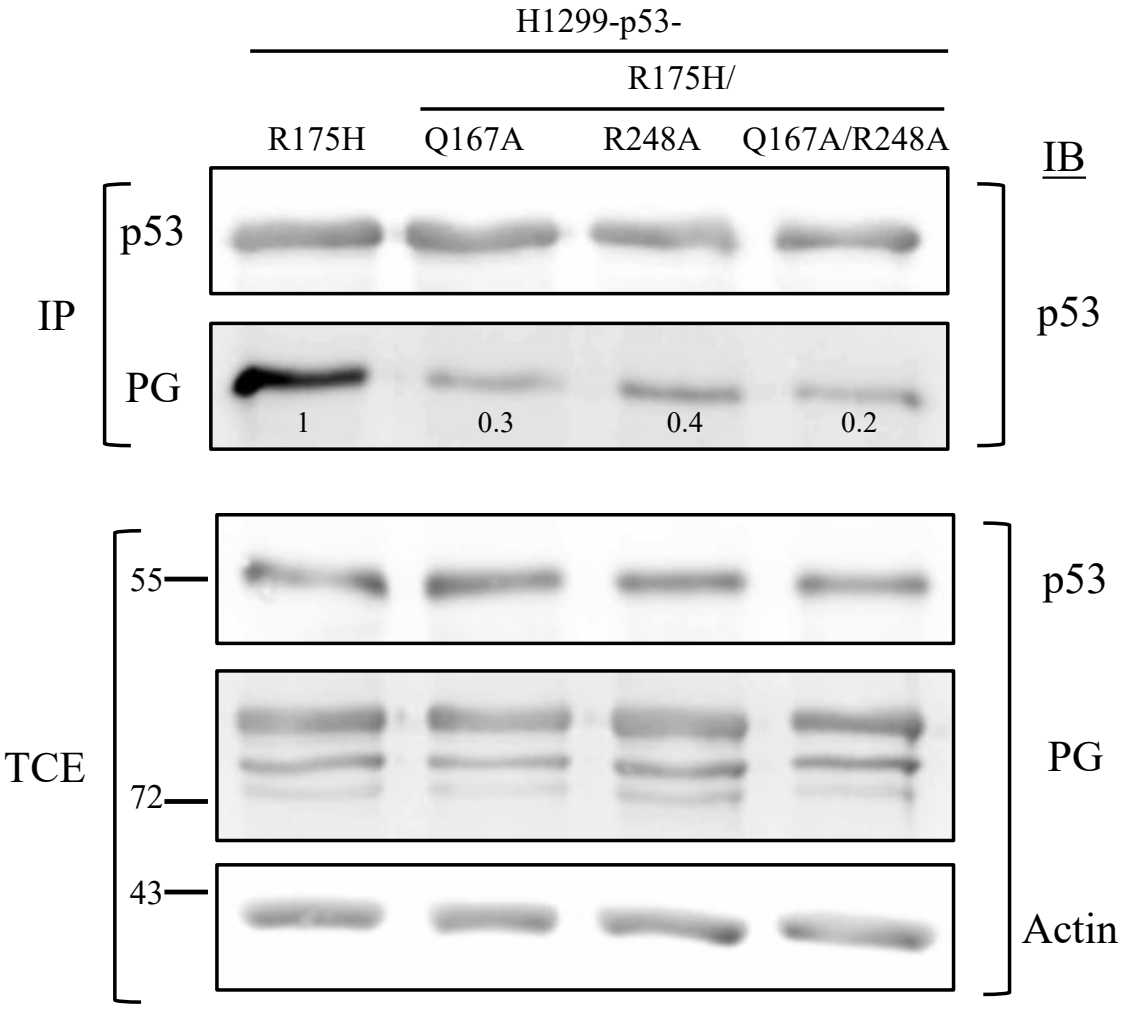

Figure 3-4. Substitution of Q167 and R248 residues by alanine (A) in p53-R175H reduced its interaction with plakoglobin (PG). Total cellular extracts **(TCE)** from H1299 cells co-expressing plakoglobin with various forms of p53-R175H, R175H/ (Q167A, R248A, or Q167A/R248A) were processed for sequential immunoprecipitation (**IP**) and immunoblotting (**IB**) using p53 and plakoglobin antibodies. Relative intensity of plakoglobin protein bands immunoprecipitated with p53 antibody were quantitated using NIH ImageJ program. Beta-actin was used as loading control.

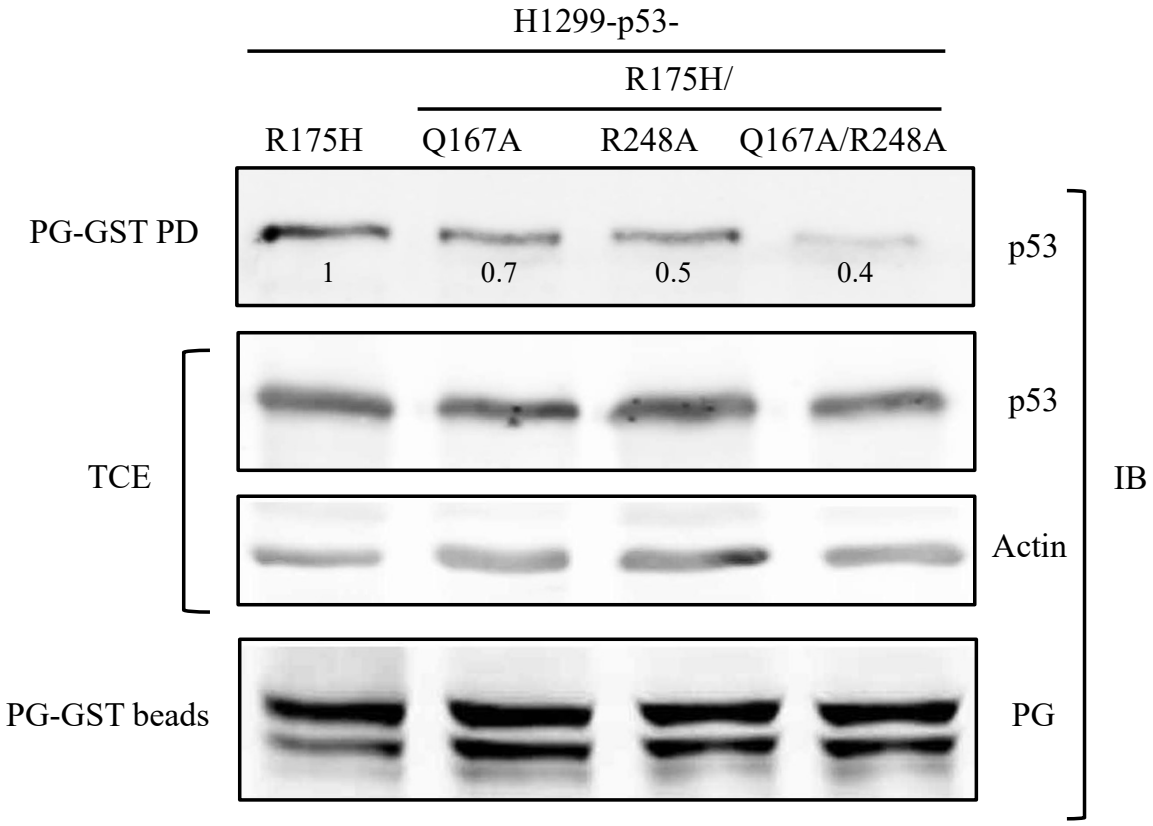

Figure 3-5. Substitution of Q167 and R248 residues by alanine (A) in p53-R175H reduced its association with GST-tagged plakoglobin (PG-GST). Total cellular extracts **(TCE)** from H1299 cells expressing various forms of p53-R175H, R175H/ (Q167A, R248A, or Q167A/R248A) were incubated with GST-tagged plakoglobin (**PG-GST**) and processed for GST-pull down assays **(PG-GST PD)** and immunoblotting **(IB)** with p53 and plakoglobin antibodies. Relative intensity of p53 protein bands pulled down with PG-GST were quantitated using NIH ImageJ program. Beta-actin was used as a loading control.

3.3.4. Plakoglobin asparagine 690 substitution by alanine has no effect on its binding to p53-R175H.

The 3D molecular dynamic modeling predicted asparagine (N) 690 in plakoglobin as being important in plakoglobin-p53-R175H interaction **(Table 3-2)**. To test the validity of this prediction, duplicate cultures of H1299-p53-R175H cells were transfected with PG-WT or PG-N690A. Transfectants were then processed for co-immunoprecipitation followed by immunoblotting with p53 and plakoglobin antibodies. As shown in **Figure 3-6**, immunoblotting of the total cellular extracts (TCEs) from H199-p53-R175H- PG-WT or PG-N690A transfectants showed similar level of PG and p53. Similarly, immunoblotting of plakoglobin immunoprecipitates with p53 antibodies detected similar levels of p53 in H199-PG-WT-p53-R175H and PG-N690A-p53-R175H transfectants (**Figure 3-6**). Overall, these results showed N690A substitution in plakoglobin has no detectable effect in its interaction with p53-R175H.

3.3.5 Plakoglobin co-expression decreased invasiveness of all p53-R175H/(Q167, R248, Q167/ R248) expressing H1299 cells

Previously, we have demonstrated that plakoglobin interaction with several p53 mutants in various carcinoma cell lines restored mutant p53 tumor suppressor function *in vitro.* Specifically, we have shown that while p53-R175H expression in H1299 cells increased cellular migration and invasion and plakoglobin co-expression in H1299-PG-p53-R175H transfectants significantly reduced these properties by >70% (72). Based on these observations, we performed invasion assays to determine if the reduced plakoglobin interaction with p53-R175H-(Q167A, R248A, Q167A-R248A) transfectants affected their invasiveness *in vitro* (**Figure 3-7)**.

Matrigel transwell invasion assays showed no difference in the invasiveness of H1299-R175H-Q167A transfectants relative to H1299-R175H cells. In contrast, the number of invaded cells increased by ~43% in both H1299-p53-R175H-R248A and p53-R175H-Q167A-R248A cell lines (**Figure 3-7).** R248 residue in p53-WT is directly involved in its binding to DNA. Mutations in this residue are known as hotspot p53 GOF contact mutants and many of them have been shown to gain oncogenic functions and activate tumorigenic and metastatic pathways (42, 184, 201, 202).

Among various mutations in R248 residue (R248W, R248Q, R248P, R248G, R248L) p53-R248L in which arginine is mutated to leucine (L), is biochemically similar to alanine substitution

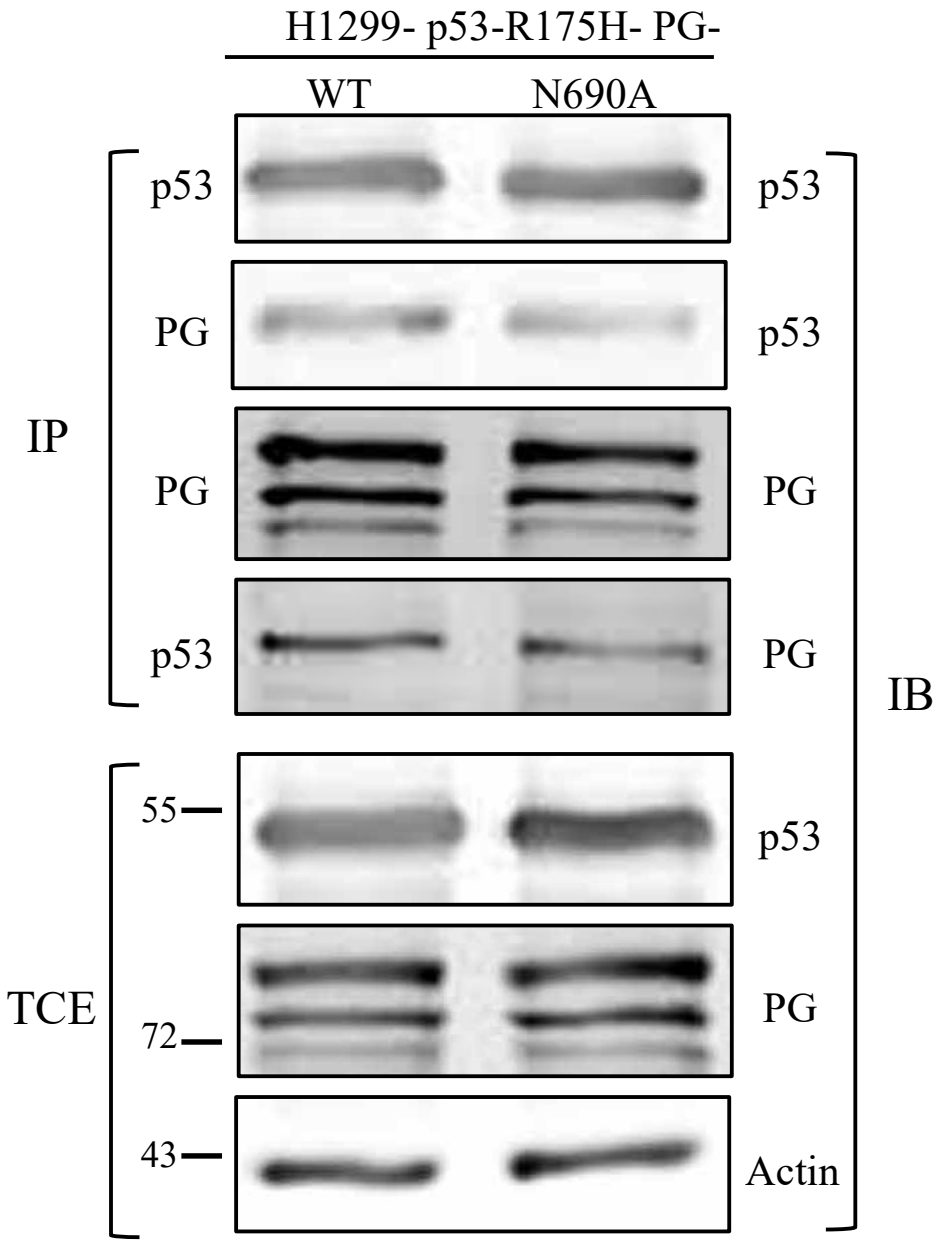

Figure 3-6. Plakoglobin (PG) asparagine 690 substitution by alanine (PG-N690A) does not interfere with plakoglobin -p53-R175H interaction. Total cellular extracts **(TCE)** from H1299-p53-R175H cells co-expressing **PG-WT** or **PG-N690A** were processed for sequential immunoprecipitation (**IP**) and immunoblotting (**IB**) using p53 and plakoglobin antibodies. Beta-actin was used as loading control.

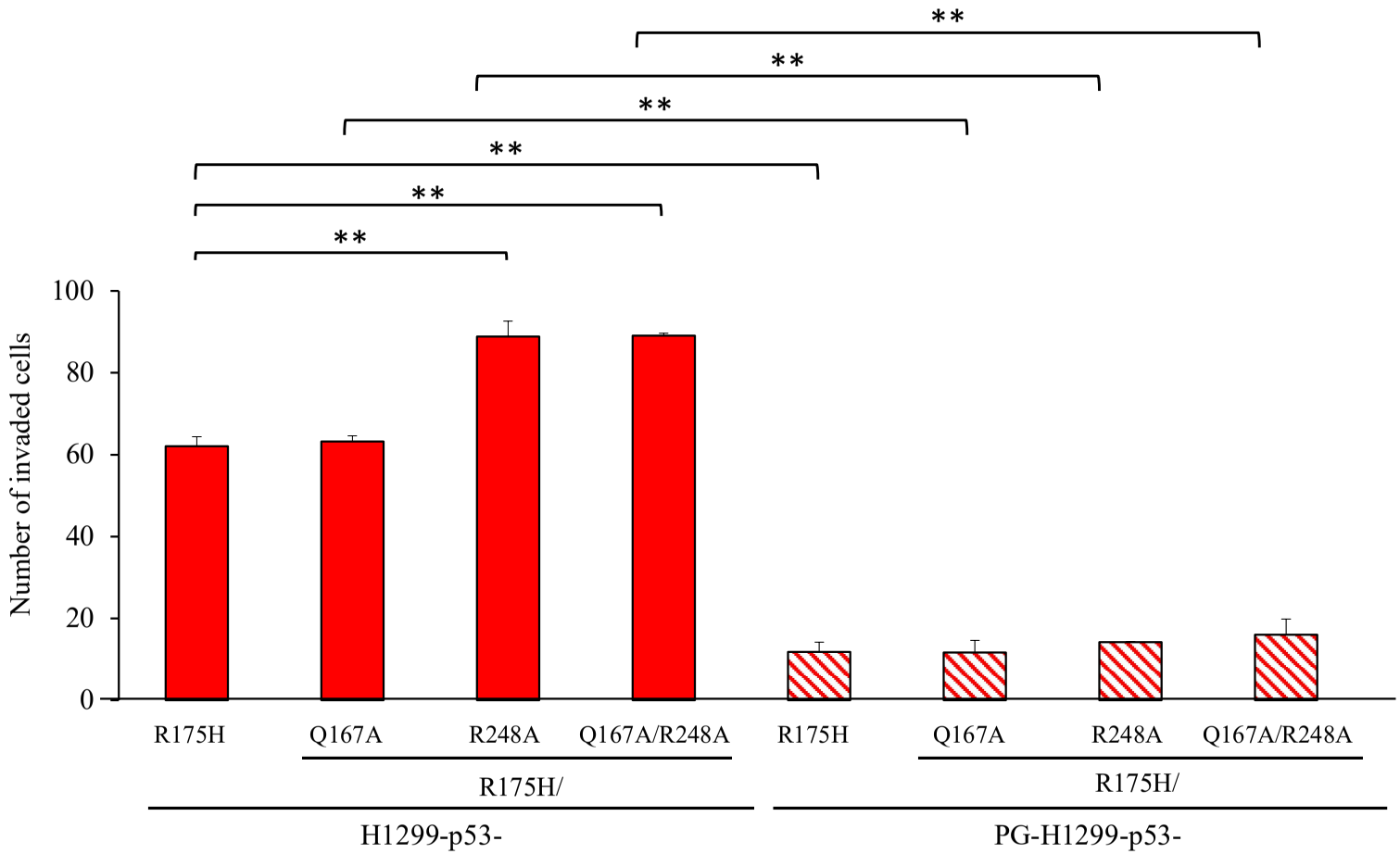

Figure 3- 7. Decreased *in vitro* invasiveness of H1299-p53-R175H and H1299-p53-R175H/ (Q167A, R248A, Q167A/R248A) transfectants by plakoglobin (PG) co-expression transfectants. Twenty-four- hour invasion assays were performed in triplicates in Matrigel coated transwell membranes. Membranes were fixed, stained and the number of invaded cells were counted in five random fields for each membrane using the ImageJ Cell Counter program and averaged. Histograms represent the average ± SD of the number of invaded cells for each cell line. **p <0.02.

used in the current study. R248L mutant has been shown to impair UV-induced apoptosis in glioblastoma cell lines and to promote inflammation and chemotaxis in glioblastoma xenografts (203, 204). The overexpression of DNA methyltransferase 1 (DNMT1) has been suggested to be a mechanism for oncogenicity of p53-R248L and associated with poor prognosis in lung cancer patients (205). Using H1299 cells, Lin *et al*. showed DNMT1 expression was suppressed by the exogenous expression of p53-WT but not p53-R248L. The overexpression of DNMT1 in H1299-p53-R248L cells led to the hypermethylation of several tumor suppressor genes including p16 (205). Together, these studies are indicative of tumorigenic properties of p53-R248L either by GOF or loss of p53-WT function. Interestingly, DNMT (1, 3A and 3B) has been shown to downregulate the plakoglobin gene (*JUP*) (206), which has been associated with metastasis in many cancers (85, 94).

The increased invasiveness of p53-R175H-R248A and p53-R175H-Q167-R248A transfectants may be explained by the presence of a conformational and a contact mutant in the same protein and acquiring new oncogenic properties including epigenetic modification of growth/metastasis regulating genes. Interestingly, when plakoglobin was co-expressed with any of p53-R175H constructs, invasiveness was significantly reduced by >80% in all transfectants.

In summary, our data from *in silico* modeling and the experimental results suggested that amino acid residues Q167 and R248 are important for p53-R175H interaction with plakoglobin. However, invasion assays showed cells expressing p53-R175H-Q167A exhibited similar invasiveness as p53-R175H expressing cells, whereas transfectants expressing p53-R175H-R248A or p53-R175H-Q167A-R248A constructs showed increased invasiveness relative to p53-R175H cells. This suggests that while Q167A did not change tumorigenicity of p53-R175H, R248A increased R175H tumorigenic properties. Plakoglobin co-expression reduced invasiveness of all transfectants significantly and similarly regardless of p53 status. The reduction in the invasiveness of cells expressing p53-R175H was not surprising and was consistent with our previous observations (72). However, the reduced invasiveness of cells expressing various alanine substituted residues and exhibiting decreased PG-p53-R175H interaction was somewhat unexpected and warrants further investigation. Moreover, considering that Q167A had no effect on R175H invasiveness, while R248A or Q167A-R248A significantly increased invasiveness, it

was surprising that plakoglobin co-expression reduced invasiveness of all transfectants to similar degrees.

Our previous studies suggested that plakoglobin binding to conformational mutants may potentially change their conformation into WT and restore the activation of p53-WT target genes (72). It may be possible that Q167A and R248A substitutions, individually or together, did not severely change the p53-R175H conformation. While these substitutions decreased plakoglobin-p53-R175H interaction, as a transcriptional complex, there may exist a low threshold requirement to trigger changes in the expression of genes involved in tumor suppression. Alternatively, the tumor suppressing effect induced by plakoglobin may be, at least partially, independent of its interaction with p53-R175H. We previously showed that plakoglobin expression in H1299-p53-R175H cells with upregulated β-catenin level, decreased the expression *c-MYC and S100A4*, well-known tumor/metastasis promoter and targets of Wnt/β-catenin, by increasing β-catenin degradation and decreasing its nuclear distribution (72). It is also possible that plakoglobin-mediated tumor suppressing effects through p53-R175H may not be dependent on their interaction, but through alternative mechanisms such as regulation of gene products induced by p53-R175H expression. In this respect, recent studies have shown that oncogenic activities of mutant p53 are mediated by its interplay with hypoxia and HIF signaling pathways (207) and plakoglobin inhibits the stability and transcriptional activity of HIF2α (154).

3.4. CONCLUSION

Overall, our studies have suggested that plakoglobin can restore tumor suppressor activity of conformational p53 mutants. However, the larger implication of the studies presented here is the potential for exploring plakoglobin-mutant p53 interaction for development of cancer therapeutics. The advantage of developing compounds that mimic mutant p53-pakoglobin interaction to restore the tumor suppressor activity is that these compounds may have the benefit of representing a naturally occurring biological interaction that positively regulates p53 tumor/metastasis suppressor function with less potential side effects. Furthermore, since plakoglobin also interacts with p53-WT and regulates p53-WT gene expression (70, 71, 108), it may be less likely to cause detrimental effects in normal cells expressing p53-WT. This study may

provide a framework for future research into utilizing plakoglobin-p53 interaction as a potential p53-targeted therapy.

CHAPTER 4: GENERAL CONCLUSION AND FUTURE STUDIES

4.1 Overview

p53 is one of the most important tumor suppressors and one of the most frequently mutated protein found in cancer cells. Single missense mutations in the DBD of p53 can lead to altered protein conformation, change in its binding affinity to interacting partners, and loss of tumor suppress and/or gain of oncogenic function (GOF) that contribute to tumorigenesis.(42) In general, there are two categorizes of GOF mutants: conformational and contact. Conformational p53 mutant loses WT-p53 conformation, making it incapable of DNA-binding whereas in contact mutants a single amino acid residue directly involved in DNA-binding is mutated.(42) Consistent with their differential mechanisms that compromise their DNA binding ability, studies have demonstrated that these two types of mutants promote carcinogenesis via different pathways. Since majority of tumors have non-functional or GOF mutants, significant effort is invested to develop p53 targeted therapies and drugs that either reactivate p53-WT function or restore tumor suppressor function of GOF mutants.(208) It is also clear that the efficiency of p53-targeted therapies, that aim to restore GOF mutants' tumor suppressor activity, may be dependent on whether they belong to the conformation vs. contact category.

Our laboratory has shown that plakoglobin, a dual cell-cell adhesion and signaling protein act as a tumor suppressor via several mechanisms one of which is by interacting with p53.[(70), (71), (72)] Plakoglobin has been shown to interact with both p53-WT and mutants (both conformational and contact) and its interaction with p53 mutants restores their tumor suppressor activity *in vitro.* The larger implication of our studies is the potential of plakoglobin as a therapeutic target in cancers.

In this thesis, we compared the effect of plakoglobin co-expression with p53 conformational and contact mutants in the same cellular background. Additionally, we furthered our understanding in p53-R175H and plakoglobin interaction by validating an *in silico* model of p53-R175H and plakoglobin interacting interface, which identified amino acid residues on both proteins that are critical for their interaction. Overall, characterization of the differential effect of plakoglobin in restoring tumor suppressor activity of conformational vs. contact mutants and validation of the *in silico* model of plakoglobin- p53-R175H conformational mutant have provided important insights for exploiting the potential of p53-plakoglobin interaction in development of cancer therapeutics.

4.2 Assessment of the differential Effect of Plakoglobin on Conformational vs. Contact p53 Mutants

Most frequent p53 conformational mutations occur on R175, G245, R249, and R282, residues, which are important for stabilization of p53 structure (via van-der Waal force, hydrogen bonding and electrostatic force). On the other hand, the most common contact mutations occur on R248 and R273 residues that are important for direct contact between p53 and DNA's minor and major grooves.(209) It is not clear whether the categorization of conformational and contact mutants are meaningful in the context of tumorigenicity and therapeutics. Currently, several compounds capable of restoring mutant p53 tumor suppressor activity such as APR-246 and COTI-2 have been identified and have completed phase 3 clinical trial for treatment of *TP53* mutant myelodysplastic syndromes (MDS) or in phase I trial for malignancies, respectively, as of Sept 2022**.** However, in many cases these compounds are not targeted to specific mutant types and is unclear how they restore their tumor suppressive function.

While our group has previously demonstrated that plakoglobin can interact with WT-p53 and several mutant p53s, and that this interaction can potentially participate in restoration of WT-p53 activities in several carcinoma cell lines, we lacked a direct comparison of the effect of plakoglobin on p53 conformational and p53 contact mutants in the same genetic and cellular background. The effects of mutant p53 expression are cellular context-dependent, and results from previous studies that used several cell lines expressing different mutant p53s can be complex to interpret and conclude. To this end, we established an *in vitro* cellular model by expressing p53-R175H or p53-R273H, with or without plakoglobin in the p53-null and plakoglobin deficient H1299 non-small cell lung carcinoma cell line. This model allowed unequivocal comparison on the effect of plakoglobin co-expression with either conformational or contact p53 mutant. In general, p53-R175H expression in H1299 cells led to strong oncogenic phenotypes, whereas p53-R273H expressing cells exhibited phenotypes more reflective of cells expressing p53-WT. Consistent with these observations, our data demonstrated that the tumor suppressing effect of plakoglobin is strongest when co-expressed with conformational p53-R175H mutant. Plakoglobin co-expression significantly suppressed p53-R175H tumorigenic properties such as cellular migration, invasion, and anchorage independent growth and these phenotypic changes were concurrent with decreased nuclear β-catenin level and increased NPM nuclear distribution. In

contrast, when co-expressed with p53-R273H contact mutant, plakoglobin only reduced anchorage-independent growth and this decrease was concurrent with reduction in pAkt level.

4.2.1 Plakoglobin decreases β-catenin nuclear distribution

Work from various groups including ours has shown that plakoglobin can regulate β-catenin level in the cytoplasm and its signaling activities in the nucleus. [91], [107], [156], [179] Our previous studies have also demonstrated that plakoglobin co-expression with p53-R175H increased β-catenin degradation, decreased nuclear β-catenin level and expression of Wnt/β-catenin target genes c-*MYC* and *S100A4*, concurrent with decreased cellular migration and invasion.(72) Here, we showed that plakoglobin co-expression with p53-R273H did not affect nuclear β-catenin level, which is consistent with the less tumorigenic properties of this mutant and its similarity to p53-WT with respect to its growth, migratory and invasive properties.

4.2.2 Plakoglobin increases NPM nuclear distribution

Similar to β-catenin, NPM is a nucleocytoplasmic protein that shuttles in and out of the nucleolus/nucleus and cytoplasm and based on its subcellular distribution has tumor suppressor or oncogenic function.[114], [117], [210] NPM plays important roles in the stability of p53 by interacting with p53, $p14^{ARF}$ and MDM2 and inhibiting MDM2-mediated p53 degradation.(117) Previously, we identified NPM as a differentially expressed protein in our proteomic analysis of carcinoma cell lines expressing no/low plakoglobin and their plakoglobin expressing transfectants.[108], [110] Further studies demonstrated that in these cells, the exogenously expressed plakoglobin interacted with NPM, increased its nuclear distribution, and concurrently decreased their oncogenic potential *in vitro*.(109) In keeping with these observations, plakoglobin expression increased nuclear NPM distribution in H1299 cells expressing p53-WT, -R175H and -R273H **(Chapter 2)**. Results from these studies suggested that plakoglobin may alter the localization of p53-interacting protein, and that this may associate with the decrease in tumorigenic properties we observe in these cells.

4.2.3 Plakoglobin and Akt

Activated AKT, pAKT, can promote tumorigenesis by activating pathways such as the mTOR signaling or the Wnt/β-catenin signaling.[211], [212] pAKT can also phosphorylate NPM and

promote dissociation of MDM2 from mutant p53 and increase mutant p53 stability.(118) Several studies have demonstrated p53-R273H mutant can promote anchorage independent growth.[213], [214], [159] Several studies have also shown specific elevation of pAkt level, but not the total Akt level, was elevated in several carcinoma cell lines expressing p53-R273H, and that this was associated with increased resistance to anoikis and cellular migration.[159, 215], [216] Consistent with these observations, we detected significantly increased pAkt level in H1299-p53-R273H cells relative to that of H1299-p53-WT cells. Plakoglobin co-expression with p53-R273H significantly decreased pAkt level and soft agar colonies formation in H1299-PG-p53-R273H cells without affecting their migratory and invasive properties. These observations suggested that plakoglobin may affect the Akt signaling pathway by regulation of Akt phosphorylation.

Together with the effect of plakoglobin on NPM and β-catenin cellular distribution, these observations suggest that conformational and contact mutant p53 contribute to tumorigenesis via distinctive pathways under same cellular conditions and that plakoglobin's co-expression differentially affected these pathways and the tumorigenic properties in cells expressing either type of mutant.

4.3 Validation of *in silico* model simulating p53-R175H and plakoglobin interaction

In silico modeling of p53-R175H and plakoglobin interaction identified Q167 and R248 residues in p53-R175H and N690 in plakoglobin as potentially important for their interaction. To validate the model prediction, we used site-directed mutagenesis to substitute the identified residues in both proteins with alanine and assessed the effects. Results of this study demonstrated that Q167A and R248A substitutions, whether individually or together, decreased p53-R175H interaction with plakoglobin by $\geq$ 50%. In contrast, substitution of N690 in plakoglobin by alanine had no effect on it binding to p53-R175H. Interestingly, despite the decreased interaction of plakoglobin with p53-R175H/Q167A, p53-R175H/R248A, and p53-R175H/Q167A/R248A relative to p53-R175H, plakoglobin co-expression decreased cellular invasion in all transfectants similarly. These results suggested that low threshold level of p53-R175H-plakoglobin interaction may be sufficient to promote tumor suppression. Alternatively, these observations may suggest that tumor suppression induced by plakoglobin co-expression may be independent of p53-

plakoglobin interaction, which is consistent with p53-independent tumor suppression function of plakoglobin.

4.4 Conclusion:

Overall, the studies in this thesis provided important framework for future research into utilizing plakoglobin interaction with p53 as a potential p53-targeted therapy. Our results demonstrated that plakoglobin conferred a preferential and significant decrease in tumorigenicity when co-expressed with conformational mutant p53-R175H. A possibility that may also be supported by the fact that plakoglobin still interacted (although significantly less) with p53-R175H in which the residues involved in their interaction were substituted by alanine. These observations may also be an indication of potential plakoglobin interaction with other conformational mutants.

Together, our studies suggest that plakoglobin may potentially repress p53 mutant oncogenic activities by at least two mechanisms; **(1)** regulation of subcellular localization and function of proteins involved in p53 (WT and mutant) growth regulating pathways and (**2)** modulation of p53 mutant target genes expression. **Figure 4-1** is a conceivable model of how plakoglobin may act as a tumor suppressor by interacting and regulating p53 (WT and mutants) tumor suppressor function. In this model, plakoglobin and β-catenin interact with cadherins in a mutually exclusive manner at the membrane to form adherens junction and maintain the integrity and function of epithelium. In normal cells, excess cadherin independent cytoplasmic β-catenin is ubiquitinated and degraded by the proteosome pathway**. (4-1.1a)** Plakoglobin and p53-WT promote, whereas mutant p53 inhibits the proteosomal degradation of excess cytoplasmic and oncogenic competent/nuclear β-catenin. Similarly, plakoglobin interact with and promotes nuclear localization of NPM and its tumor suppressor activity of NPM. **(4-1.1b)** If not degraded, β-catenin translocates into the nucleus and together with TCF/LEF activate the expression of tumor/metastasis promoting target genes. Plakoglobin counters the oncogenic function of β-catenin in the nucleus by binding to and replacing β-catenin in the β-catenin-TCF complex and inhibiting the expression of tumor promoting genes. **(4-1.2a)** Plakoglobin interacts with p53-WT and together they regulate the expression of genes involved in inhibition of tumorigenesis and metastasis. **(4-1.2b)** Plakoglobin interacts with the p53-R175H conformational mutant, potentially changes its conformation to wild-type and activates p53-WT growth inhibitory target genes expression while inhibiting the expression of oncogenic targets. **(4-1.2c)** Plakoglobin interacts

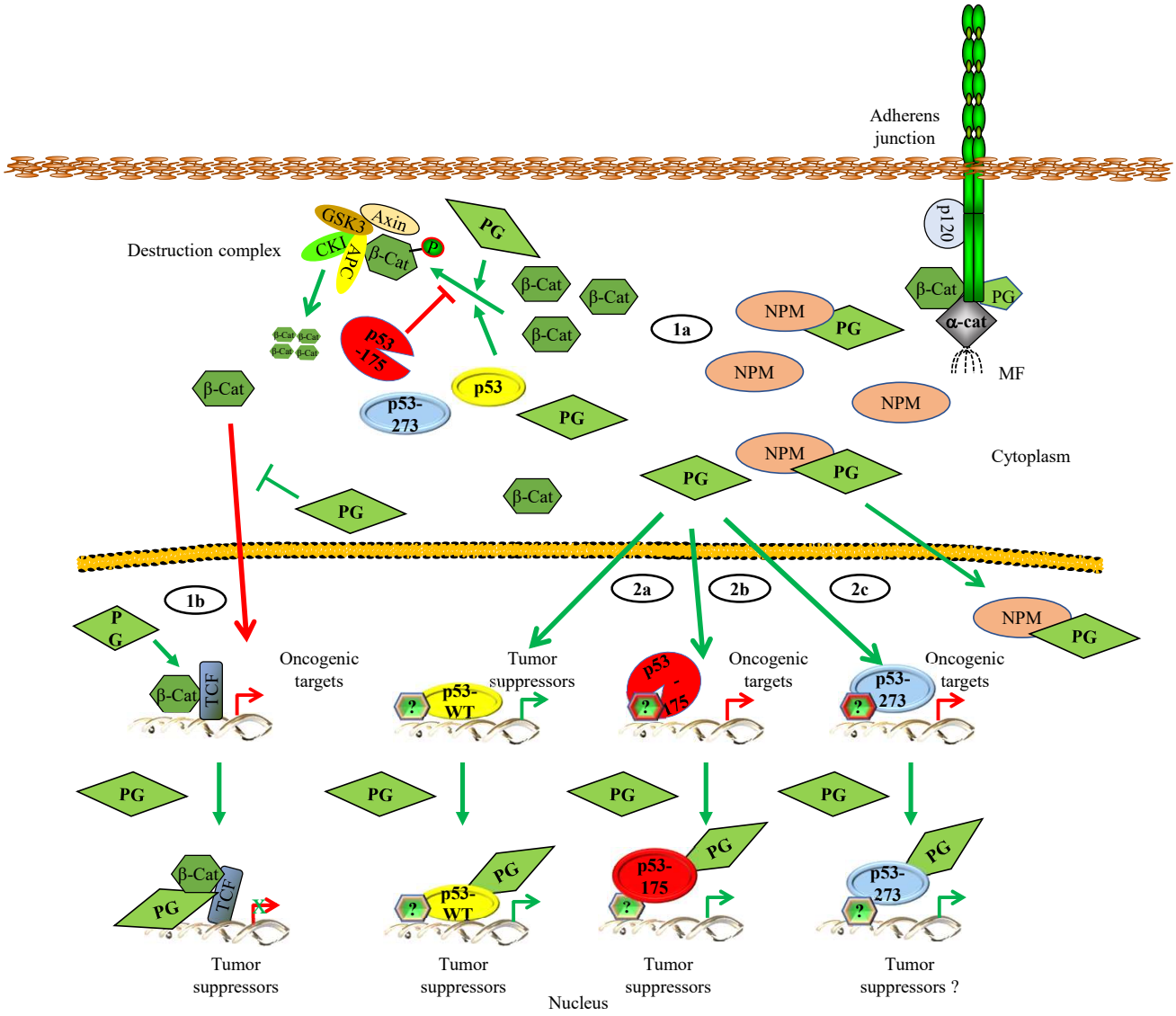

Figure 4-1. A potential model of plakoglobin tumor suppressor activity via regulation of gene expression and cell signaling in a p53-independent and p53-dependent manner. (**1a**) Plakoglobin (**PG**) and β-catenin (**β-cat**) interact with cadherins in a mutually exclusive manner and participate in the adherens junction formation. Excess cytoplasmic β-catenin is recruited to the destruction complex for phosphorylation, ubiquitination and proteasomal degradation. Plakoglobin and p53 promote cytoplasmic β-catenin degradation while mutant p53s inhibit this process; plakoglobin interferes with this inhibition via its interaction with mutant p53s. (**1b**) Excess cytoplasmic β-catenin translocates to the nucleus where it interacts with **TCF** and together they activate oncogenic gene transcription. Plakoglobin displaces β-catenin in the β-catenin/TCF complex and inhibits the activation of oncogenic genes. (**2a**) Plakoglobin interacts with p53-WT and together they regulate the expression of genes involved in suppression of tumorigenesis/metastasis. (**2b**) Conformational mutant $p53^{R175H}$ (**p53-175**) activates oncogenic targets. Interaction with plakoglobin changes the mutant conformation to wild-type and activation of tumor suppressor targets. **(2c)** Contact mutant $p53^{R273H}$ (**p53-273**) loses the ability to bind to p53-WT target DNA, and instead interacts with nuclear factors that activate oncogenic gene expression. Upon binding to plakoglobin, $p53^{R273H}$ oncogenic partners are replaced with nuclear factors that promote activation of growth/metastasis inhibitory targets. α-cat, α-catenin; MF, microfilaments; GSK3β, glycogen synthase 3β; CK1, casein kinase 1; APC, adenomatous polyposis coli; TCF, T-cell factor.

with the p53-R273H contact mutant and while it does not change its conformation, it may modify its interaction with co-activators that regulate the expression of its target gene(s) involved in tumorigenesis.

4.5 Future Directions

The overall goal of this project is to explore the potential therapeutic properties of plakoglobin and discover compounds that mimic the interaction of plakoglobin, an endogenous cellular protein, with mutant p53 and target cancer cells with minimal effects on healthy tissues. To this end and in collaboration with Drs. Tuszynski and West groups, we have screened protein-protein interaction modulator libraries and identified four compounds that potentially mimic plakoglobin and p53-R175H interaction. Future *in vitro* and *in vivo* assessment of the functional effects of these drugs on p53-R175H expressing cells will provide valuable information and insights into development of compounds that mimic plakoglobin-conformational p53 mutants interaction for effective p53-targeted cancer therapies.

Another future study, based on this thesis, is planned in collaboration with Dr. Jahroudi's team, we have obtained preliminary results which suggests a novel potential mechanism for p53-R175H-mediated tumorigenesis via activation of de *novo* expression of Von Willebrand Factor (VWF). VWF is a glycosylated protein released by endothelial cells to mediate platelet aggregation and blood coagulation during hemostasis.(217) VWF expression is normally restricted to endothelial cells and megakaryocytes, but recently has been detected in tumor cells of non-endothelial origin such as osteosarcoma, hepatocellular carcinoma, glioma and gastric cancer.[218, 219] Increased levels of VWF in primary tumor tissues of non-endothelial origin *in situ* was associated with increased metastasis and clinicopathologic staging.(218) These observations suggest that some cancer cells may gain *de novo* expression of VWF that facilitate the adhesion of cancer cells and platelets to endothelial walls and consequently promote their metastatic potential. Our preliminary results from qRT-PCR and immunofluorescence have shown that exogenous expression of p53-R175H but not p53-WT in H1299 cells induced VWF expression. Interestingly, co-expression of plakoglobin (H1299-PG-p53-R175H) significantly reduced *VWF* message in these cells. These observations propose a novel mechanism by which plakoglobin may act as a tumor suppressor and warrant further investigation.

BIBLIOGRAPHY

1. Lane DP, Crawford LV. T antigen is bound to a host protein in SV40-transformed cells. Nature. 1979;278(5701):261-3.
2. Parada LF, Land H, Weinberg RA, Wolf D, Rotter V. Cooperation between gene encoding p53 tumour antigen and ras in cellular transformation. Nature. 1984;312(5995):649-51.
3. Eliyahu D, Raz A, Gruss P, Givol D, Oren M. Participation of p53 cellular tumour antigen in transformation of normal embryonic cells. Nature. 1984;312(5995):646-9.
4. Jenkins JR, Rudge K, Currie GA. Cellular immortalization by a cDNA clone encoding the transformation-associated phosphoprotein p53. Nature. 1984;312(5995):651-4.
5. May P, May E. Twenty years of p53 research: structural and functional aspects of the p53 protein. Oncogene. 1999;18(53):7621-36.
6. Prokocimer M, Shaklai M, Bassat HB, Wolf D, Goldfinger N, Rotter V. Expression of p53 in human leukemia and lymphoma. Blood. 1986;68(1):113-8.
7. Finlay CA, Hinds PW, Tan TH, Eliyahu D, Oren M, Levine AJ. Activating mutations for transformation by p53 produce a gene product that forms an hsc70-p53 complex with an altered half-life. Mol Cell Biol. 1988;8(2):531-9.
8. Hinds PW, Finlay CA, Frey AB, Levine AJ. Immunological evidence for the association of p53 with a heat shock protein, hsc70, in p53-plus-ras-transformed cell lines. Mol Cell Biol. 1987;7(8):2863-9.
9. Hinds P, Finlay C, Levine AJ. Mutation is required to activate the p53 gene for cooperation with the ras oncogene and transformation. J Virol. 1989;63(2):739-46.
10. Finlay CA, Hinds PW, Levine AJ. The p53 proto-oncogene can act as a suppressor of transformation. Cell. 1989;57(7):1083-93.
11. Eliyahu D, Michalovitz D, Eliyahu S, Pinhasi-Kimhi O, Oren M. Wild-type p53 can inhibit oncogene-mediated focus formation. Proc Natl Acad Sci U S A. 1989;86(22):8763-7.
12. Cheng J, Haas M. Frequent mutations in the p53 tumor suppressor gene in human leukemia T-cell lines. Mol Cell Biol. 1990;10(10):5502-9.
13. Takahashi T, Nau MM, Chiba I, Birrer MJ, Rosenberg RK, Vinocour M, et al. p53: a frequent target for genetic abnormalities in lung cancer. Science. 1989;246(4929):491-4.
14. Romano JW, Ehrhart JC, Duthu A, Kim CM, Appella E, May P. Identification and characterization of a p53 gene mutation in a human osteosarcoma cell line. Oncogene. 1989;4(12):1483-8.

15. Stein Y, Rotter V, Aloni-Grinstein R. Gain-of-Function Mutant p53: All the Roads Lead to Tumorigenesis. Int J Mol Sci. 2019;20(24).
16. Kastenhuber ER, Lowe SW. Putting p53 in Context. Cell. 2017;170(6):1062-78.
17. Brady CA, Attardi LD. p53 at a glance. J Cell Sci. 2010;123(Pt 15):2527-32.
18. Li FP, Fraumeni JF, Mulvihill JJ, Blattner WA, Dreyfus MG, Tucker MA, et al. A cancer family syndrome in twenty-four kindreds. Cancer Res. 1988;48(18):5358-62.
19. Olivier M, Goldgar DE, Sodha N, Ohgaki H, Kleihues P, Hainaut P, et al. Li-Fraumeni and related syndromes: correlation between tumor type, family structure, and TP53 genotype. Cancer Res. 2003;63(20):6643-50.
20. Hanahan D. Hallmarks of Cancer: New Dimensions. Cancer Discov. 2022;12(1):31-46.
21. Hanahan D, Weinberg RA. Hallmarks of cancer: the next generation. Cell. 2011;144(5):646-74.
22. Hanahan D, Weinberg RA. The hallmarks of cancer. Cell. 2000;100(1):57-70.
23. Joerger AC, Fersht AR. The tumor suppressor p53: from structures to drug discovery. Cold Spring Harb Perspect Biol. 2010;2(6):a000919.
24. Lill NL, Grossman SR, Ginsberg D, DeCaprio J, Livingston DM. Binding and modulation of p53 by p300/CBP coactivators. Nature. 1997;387(6635):823-7.
25. Lee CW, Martinez-Yamout MA, Dyson HJ, Wright PE. Structure of the p53 transactivation domain in complex with the nuclear receptor coactivator binding domain of CREB binding protein. Biochemistry. 2010;49(46):9964-71.
26. Chi SW, Lee SH, Kim DH, Ahn MJ, Kim JS, Woo JY, et al. Structural details on mdm2-p53 interaction. J Biol Chem. 2005;280(46):38795-802.
27. Tibbetts RS, Brumbaugh KM, Williams JM, Sarkaria JN, Cliby WA, Shieh SY, et al. A role for ATR in the DNA damage-induced phosphorylation of p53. Genes Dev. 1999;13(2):152-7.
28. Shieh SY, Ikeda M, Taya Y, Prives C. DNA damage-induced phosphorylation of p53 alleviates inhibition by MDM2. Cell. 1997;91(3):325-34.
29. Khanna KK, Keating KE, Kozlov S, Scott S, Gatei M, Hobson K, et al. ATM associates with and phosphorylates p53: mapping the region of interaction. Nat Genet. 1998;20(4):398-400.

30. Inoue T, Geyer RK, Howard D, Yu ZK, Maki CG. MDM2 can promote the ubiquitination, nuclear export, and degradation of p53 in the absence of direct binding. J Biol Chem. 2001;276(48):45255-60.
31. Hoyos D, Greenbaum B, Levine AJ. The genotypes and phenotypes of missense mutations in the proline domain of the p53 protein. Cell Death Differ. 2022;29(5):938-45.
32. Toledo F, Krummel KA, Lee CJ, Liu CW, Rodewald LW, Tang M, et al. A mouse p53 mutant lacking the proline-rich domain rescues Mdm4 deficiency and provides insight into the Mdm2-Mdm4-p53 regulatory network. Cancer Cell. 2006;9(4):273-85.
33. Guha T, Malkin D. Inherited. Cold Spring Harb Perspect Med. 2017;7(4).
34. Nicholls CD, McLure KG, Shields MA, Lee PW. Biogenesis of p53 involves cotranslational dimerization of monomers and posttranslational dimerization of dimers. Implications on the dominant negative effect. J Biol Chem. 2002;277(15):12937-45.
35. Liang SH, Clarke MF. A bipartite nuclear localization signal is required for p53 nuclear import regulated by a carboxyl-terminal domain. J Biol Chem. 1999;274(46):32699-703.
36. O'Brate A, Giannakakou P. The importance of p53 location: nuclear or cytoplasmic zip code? Drug Resist Updat. 2003;6(6):313-22.
37. Chène P. The role of tetramerization in p53 function. Oncogene. 2001;20(21):2611-7.
38. Kubbutat MH, Jones SN, Vousden KH. Regulation of p53 stability by Mdm2. Nature. 1997;387(6630):299-303.
39. Haupt Y, Maya R, Kazaz A, Oren M. Mdm2 promotes the rapid degradation of p53. Nature. 1997;387(6630):296-9.
40. Mayo LD, Donner DB. A phosphatidylinositol 3-kinase/Akt pathway promotes translocation of Mdm2 from the cytoplasm to the nucleus. Proc Natl Acad Sci U S A. 2001;98(20):11598-603.
41. Barak Y, Gottlieb E, Juven-Gershon T, Oren M. Regulation of mdm2 expression by p53: alternative promoters produce transcripts with nonidentical translation potential. Genes Dev. 1994;8(15):1739-49.
42. Yamamoto S, Iwakuma T. Regulators of Oncogenic Mutant TP53 Gain of Function. Cancers (Basel). 2018;11(1).
43. Pilley S, Rodriguez TA, Vousden KH. Mutant p53 in cell-cell interactions. Genes Dev. 2021;35(7-8):433-48.

44. Yeudall WA, Vaughan CA, Miyazaki H, Ramamoorthy M, Choi MY, Chapman CG, et al. Gain-of-function mutant p53 upregulates CXC chemokines and enhances cell migration. Carcinogenesis. 2012;33(2):442-51.
45. Zhang S, Wang C, Ma B, Xu M, Xu S, Liu J, et al. Mutant p53 Drives Cancer Metastasis via RCP-Mediated Hsp90α Secretion. Cell Rep. 2020;32(1):107879.
46. Brokx RD, Bolewska-Pedyczak E, Gariépy J. A stable human p53 heterotetramer based on constructive charge interactions within the tetramerization domain. J Biol Chem. 2003;278(4):2327-32.
47. Lang GA, Iwakuma T, Suh YA, Liu G, Rao VA, Parant JM, et al. Gain of function of a p53 hot spot mutation in a mouse model of Li-Fraumeni syndrome. Cell. 2004;119(6):861-72.
48. Wiech M, Olszewski MB, Tracz-Gaszewska Z, Wawrzynow B, Zylicz M, Zylicz A. Molecular mechanism of mutant p53 stabilization: the role of HSP70 and MDM2. PLoS One. 2012;7(12):e51426.
49. Peng Y, Chen L, Li C, Lu W, Agrawal S, Chen J. Stabilization of the MDM2 oncoprotein by mutant p53. J Biol Chem. 2001;276(9):6874-8.
50. Yue X, Zhao Y, Xu Y, Zheng M, Feng Z, Hu W. Mutant p53 in Cancer: Accumulation, Gain-of-Function, and Therapy. J Mol Biol. 2017;429(11):1595-606.
51. Vijayakumaran R, Tan KH, Miranda PJ, Haupt S, Haupt Y. Regulation of Mutant p53 Protein Expression. Front Oncol. 2015;5:284.
52. Zhou JX, Lee CH, Qi CF, Wang H, Naghashfar Z, Abbasi S, et al. IFN regulatory factor 8 regulates MDM2 in germinal center B cells. J Immunol. 2009;183(5):3188-94.
53. Zhang X, Zhang Z, Cheng J, Li M, Wang W, Xu W, et al. Transcription factor NFAT1 activates the mdm2 oncogene independent of p53. J Biol Chem. 2012;287(36):30468-76.
54. Zhao Y, Yu H, Hu W. The regulation of MDM2 oncogene and its impact on human cancers. Acta Biochim Biophys Sin (Shanghai). 2014;46(3):180-9.
55. Yue X, Zhao Y, Liu J, Zhang C, Yu H, Wang J, et al. BAG2 promotes tumorigenesis through enhancing mutant p53 protein levels and function. Elife. 2015;4.
56. Lukashchuk N, Vousden KH. Ubiquitination and degradation of mutant p53. Mol Cell Biol. 2007;27(23):8284-95.

57. Melnikova VO, Santamaria AB, Bolshakov SV, Ananthaswamy HN. Mutant p53 is constitutively phosphorylated at Serine 15 in UV-induced mouse skin tumors: involvement of ERK1/2 MAP kinase. Oncogene. 2003;22(38):5958-66.
58. Aschauer L, Muller PA. Novel targets and interaction partners of mutant p53 Gain-Of-Function. Biochem Soc Trans. 2016;44(2):460-6.
59. Dong P, Karaayvaz M, Jia N, Kaneuchi M, Hamada J, Watari H, et al. Mutant p53 gain-of-function induces epithelial-mesenchymal transition through modulation of the miR-130b-ZEB1 axis. Oncogene. 2013;32(27):3286-95.
60. Kogan-Sakin I, Tabach Y, Buganim Y, Molchadsky A, Solomon H, Madar S, et al. Mutant p53(R175H) upregulates Twist1 expression and promotes epithelial-mesenchymal transition in immortalized prostate cells. Cell Death Differ. 2011;18(2):271-81.
61. Wang SP, Wang WL, Chang YL, Wu CT, Chao YC, Kao SH, et al. p53 controls cancer cell invasion by inducing the MDM2-mediated degradation of Slug. Nat Cell Biol. 2009;11(6):694-704.
62. Zhang C, Liu J, Liang Y, Wu R, Zhao Y, Hong X, et al. Tumour-associated mutant p53 drives the Warburg effect. Nat Commun. 2013;4:2935.
63. Sampath J, Sun D, Kidd VJ, Grenet J, Gandhi A, Shapiro LH, et al. Mutant p53 cooperates with ETS and selectively up-regulates human MDR1 not MRP1. J Biol Chem. 2001;276(42):39359-67.
64. Thottassery JV, Zambetti GP, Arimori K, Schuetz EG, Schuetz JD. p53-dependent regulation of MDR1 gene expression causes selective resistance to chemotherapeutic agents. Proc Natl Acad Sci U S A. 1997;94(20):11037-42.
65. Weissmueller S, Manchado E, Saborowski M, Morris JP, Wagenblast E, Davis CA, et al. Mutant p53 drives pancreatic cancer metastasis through cell-autonomous PDGF receptor β signaling. Cell. 2014;157(2):382-94.
66. Alam SK, Yadav VK, Bajaj S, Datta A, Dutta SK, Bhattacharyya M, et al. DNA damage-induced ephrin-B2 reverse signaling promotes chemoresistance and drives EMT in colorectal carcinoma harboring mutant p53. Cell Death Differ. 2016;23(4):707-22.
67. Freed-Pastor WA, Mizuno H, Zhao X, Langerød A, Moon SH, Rodriguez-Barrueco R, et al. Mutant p53 disrupts mammary tissue architecture via the mevalonate pathway. Cell. 2012;148(1-2):244-58.

68. Xiong S, Tu H, Kollareddy M, Pant V, Li Q, Zhang Y, et al. Pla2g16 phospholipase mediates gain-of-function activities of mutant p53. Proc Natl Acad Sci U S A. 2014;111(30):11145-50.
69. Arjonen A, Kaukonen R, Mattila E, Rouhi P, Högnäs G, Sihto H, et al. Mutant p53-associated myosin-X upregulation promotes breast cancer invasion and metastasis. J Clin Invest. 2014;124(3):1069-82.
70. Alaee M, Padda A, Mehrabani V, Churchill L, Pasdar M. The physical interaction of p53 and plakoglobin is necessary for their synergistic inhibition of migration and invasion. Oncotarget. 2016;7(18):26898-915.
71. Aktary Z, Kulak S, Mackey J, Jahroudi N, Pasdar M. Plakoglobin interacts with the transcription factor p53 and regulates the expression of 14-3-3σ. J Cell Sci. 2013;126(Pt 14):3031-42.
72. Alaee M, Nool K, Pasdar M. Plakoglobin restores tumor suppressor activity of p53. Cancer Sci. 2018;109(6):1876-88.
73. McCrea PD, Turck CW, Gumbiner B. A homolog of the armadillo protein in Drosophila (plakoglobin) associated with E-cadherin. Science. 1991;254(5036):1359-61.
74. Lewis JE, Wahl JK, Sass KM, Jensen PJ, Johnson KR, Wheelock MJ. Cross-talk between adherens junctions and desmosomes depends on plakoglobin. J Cell Biol. 1997;136(4):919-34.
75. Nagar B, Overduin M, Ikura M, Rini JM. Structural basis of calcium-induced E-cadherin rigidification and dimerization. Nature. 1996;380(6572):360-4.
76. Kim SA, Tai CY, Mok LP, Mosser EA, Schuman EM. Calcium-dependent dynamics of cadherin interactions at cell-cell junctions. Proc Natl Acad Sci U S A. 2011;108(24):9857-62.
77. Leckband DE, de Rooij J. Cadherin adhesion and mechanotransduction. Annu Rev Cell Dev Biol. 2014;30:291-315.
78. Yu W, Yang L, Li T, Zhang Y. Cadherin Signaling in Cancer: Its Functions and Role as a Therapeutic Target. Front Oncol. 2019;9:989.
79. Ozawa M, Baribault H, Kemler R. The cytoplasmic domain of the cell adhesion molecule uvomorulin associates with three independent proteins structurally related in different species. EMBO J. 1989;8(6):1711-7.
80. Rübsam M, Broussard JA, Wickström SA, Nekrasova O, Green KJ, Niessen CM. Adherens Junctions and Desmosomes Coordinate Mechanics and Signaling to Orchestrate Tissue

Morphogenesis and Function: An Evolutionary Perspective. Cold Spring Harb Perspect Biol. 2018;10(11).
81. Desai BV, Harmon RM, Green KJ. Desmosomes at a glance. J Cell Sci. 2009;122(Pt 24):4401-7.
82. Hatzfeld M, Keil R, Magin TM. Desmosomes and Intermediate Filaments: Their Consequences for Tissue Mechanics. Cold Spring Harb Perspect Biol. 2017;9(6).
83. Yin T, Getsios S, Caldelari R, Godsel LM, Kowalczyk AP, Müller EJ, et al. Mechanisms of plakoglobin-dependent adhesion: desmosome-specific functions in assembly and regulation by epidermal growth factor receptor. J Biol Chem. 2005;280(48):40355-63.
84. Näthke IS, Hinck L, Swedlow JR, Papkoff J, Nelson WJ. Defining interactions and distributions of cadherin and catenin complexes in polarized epithelial cells. J Cell Biol. 1994;125(6):1341-52.
85. Aktary Z, Alaee M, Pasdar M. Beyond cell-cell adhesion: Plakoglobin and the regulation of tumorigenesis and metastasis. Oncotarget. 2017;8(19):32270-91.
86. MacDonald BT, Tamai K, He X. Wnt/beta-catenin signaling: components, mechanisms, and diseases. Dev Cell. 2009;17(1):9-26.
87. Komiya Y, Habas R. Wnt signal transduction pathways. Organogenesis. 2008;4(2):68-75.
88. Amitay R, Nass D, Meitar D, Goldberg I, Davidson B, Trakhtenbrot L, et al. Reduced expression of plakoglobin correlates with adverse outcome in patients with neuroblastoma. Am J Pathol. 2001;159(1):43-9.
89. Närkiö-Mäkelä M, Pukkila M, Lagerstedt E, Virtaniemi J, Pirinen R, Johansson R, et al. Reduced gamma-catenin expression and poor survival in oral squamous cell carcinoma. Arch Otolaryngol Head Neck Surg. 2009;135(10):1035-40.
90. Baumgart E, Cohen MS, Silva Neto B, Jacobs MA, Wotkowicz C, Rieger-Christ KM, et al. Identification and prognostic significance of an epithelial-mesenchymal transition expression profile in human bladder tumors. Clin Cancer Res. 2007;13(6):1685-94.
91. Fang WK, Liao LD, Gu W, Chen B, Wu ZY, Wu JY, et al. Down-regulated γ-catenin expression is associated with tumor aggressiveness in esophageal cancer. World J Gastroenterol. 2014;20(19):5839-48.

92. Pantel K, Passlick B, Vogt J, Stosiek P, Angstwurm M, Seen-Hibler R, et al. Reduced expression of plakoglobin indicates an unfavorable prognosis in subsets of patients with non-small-cell lung cancer. J Clin Oncol. 1998;16(4):1407-13.
93. Kanazawa Y, Ueda Y, Shimasaki M, Katsuda S, Yamamoto N, Tomita K, et al. Down-regulation of plakoglobin in soft tissue sarcoma is associated with a higher risk of pulmonary metastasis. Anticancer Res. 2008;28(2A):655-64.
94. Aktary Z, Pasdar M. Plakoglobin: role in tumorigenesis and metastasis. Int J Cell Biol. 2012;2012:189521.
95. Fung TK, Gandillet A, So CW. Selective treatment of mixed-lineage leukemia leukemic stem cells through targeting glycogen synthase kinase 3 and the canonical Wnt/β-catenin pathway. Curr Opin Hematol. 2012;19(4):280-6.
96. Xu J, Wu W, Shen W, Liu P. The clinical significance of γ-catenin in acute myeloid leukemia. Onco Targets Ther. 2016;9:3861-71.
97. Morgan RG, Pearn L, Liddiard K, Pumford SL, Burnett AK, Tonks A, et al. γ-Catenin is overexpressed in acute myeloid leukemia and promotes the stabilization and nuclear localization of β-catenin. Leukemia. 2013;27(2):336-43.
98. Qian J, Huang X, Zhang Y, Ye X, Qian W. γ-Catenin Overexpression in AML Patients May Promote Tumor Cell Survival via Activation of the Wnt/β-Catenin Axis. Onco Targets Ther. 2020;13:1265-76.
99. Niu CC, Zhao C, Yang ZD, Zhang XL, Wu WR, Pan J, et al. Downregulation of γ-catenin inhibits CML cell growth and potentiates the response of CML cells to imatinib through β-catenin inhibition. Int J Mol Med. 2013;31(2):453-8.
100. Luong-Gardiol N, Siddiqui I, Pizzitola I, Jeevan-Raj B, Charmoy M, Huang Y, et al. γ-Catenin-Dependent Signals Maintain BCR-ABL1. Cancer Cell. 2019;35(4):649-63.e10.
101. Goto W, Kashiwagi S, Asano Y, Takada K, Takahashi K, Hatano T, et al. Circulating tumor cell clusters-associated gene plakoglobin is a significant prognostic predictor in patients with breast cancer. Biomark Res. 2017;5:19.
102. Aceto N, Bardia A, Miyamoto DT, Donaldson MC, Wittner BS, Spencer JA, et al. Circulating tumor cell clusters are oligoclonal precursors of breast cancer metastasis. Cell. 2014;158(5):1110-22.

103. Amintas S, Bedel A, Moreau-Gaudry F, Boutin J, Buscail L, Merlio JP, et al. Circulating Tumor Cell Clusters: United We Stand Divided We Fall. Int J Mol Sci. 2020;21(7).
104. Schuster E, Taftaf R, Reduzzi C, Albert MK, Romero-Calvo I, Liu H. Better together: circulating tumor cell clustering in metastatic cancer. Trends Cancer. 2021;7(11):1020-32.
105. Parker HR, Li Z, Sheinin H, Lauzon G, Pasdar M. Plakoglobin induces desmosome formation and epidermoid phenotype in N-cadherin-expressing squamous carcinoma cells deficient in plakoglobin and E-cadherin. Cell Motil Cytoskeleton. 1998;40(1):87-100.
106. Hakimelahi S, Parker HR, Gilchrist AJ, Barry M, Li Z, Bleackley RC, et al. Plakoglobin regulates the expression of the anti-apoptotic protein BCL-2. J Biol Chem. 2000;275(15):10905-11.
107. Li L, Chapman K, Hu X, Wong A, Pasdar M. Modulation of the oncogenic potential of beta-catenin by the subcellular distribution of plakoglobin. Mol Carcinog. 2007;46(10):824-38.
108. Aktary Z, Chapman K, Lam L, Lo A, Ji C, Graham K, et al. Plakoglobin interacts with and increases the protein levels of metastasis suppressor Nm23-H2 and regulates the expression of Nm23-H1. Oncogene. 2010;29(14):2118-29.
109. Lam L, Aktary Z, Bishay M, Werkman C, Kuo CY, Heacock M, et al. Regulation of subcellular distribution and oncogenic potential of nucleophosmin by plakoglobin. Oncogenesis. 2012;1:e4.
110. Aktary Z, Pasdar M. Plakoglobin represses SATB1 expression and decreases in vitro proliferation, migration and invasion. PLoS One. 2013;8(11):e78388.
111. Alaee M, Danesh G, Pasdar M. Plakoglobin Reduces the in vitro Growth, Migration and Invasion of Ovarian Cancer Cells Expressing N-Cadherin and Mutant p53. PLoS One. 2016;11(5):e0154323.
112. Aberle H, Bierkamp C, Torchard D, Serova O, Wagner T, Natt E, et al. The human plakoglobin gene localizes on chromosome 17q21 and is subjected to loss of heterozygosity in breast and ovarian cancers. Proc Natl Acad Sci U S A. 1995;92(14):6384-8.
113. Simcha I, Geiger B, Yehuda-Levenberg S, Salomon D, Ben-Ze'ev A. Suppression of tumorigenicity by plakoglobin: an augmenting effect of N-cadherin. J Cell Biol. 1996;133(1):199-209.
114. Grisendi S, Mecucci C, Falini B, Pandolfi PP. Nucleophosmin and cancer. Nat Rev Cancer. 2006;6(7):493-505.

115. Mariano AR, Colombo E, Luzi L, Martinelli P, Volorio S, Bernard L, et al. Cytoplasmic localization of NPM in myeloid leukemias is dictated by gain-of-function mutations that create a functional nuclear export signal. Oncogene. 2006;25(31):4376-80.
116. Holoubek A, Strachotová D, Otevřelová P, Röselová P, Heřman P, Brodská B. AML-Related NPM Mutations Drive p53 Delocalization into the Cytoplasm with Possible Impact on p53-Dependent Stress Response. Cancers (Basel). 2021;13(13).
117. Kurki S, Peltonen K, Latonen L, Kiviharju TM, Ojala PM, Meek D, et al. Nucleolar protein NPM interacts with HDM2 and protects tumor suppressor protein p53 from HDM2-mediated degradation. Cancer Cell. 2004;5(5):465-75.
118. Hamilton G, Abraham AG, Morton J, Sampson O, Pefani DE, Khoronenkova S, et al. AKT regulates NPM dependent ARF localization and p53mut stability in tumors. Oncotarget. 2014;5(15):6142-67.
119. Steeg PS, Bevilacqua G, Kopper L, Thorgeirsson UP, Talmadge JE, Liotta LA, et al. Evidence for a novel gene associated with low tumor metastatic potential. J Natl Cancer Inst. 1988;80(3):200-4.
120. Marino N, Marshall JC, Steeg PS. Protein-protein interactions: a mechanism regulating the anti-metastatic properties of Nm23-H1. Naunyn Schmiedebergs Arch Pharmacol. 2011;384(4-5):351-62.
121. Williams BO, Barish GD, Klymkowsky MW, Varmus HE. A comparative evaluation of beta-catenin and plakoglobin signaling activity. Oncogene. 2000;19(50):5720-8.
122. Lai YH, Cheng J, Cheng D, Feasel ME, Beste KD, Peng J, et al. SOX4 interacts with plakoglobin in a Wnt3a-dependent manner in prostate cancer cells. BMC Cell Biol. 2011;12:50.
123. Sechler M, Borowicz S, Van Scoyk M, Avasarala S, Zerayesus S, Edwards MG, et al. Novel Role for γ-Catenin in the Regulation of Cancer Cell Migration via the Induction of Hepatocyte Growth Factor Activator Inhibitor Type 1 (HAI-1). J Biol Chem. 2015;290(25):15610-20.
124. Baugh EH, Ke H, Levine AJ, Bonneau RA, Chan CS. Why are there hotspot mutations in the TP53 gene in human cancers? Cell Death Differ. 2018;25(1):154-60.
125. Tang Q, Su Z, Gu W, Rustgi AK. Mutant p53 on the Path to Metastasis. Trends Cancer. 2020;6(1):62-73.

126. Gomes AS, Ramos H, Inga A, Sousa E, Saraiva L. Structural and Drug Targeting Insights on Mutant p53. Cancers (Basel). 2021;13(13).
127. Zhou X, Hao Q, Lu H. Mutant p53 in cancer therapy-the barrier or the path. J Mol Cell Biol. 2019;11(4):293-305.
128. Chasov V, Mirgayazova R, Zmievskaya E, Khadiullina R, Valiullina A, Stephenson Clarke J, et al. Key Players in the Mutant p53 Team: Small Molecules, Gene Editing, Immunotherapy. Front Oncol. 2020;10:1460.
129. Lane DP. Cancer. p53, guardian of the genome. Nature. 1992;358(6381):15-6.
130. Abdel-Magid AF. Reactivation of the Guardian of the Genome P53: A Promising Strategy for Treatment of Cancer. ACS Med Chem Lett. 2021;12(3):331-3.
131. Sabapathy K, Lane DP. Therapeutic targeting of p53: all mutants are equal, but some mutants are more equal than others. Nat Rev Clin Oncol. 2018;15(1):13-30.
132. Goh AM, Coffill CR, Lane DP. The role of mutant p53 in human cancer. J Pathol. 2011;223(2):116-26.
133. Wang H, Liao P, Zeng SX, Lu H. It takes a team: a gain-of-function story of p53-R249S. J Mol Cell Biol. 2019;11(4):277-83.
134. Alvarado-Ortiz E, de la Cruz-López KG, Becerril-Rico J, Sarabia-Sánchez MA, Ortiz-Sánchez E, García-Carrancá A. Mutant p53 Gain-of-Function: Role in Cancer Development, Progression, and Therapeutic Approaches. Front Cell Dev Biol. 2020;8:607670.
135. Stein Y, Aloni-Grinstein R, Rotter V. Mutant p53 oncogenicity: dominant-negative or gain-of-function? Carcinogenesis. 2020;41(12):1635-47.
136. Moxley AH, Reisman D. Context is key: Understanding the regulation, functional control, and activities of the p53 tumour suppressor. Cell Biochem Funct. 2021;39(2):235-47.
137. Pitolli C, Wang Y, Mancini M, Shi Y, Melino G, Amelio I. Do Mutations Turn p53 into an Oncogene? Int J Mol Sci. 2019;20(24).
138. Bouaoun L, Sonkin D, Ardin M, Hollstein M, Byrnes G, Zavadil J, et al. TP53 Variations in Human Cancers: New Lessons from the IARC TP53 Database and Genomics Data. Hum Mutat. 2016;37(9):865-76.
139. Mello SS, Attardi LD. Not all p53 gain-of-function mutants are created equal. Cell Death Differ. 2013;20(7):855-7.

140. Brady SW, Gout AM, Zhang J. Therapeutic and prognostic insights from the analysis of cancer mutational signatures. Trends Genet. 2022;38(2):194-208.
141. Thut CJ, Goodrich JA, Tjian R. Repression of p53-mediated transcription by MDM2: a dual mechanism. Genes Dev. 1997;11(15):1974-86.
142. Oliner JD, Pietenpol JA, Thiagalingam S, Gyuris J, Kinzler KW, Vogelstein B. Oncoprotein MDM2 conceals the activation domain of tumour suppressor p53. Nature. 1993;362(6423):857-60.
143. Levine AJ. p53: 800 million years of evolution and 40 years of discovery. Nat Rev Cancer. 2020;20(8):471-80.
144. Midgley CA, Lane DP. p53 protein stability in tumour cells is not determined by mutation but is dependent on Mdm2 binding. Oncogene. 1997;15(10):1179-89.
145. Terzian T, Suh YA, Iwakuma T, Post SM, Neumann M, Lang GA, et al. The inherent instability of mutant p53 is alleviated by Mdm2 or p16INK4a loss. Genes Dev. 2008;22(10):1337-44.
146. Frum RA, Grossman SR. Mechanisms of mutant p53 stabilization in cancer. Subcell Biochem. 2014;85:187-97.
147. Billant O, Friocourt G, Roux P, Voisset C. p53, A Victim of the Prion Fashion. Cancers (Basel). 2021;13(2).
148. Liu Y, Tavana O, Gu W. p53 modifications: exquisite decorations of the powerful guardian. J Mol Cell Biol. 2019;11(7):564-77.
149. Lees A, Sessler T, McDade S. Dying to Survive-The p53 Paradox. Cancers (Basel). 2021;13(13).
150. Peifer M, McCrea PD, Green KJ, Wieschaus E, Gumbiner BM. The vertebrate adhesive junction proteins beta-catenin and plakoglobin and the Drosophila segment polarity gene armadillo form a multigene family with similar properties. J Cell Biol. 1992;118(3):681-91.
151. Chatterjee A, Paul S, Bisht B, Bhattacharya S, Sivasubramaniam S, Paul MK. Advances in targeting the WNT/β-catenin signaling pathway in cancer. Drug Discov Today. 2021.
152. Wang Z, Li Z, Ji H. Direct targeting of β-catenin in the Wnt signaling pathway: Current progress and perspectives. Med Res Rev. 2021;41(4):2109-29.
153. Bugter JM, Fenderico N, Maurice MM. Publisher Correction: Mutations and mechanisms of WNT pathway tumour suppressors in cancer. Nat Rev Cancer. 2021;21(1):64.

154. Chen K, Zeng J, Sun Y, Ouyang W, Yu G, Zhou H, et al. Junction plakoglobin regulates and destabilizes HIF2α to inhibit tumorigenesis of renal cell carcinoma. Cancer Commun (Lond). 2021;41(4):316-32.
155. Charpentier E, Lavker RM, Acquista E, Cowin P. Plakoglobin suppresses epithelial proliferation and hair growth in vivo. J Cell Biol. 2000;149(2):503-20.
156. Salomon D, Sacco PA, Roy SG, Simcha I, Johnson KR, Wheelock MJ, et al. Regulation of beta-catenin levels and localization by overexpression of plakoglobin and inhibition of the ubiquitin-proteasome system. J Cell Biol. 1997;139(5):1325-35.
157. Valenti F, Ganci F, Fontemaggi G, Sacconi A, Strano S, Blandino G, et al. Gain of function mutant p53 proteins cooperate with E2F4 to transcriptionally downregulate RAD17 and BRCA1 gene expression. Oncotarget. 2015;6(8):5547-66.
158. Choi HJ, Gross JC, Pokutta S, Weis WI. Interactions of plakoglobin and beta-catenin with desmosomal cadherins: basis of selective exclusion of alpha- and beta-catenin from desmosomes. J Biol Chem. 2009;284(46):31776-88.
159. Tan BS, Tiong KH, Choo HL, Chung FF, Hii LW, Tan SH, et al. Mutant p53-R273H mediates cancer cell survival and anoikis resistance through AKT-dependent suppression of BCL2-modifying factor (BMF). Cell Death Dis. 2015;6:e1826.
160. Muller PA, Caswell PT, Doyle B, Iwanicki MP, Tan EH, Karim S, et al. Mutant p53 drives invasion by promoting integrin recycling. Cell. 2009;139(7):1327-41.
161. Mukherjee S, Maddalena M, Lü Y, Martinez S, Nataraj NB, Noronha A, et al. Cross-talk between mutant p53 and p62/SQSTM1 augments cancer cell migration by promoting the degradation of cell adhesion proteins. Proc Natl Acad Sci U S A. 2022;119(17):e2119644119.
162. Hassin O, Nataraj NB, Shreberk-Shaked M, Aylon Y, Yaeger R, Fontemaggi G, et al. Different hotspot p53 mutants exert distinct phenotypes and predict outcome of colorectal cancer patients. Nat Commun. 2022;13(1):2800.
163. Lv T, Wu X, Sun L, Hu Q, Wan Y, Wang L, et al. p53-R273H upregulates neuropilin-2 to promote cell mobility and tumor metastasis. Cell Death Dis. 2017;8(8):e2995.
164. Kadosh E, Snir-Alkalay I, Venkatachalam A, May S, Lasry A, Elyada E, et al. The gut microbiome switches mutant p53 from tumour-suppressive to oncogenic. Nature. 2020;586(7827):133-8.

165. Dusek RL, Godsel LM, Chen F, Strohecker AM, Getsios S, Harmon R, et al. Plakoglobin deficiency protects keratinocytes from apoptosis. J Invest Dermatol. 2007;127(4):792-801.
166. Xiao Q, Werner J, Venkatachalam N, Boonekamp KE, Ebert MP, Zhan T. Cross-Talk between p53 and Wnt Signaling in Cancer. Biomolecules. 2022;12(3).
167. Bouvard V, Zaitchouk T, Vacher M, Duthu A, Canivet M, Choisy-Rossi C, et al. Tissue and cell-specific expression of the p53-target genes: bax, fas, mdm2 and waf1/p21, before and following ionising irradiation in mice. Oncogene. 2000;19(5):649-60.
168. Miyashita T, Reed JC. Tumor suppressor p53 is a direct transcriptional activator of the human bax gene. Cell. 1995;80(2):293-9.
169. Nakano K, Vousden KH. PUMA, a novel proapoptotic gene, is induced by p53. Mol Cell. 2001;7(3):683-94.
170. Hikisz P, Kiliańska ZM. PUMA, a critical mediator of cell death--one decade on from its discovery. Cell Mol Biol Lett. 2012;17(4):646-69.
171. Beyfuss K, Hood DA. A systematic review of p53 regulation of oxidative stress in skeletal muscle. Redox Rep. 2018;23(1):100-17.
172. Hernández Borrero LJ, El-Deiry WS. Tumor suppressor p53: Biology, signaling pathways, and therapeutic targeting. Biochim Biophys Acta Rev Cancer. 2021;1876(1):188556.
173. Wu X, Deng Y. Bax and BH3-domain-only proteins in p53-mediated apoptosis. Front Biosci. 2002;7:d151-6.
174. Sinha S, Malonia SK, Mittal SP, Singh K, Kadreppa S, Kamat R, et al. Coordinated regulation of p53 apoptotic targets BAX and PUMA by SMAR1 through an identical MAR element. EMBO J. 2010;29(4):830-42.
175. Willis SN, Adams JM. Life in the balance: how BH3-only proteins induce apoptosis. Curr Opin Cell Biol. 2005;17(6):617-25.
176. Bjørnland K, Winberg JO, Odegaard OT, Hovig E, Loennechen T, Aasen AO, et al. S100A4 involvement in metastasis: deregulation of matrix metalloproteinases and tissue inhibitors of matrix metalloproteinases in osteosarcoma cells transfected with an anti-S100A4 ribozyme. Cancer Res. 1999;59(18):4702-8.
177. Shen W, Chen D, Liu S, Chen L, Yu A, Fu H, et al. S100A4 interacts with mutant p53 and affects gastric cancer MKN1 cell autophagy and differentiation. Int J Oncol. 2015;47(6):2123-30.

178. Miravet S, Piedra J, Miró F, Itarte E, García de Herreros A, Duñach M. The transcriptional factor Tcf-4 contains different binding sites for beta-catenin and plakoglobin. J Biol Chem. 2002;277(3):1884-91.
179. Yang L, Chen Y, Cui T, Knösel T, Zhang Q, Albring KF, et al. Desmoplakin acts as a tumor suppressor by inhibition of the Wnt/β-catenin signaling pathway in human lung cancer. Carcinogenesis. 2012;33(10):1863-70.
180. Yang J, Nie J, Ma X, Wei Y, Peng Y, Wei X. Targeting PI3K in cancer: mechanisms and advances in clinical trials. Mol Cancer. 2019;18(1):26.
181. Hoxhaj G, Manning BD. The PI3K-AKT network at the interface of oncogenic signalling and cancer metabolism. Nat Rev Cancer. 2020;20(2):74-88.
182. Huang B, Wu G, Peng C, Peng X, Huang M, Ding J, et al. miR-126 regulates the proliferation, migration, invasion, and apoptosis of non-small lung cancer cells via AKT2/HK2 axis. IUBMB Life. 2021.
183. Tsubochi H, Minegishi K, Goto A, Nakamura R, Matsubara D, Dobashi Y. EphA2, a possible target of miR-200a, functions through the AKT2 pathway in human lung carcinoma. Int J Clin Exp Pathol. 2020;13(8):2201-10.
184. Hanel W, Marchenko N, Xu S, Yu SX, Weng W, Moll U. Two hot spot mutant p53 mouse models display differential gain of function in tumorigenesis. Cell Death Differ. 2013;20(7):898-909.
185. Fang D, Hawke D, Zheng Y, Xia Y, Meisenhelder J, Nika H, et al. Phosphorylation of beta-catenin by AKT promotes beta-catenin transcriptional activity. J Biol Chem. 2007;282(15):11221-9.
186. Yu J, Zhang L, Hwang PM, Kinzler KW, Vogelstein B. PUMA induces the rapid apoptosis of colorectal cancer cells. Mol Cell. 2001;7(3):673-82.
187. Leszczynska KB, Foskolou IP, Abraham AG, Anbalagan S, Tellier C, Haider S, et al. Hypoxia-induced p53 modulates both apoptosis and radiosensitivity via AKT. J Clin Invest. 2015;125(6):2385-98.
188. Jenkinson SR, Barraclough R, West CR, Rudland PS. S100A4 regulates cell motility and invasion in an in vitro model for breast cancer metastasis. Br J Cancer. 2004;90(1):253-62.

189. Sack U, Walther W, Scudiero D, Selby M, Aumann J, Lemos C, et al. S100A4-induced cell motility and metastasis is restricted by the Wnt/β-catenin pathway inhibitor calcimycin in colon cancer cells. Mol Biol Cell. 2011;22(18):3344-54.
190. SI O, F W, M P, JT T. Plakoglobin to the rescue: predicting the mutant p53-plakoglobin complex structure *in silico* Canadian Cancer Research Conference; Ottawa2019.
191. Panatta E, Zampieri C, Melino G, Amelio I. Understanding p53 tumour suppressor network. Biol Direct. 2021;16(1):14.
192. de Andrade KC, Lee EE, Tookmanian EM, Kesserwan CA, Manfredi JJ, Hatton JN, et al. The TP53 Database: transition from the International Agency for Research on Cancer to the US National Cancer Institute. Cell Death Differ. 2022;29(5):1071-3.
193. Zhang S, Carlsen L, Hernandez Borrero L, Seyhan AA, Tian X, El-Deiry WS. Advanced Strategies for Therapeutic Targeting of Wild-Type and Mutant p53 in Cancer. Biomolecules. 2022;12(4).
194. Huang J. Current developments of targeting the p53 signaling pathway for cancer treatment. Pharmacol Ther. 2021;220:107720.
195. Chiang YT, Chien YC, Lin YH, Wu HH, Lee DF, Yu YL. The Function of the Mutant p53-R175H in Cancer. Cancers (Basel). 2021;13(16).
196. Mukherjee S, Zhang Y. Protein-protein complex structure predictions by multimeric threading and template recombination. Structure. 2011;19(7):955-66.
197. Case DA, Ben-Shalom IY, Brozell SR, Cerutti DS, Cheatham TEI, Cruzeiro VWD, et al. AMBER 2018. University of California, San Francisco.2018.
198. Miller BR, McGee TD, Swails JM, Homeyer N, Gohlke H, Roitberg AE. MMPBSA.py: An Efficient Program for End-State Free Energy Calculations. J Chem Theory Comput. 2012;8(9):3314-21.
199. Leng RP, Lin Y, Ma W, Wu H, Lemmers B, Chung S, et al. Pirh2, a p53-induced ubiquitin-protein ligase, promotes p53 degradation. Cell. 2003;112(6):779-91.
200. Case DA, Darden TA, Cheatham TEI, Simmerling CL, Wang J, Luo R, et al. AMBER 12. University of California, San Francisco.; 2012.
201. Solomon H, Buganim Y, Kogan-Sakin I, Pomeraniec L, Assia Y, Madar S, et al. Various p53 mutant proteins differently regulate the Ras circuit to induce a cancer-related gene signature. J Cell Sci. 2012;125(Pt 13):3144-52.

202. Lai ZY, Tsai KY, Chang SJ, Chuang YJ. Gain-of-Function Mutant TP53 R248Q Overexpressed in Epithelial Ovarian Carcinoma Alters AKT-Dependent Regulation of Intercellular Trafficking in Responses to EGFR/MDM2 Inhibitor. Int J Mol Sci. 2021;22(16).
203. Kondo E, Tanaka T, Miyake T, Ichikawa T, Hirai M, Adachi M, et al. Potent synergy of dual antitumor peptides for growth suppression of human glioblastoma cell lines. Mol Cancer Ther. 2008;7(6):1461-71.
204. Ham SW, Jeon HY, Jin X, Kim EJ, Kim JK, Shin YJ, et al. TP53 gain-of-function mutation promotes inflammation in glioblastoma. Cell Death Differ. 2019;26(3):409-25.
205. Lin RK, Wu CY, Chang JW, Juan LJ, Hsu HS, Chen CY, et al. Dysregulation of p53/Sp1 control leads to DNA methyltransferase-1 overexpression in lung cancer. Cancer Res. 2010;70(14):5807-17.
206. Shafiei F, Rahnama F, Pawella L, Mitchell MD, Gluckman PD, Lobie PE. DNMT3A and DNMT3B mediate autocrine hGH repression of plakoglobin gene transcription and consequent phenotypic conversion of mammary carcinoma cells. Oncogene. 2008;27(18):2602-12.
207. Zhang C, Liu J, Wang J, Zhang T, Xu D, Hu W, et al. The Interplay Between Tumor Suppressor p53 and Hypoxia Signaling Pathways in Cancer. Front Cell Dev Biol. 2021;9:648808.
208. Duffy MJ, Synnott NC, O'Grady S, Crown J. Targeting p53 for the treatment of cancer. Semin Cancer Biol. 2022;79:58-67.
209. Cho Y, Gorina S, Jeffrey PD, Pavletich NP. Crystal structure of a p53 tumor suppressor-DNA complex: understanding tumorigenic mutations. Science. 1994;265(5170):346-55.
210. Colombo E, Marine JC, Danovi D, Falini B, Pelicci PG. Nucleophosmin regulates the stability and transcriptional activity of p53. Nat Cell Biol. 2002;4(7):529-33.
211. Tan AC. Targeting the PI3K/Akt/mTOR pathway in non-small cell lung cancer (NSCLC). Thorac Cancer. 2020;11(3):511-8.
212. Jiang N, Dai Q, Su X, Fu J, Feng X, Peng J. Role of PI3K/AKT pathway in cancer: the framework of malignant behavior. Mol Biol Rep. 2020;47(6):4587-629.
213. Dittmer D, Pati S, Zambetti G, Chu S, Teresky AK, Moore M, et al. Gain of function mutations in p53. Nat Genet. 1993;4(1):42-6.
214. Shi XB, Nesslinger NJ, Deitch AD, Gumerlock PH, deVere White RW. Complex functions of mutant p53 alleles from human prostate cancer. Prostate. 2002;51(1):59-72.

215. Lv T, Lv H, Fei J, Xie Y, Lian D, Hu J, et al. p53-R273H promotes cancer cell migration via upregulation of neuraminidase-1. J Cancer. 2020;11(23):6874-82.
216. Guo F, Chen H, Chang J, Zhang L. Mutation R273H confers p53 a stimulating effect on the IGF-1R-AKT pathway via miR-30a suppression in breast cancer. Biomed Pharmacother. 2016;78:335-41.
217. Harris NS, Pelletier JP, Marin MJ, Winter WE. Von Willebrand factor and disease: a review for laboratory professionals. Crit Rev Clin Lab Sci. 2022;59(4):241-56.
218. Mojiri A, Alavi P, Jahroudi N. Von Willebrand factor contribution to pathophysiology outside of von Willebrand disease. Microcirculation. 2018:e12510.
219. Luo GP, Ni B, Yang X, Wu YZ. von Willebrand factor: more than a regulator of hemostasis and thrombosis. Acta Haematol. 2012;128(3):158-69.